

**PROGRESS TOWARDS THE TOTAL SYNTHESIS OF
HIBARIMICIN B AND ITS CONGENERS**

A Thesis

by

NATHAN PAUL REISING

Submitted to the Office of Graduate Studies of
Texas A&M University
in partial fulfillment of the requirements for the degree of
MASTER OF SCIENCE

December 2003

Major Subject: Chemistry

**PROGRESS TOWARDS THE TOTAL SYNTHESIS OF
HIBARIMICIN B AND ITS CONGENERS**

A Thesis

by

NATHAN PAUL REISING

Submitted to Texas A&M University
in partial fulfillment of the requirements
for the degree of

MASTER OF SCIENCE

Approved as to style and content by:

Gary A. Sulikowski
(Chair of Committee)

James Hu
(Member)

Daniel Romo
(Member)

Emile Schweikert
(Head of Department)

December 2003

Major Subject: Chemistry

ABSTRACT

Progress Towards Total Synthesis of Hibarimicin B and Its Congeners.

(December 2003)

Nathan Paul Reising, B.A., Wabash College

Chair of Advisory Committee: Dr. Gary A. Sulikowski

Hibarimicin B (**I**) was isolated from a soil sample collected in Hibari, Japan, in 1995, and was identified to be a potent inhibitor of tyrosine kinase via a multi-protein assay. Chapter I of this thesis describes the biological activity of the hibarimicins, in addition to an investigation of the biosynthetic pathway leading to the hibarimicins. Based on this biosynthetic study, we have identified hibarimicinone (**II**) and HMP-Y1 (**III**) as key synthetic targets. Chapter II describes a model study investigating the key Hauser annulation for the synthesis of hibarimicinone (**II**). Synthetic progress towards one of the key intermediates in the synthesis of HMP-Y1 (**III**) is also presented. Chapter III summarizes the work accomplished to date and provides an overview of the necessary work needed for the total synthesis of hibarimicinone (**II**) and HMP-Y1 (**III**).

ACKNOWLEDGEMENTS

I would like to thank my advisor, Dr. Gary Sulikowski, for his guidance and leadership during my graduate career. Thanks also to Dr. Daniel Romo and Dr. James Hu for serving on my advisory committee. I would also like to thank the members of the Sulikowski group who helped my development and training: Dr. Chee-Seng Lee, Dr. Fabio Agnelli, Dr. Weidong Liu, Dr. Umar Maharroof, Dr. Kurt Kiewel, Dr. Bohan Jin, Dr. Steve Luo Ron Pongdee, Bin Wu, Brant Boren, Tao Qu, Qingsong Liu, Junyan Han and especially, Dr. Kwangho Kim. Finally, I would like to thank my family, especially my parents and my sister, for their years of unconditional love, support and guidance. I would not be where I am today without you. Thank you.

TABLE OF CONTENTS

CHAPTER	Page
I	INTRODUCTION..... 1
	1.1 Isolation and Biological Activity of the Hibarimicins..... 1
	1.2 Biosynthetic Studies of the Hibarimicins..... 4
	1.3 Synthetic Analysis of Hibarimicinone (1.6) and HMP-Y1(1.10)..... 12
	1.3a Synthetic Analysis of Hibarimicinone (1.6)..... 13
	1.3b Synthetic Analysis of HMP-Y1 (1.10): Cross- Coupling Approach..... 15
	1.3c Synthetic Analysis of HMP-Y1 (1.10): Bi-Directional Approach..... 16
	1.4 Literature Precedent for Aryl-Quinone and Aryl-Aryl Bond Formation..... 17
	1.5 Literature Precedent for Directed Ortho Metalations..... 21
II	SYNTHETIC PROGRESS TOWARD THE AB AND GH RING SYSTEMS OF HIBARIMICINONE AND HMP-Y1 23
	2.1 Synthetic Progress Toward Hibarimicinone (1.6): Model Study..... 23
	2.2 Synthetic Progress Toward HMP-Y1 (1.10): Cross- Coupling Approach..... 26
	2.3 Synthetic Progress Toward HMP-Y1(1.10): Bi-Directional Approach..... 28
	2.4 Experimental Section..... 33
III	CONCLUSION..... 50
	3.1 Summary..... 50
	3.2 Future Work Toward the Synthesis of Hibarimicinone (1.6) 50
	3.2a Future Work Toward the ABCD Ring System 50
	3.2b Future Work Toward the Synthesis of EFGH Ring System..... 51
	3.2c Palladium Mediated Cross-Coupling 53
	3.3 Future Work Toward the Synthesis of HMP-Y1 53
	REFERENCES..... 55

	Page
APPENDIX A SPECTRA RELEVANT TO CHAPTER II.....	57
VITA.....	88

LIST OF FIGURES

Figure	Page
1.1 Structures of the hibarimicins.....	2
1.2 Structure of hibarimicinone (1.6) and HMP-P1 (1.7)	4
1.3 Incorporation pattern of ¹³ C-labeled acetate.....	6
1.4 Generalized biosynthetic pathway of hibarimicins.....	7
1.5 Proposed mechanism for the skeletal rearrangement.....	9
1.6 Proposed biosynthetic pathway to hibarimicin B (1.2).....	11
2.1 Common intermediate in the synthesis of hibarimicinone (1.6) and HMP-Y1 (1.10).....	26
A.1a The 500 MHz ¹ H NMR spectrum of dihydroquinone 2.7 in CDCl ₃	58
A.1b The 126 MHz ¹³ C NMR spectrum of dihydroquinone 2.7 in CDCl ₃	59
A.2a The 500 MHz ¹ H NMR spectrum of tricycle 2.8 in CDCl ₃	60
A.2b The 126 MHz ¹³ C NMR spectrum of tricycle 2.8 in CDCl ₃	61
A.3a The 500 MHz ¹ H NMR spectrum of phenol 2.9 in CDCl ₃	62
A.3b The 126 MHz ¹³ C NMR spectrum of phenol 2.9 in CDCl ₃	63
A.4a The 500 MHz ¹ H NMR spectrum of quinone 2.10 in CDCl ₃	64
A.4b The 126 MHz ¹³ C NMR spectrum of quinone 2.10 in CDCl ₃	65
A.5a The 500 MHz ¹ H NMR spectrum of aryl-iodide 2.15 in CDCl ₃	66
A.5b The 126 MHz ¹³ C NMR spectrum of aryl-iodide 2.15 in CDCl ₃	67

Figure	Page
A.6a The 500 MHz ^1H NMR spectrum of aryl-amide 2.16 in CDCl_3	68
A.6b The 126 MHz ^{13}C NMR spectrum of aryl-amide 2.16 in CDCl_3	69
A.7a The 500 MHz ^1H NMR spectrum of aryl-silane 2.18 in CDCl_3	70
A.7b The 126 MHz ^{13}C NMR spectrum of aryl-silane 2.18 in CDCl_3	71
A.8a The 500 MHz ^1H NMR spectrum of aryl-iodide 2.19 in CDCl_3	72
A.8b The 126 MHz ^{13}C NMR spectrum of aryl-iodide 2.19 in CDCl_3	73
A.9a The 500 MHz ^1H NMR spectrum of aryl-amide 2.20 in CDCl_3	74
A.9b The 126 MHz ^{13}C NMR spectrum of aryl-amide 2.20 in CDCl_3	75
A.10a The 500 MHz ^1H NMR spectrum of aryl-iodide 2.24 in CDCl_3	76
A.10b The 126 MHz ^{13}C NMR spectrum of aryl-iodide 2.24 in CDCl_3	77
A.11a The 500 MHz ^1H NMR spectrum of boronic acid 2.25 in CDCl_3	78
A.11b The 126 MHz ^{13}C NMR spectrum of boronic acid 2.25 in CDCl_3	79
A.12a The 500 MHz ^1H NMR spectrum of aryl-stannane 2.26 in CDCl_3	80
A.12b The 126 MHz ^{13}C NMR spectrum of aryl-stannane 2.26 in CDCl_3	81
A.13a The 500 MHz ^1H NMR spectrum of biaryl 2.27 in CDCl_3	82
A.13b The 126 MHz ^{13}C NMR spectrum of biaryl 2.27 in CDCl_3	83
A.14a The 500 MHz ^1H NMR spectrum of aryl-stannane 2.28 in CDCl_3	84
A.14b The 126 MHz ^{13}C NMR spectrum of aryl-stannane 2.28 in CDCl_3	85
A.15a The 500 MHz ^1H NMR spectrum of biaryl 2.29 in CDCl_3	86
A.15b The 126 MHz ^{13}C NMR spectrum of biaryl 2.29 in CDCl_3	87

LIST OF SCHEMES

Scheme	Page
1.1 Hauser's Synthesis of Biphysson.....	13
1.2 Retrosynthetic Analysis of Hibarimicinone.....	14
1.3 Retrosynthetic Analysis of HMP-Y1: Cross-Coupling Approach.....	16
1.4 Retrosynthetic Analysis of HMP-Y1: Bi-Directional Approach.....	17
1.5 Fukuyama's Aryl-Quinone Suzuki Coupling.....	18
1.6 Mechanism of Suzuki Coupling.....	18
1.7 Stagliano's Aryl-Quinone Coupling.....	19
1.8 Bringmann's Oxidative Coupling of Phenols.....	20
1.9 Example of Directed Ortho Metallation Reaction.....	21
2.1 Synthesis of the Known Cyanophthalide 2.5	23
2.2 Synthesis of Phenol 2.9	25
2.3 Synthesis of Quinone 30	25
2.4 Synthetic Work Toward Lactone 2.11a	27
2.5 Synthetic Work Toward Lactone 2.11b	28
2.6 Synthesis of Sesamol Derivatives.....	29
2.7 Corey Conditions for Dimerization Reaction.....	31
2.8 Proposed Mechanism for the Corey Dimerization.....	32
3.1 Future Work Toward the Synthesis of ABCD Ring System.....	51
3.2 Future Work Toward the Synthesis of EFGH Ring System.....	52
3.3 Future Work Toward the Synthesis of Hibarimicinone.....	53

Scheme	Page
3.4 Future Work Toward the Synthesis of HMP-Y1	54

LIST OF TABLES

Table	Page
1.1 <i>In vitro</i> Cytotoxicity of Hibarimicins.....	3
1.2 Effects of Hibarimicins, Hibarimicinone, and HMP-P1.....	5
1.3 Effects of Hibarimicin B and Hibarimicinone on PKC.....	5
2.1 Conditions for Suzuki Coupling Reacton.....	30

CHAPTER I

INTRODUCTION

1.1 Isolation and Biological Activity of the Hibarimicins

The hibarimicins consist of a family of at least 10 secondary metabolites that were isolated from a soil sample collected at Hibari, Toyama Prefecture, Japan on June 2, 1995. They were found during a screening of microbial products for tyrosine kinase inhibition, the producing soil microorganism was further identified as *Microbispora rosea* subsp *hibaria* TP-A0121 based on DNA-DNA homological comparison to species in this genus.¹ The structure of five of the ten isolated secondary metabolites, hibarimicin A (**1.1**), B (**1.2**), C (**1.3**), D (**1.4**), G (**1.5**), were elucidated using 2D NMR analysis, including the use of COSY, CH-COSY, HMBC, NOESY, and NOE experiments.² Following structural assignment, hibarimicin B (**1.2**) was found to be identical to angelmicin B, a secondary metabolite previously isolated in 1993 from a culture broth of a strain of *Microbispora* sp.³ Hibarimicin A (**1.1**), B (**1.2**), C (**1.3**), D (**1.4**), and G (**1.5**), all possess the same aglycon structure and differ only in the number and structure of sugars located at the periphery of the compounds. The structures of the hibarimicins are shown in Figure 1.1. Hibarimicins A (**1.1**), B (**1.2**), C (**1.3**), and D (**1.4**) were tested in a single assay that allowed simultaneous detection of inhibition of protein

This thesis follows the style and format of the *Journal of Organic Chemistry*.

kinase A (PKA), protein kinase C (PKC), protein tyrosine kinase (PTK) and calmodulin-dependent protein kinase III (CAMKIII).¹ The results of this experiment showed that all four hibarimicins specifically inhibited PTK activity, and showed little effect on PKA or PKC activity.¹ IC₅₀ values for the inhibition of PTK ranged from 10 - 40 µg / mL, with hibarimicin A (**1.1**) be the most potent of the hibarimicins at inhibiting PTK activity. In addition, all four of the hibarimicins assayed inhibited CAMKIII activity¹, which is a common phenomenon with a number of other tyrosine kinase inhibitors including herbimycin A and tyrphostins.¹

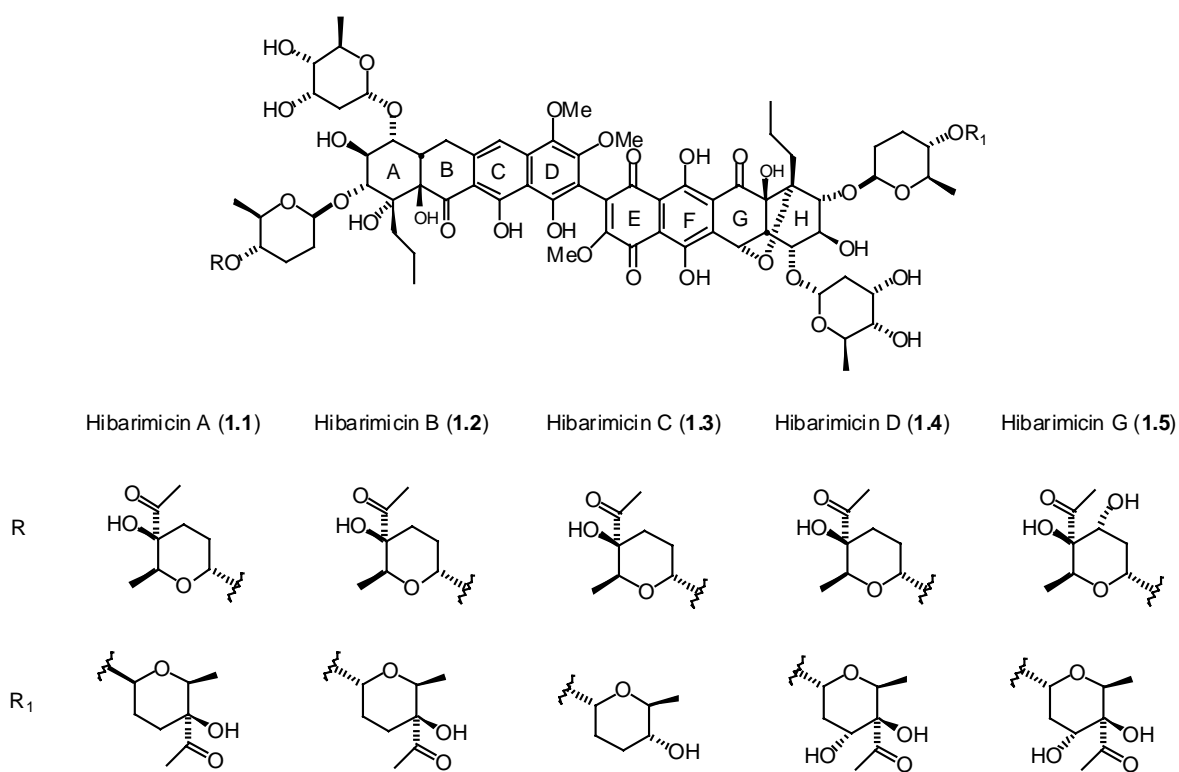


Figure 1.1. Structures of the hibarimicins.

In addition to the protein tyrosine kinase assay, hibarimicins A (**1.1**), B (**1.2**), C (**1.3**), and D (**1.4**) were also tested *in vitro* for antimicrobial activity. All four showed moderate inhibitory activity against Gram-positive bacteria with MICs of 0.8 - 12.5 $\mu\text{g} / \text{mL}$.¹ Furthermore, all four of the hibarimicins showed potent cytotoxicity against B16-F10 (murine melanoma) and HCT-116 (human colon carcinoma) cells as summarized in Table 1.1¹.

Table 1.1. *In vitro* Cytotoxicity of Hibarimicins.

	IC ₅₀ ($\mu\text{g} / \text{mL}$)	
	B16-F10	HCT-116
Hibarimicin A	1.2	2.5
Hibarimicin B	0.7	1.9
Hibarimicin C	0.8	2.7
Hibarimicin D	2.0	3.6

Uehara and co-workers further investigated the biological activity of hibarimicin A (**1.1**) and B (**1.2**), hibarimicinone (**1.6**) and HMP-P1 (**1.7**), a shunt metabolite produced from a mutant strain of *Microbispora rosea* subsp. *hibaria*, (Figure 1.2), in a multiple protein kinase assay using the postnuclear fraction of v-src transformed NIH3T3 cells.⁴ They found that all four compounds potently inhibited the Src PTK activity, as shown in Table 1.2. Hibarimicin B (**1.2**) was more effective at inhibition

than hibarimicin A (**1.1**) and hibarimicinone (**1.6**) was more effective than HMP-P1 (**1.7**).⁴ While hibarimicin B (**1.2**) and hibarimicinone (**1.6**) showed similar inhibition to v-src tyrosine kinase activity, hibarimicinone (**1.6**) showed a 5.5-fold stronger inhibition against PKC than hibarimicin B (**1.2**), Table 1.3.⁴ These results collectively indicate that while hibarimicinone (**1.6**) is a slightly stronger inhibitor of src tyrosine kinase activity than hibarimicin B (**1.2**), hibarimicin B (**1.2**) is a much more selective inhibitor than hibarimicinone (**1.6**).⁴

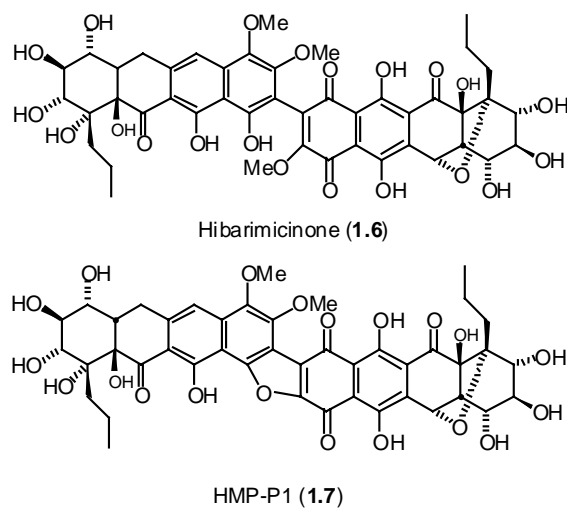


Figure 1.2. Structure of hibarimicinone (**1.6**), and HMP-P1 (**1.7**).

1.2 Biosynthetic Studies of the Hibarimicins

Recently Kajiura and coworkers studied the biosynthetic origin of the hibarimicins using stable isotope feeding experiments.⁵ Specifically, ¹³C labeled sodium acetate was added to a liquid culture of *Microbispora rosea* subsp. *hibaria* TP-A0121.

After isolation of hibarimicin B (**1.2**), NMR analysis revealed incorporation of isotope enriched carbons as summarized in Figure 1.3.⁵

Table 1.2. Effects of Hibarimicins, Hibarimicinone (**1.6**), and HMP-P1 (**1.7**) on v-src tyrosine kinase*.

Compound	v-Src tyrosin kinase inhibition
Hibarimicin A	1+
Hibarimicin B	2+
Hibarimicinone	3+
HMP-P1	2+

* + after number represents relatively stronger activity

Table 1.3. Effects of Hibarimicin B (**1.2**) and Hibarimicinone (**1.6**) on PKC.

Compound	IC ₅₀ (μM) for PKC
Hibarimicin B	36
Hibarimicinone	6.5

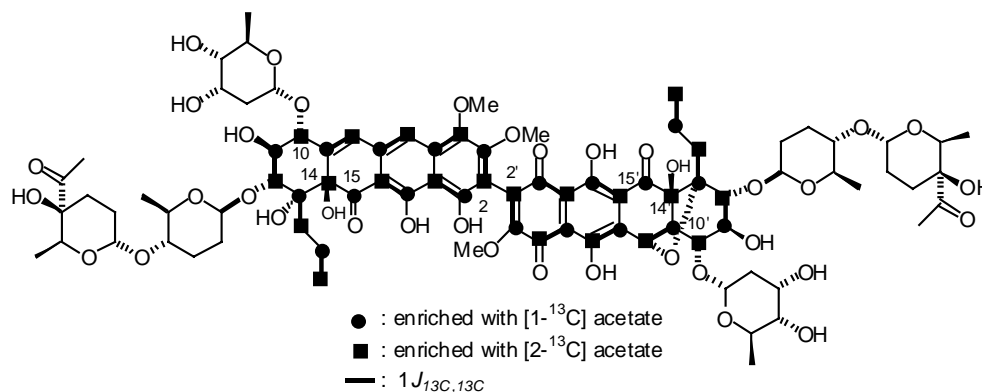


Figure 1.3. Incorporation pattern of ¹³C-labeled acetate.

Assuming a polyketide biosynthetic pathway, this experiment reveals an irregular distribution of the labeled acetates. Despite the fact that C14 and C15 correspond to carbonyl and methyl group of the labeled acetates, respectively, and are directly bound to each other, there is no ¹³C-¹³C coupling seen between them. The same results are seen for C14' and C15'.⁵ Furthermore, C10 and C10' were incorporated from the methyl group of a labeled acetate fed to the broth, but there is no carbon-carbon coupling observed in material enriched with [2-¹³C] acetate. Kajiura hypothesized that the C10 and C15 came from the same acetate unit and that C14 initially had been attached to an additional carbonyl carbon, comprising another acetate unit.⁵ The half unit was formed from a decarboxylation at C14 and a skeletal rearrangement, involving cleavage of the C10-C14 carbon-carbon bond, to give the carbon skeleton seen in the half unit of hibarimicin B (**1.2**). After intense INADEQUATE 2-D NMR analysis they found that

C10 and C15, and also C10' and C15', indeed originated from the same labeled acetate unit.⁵ From this information they concluded that the aglycon of hibarimicin B (**1.2**) was

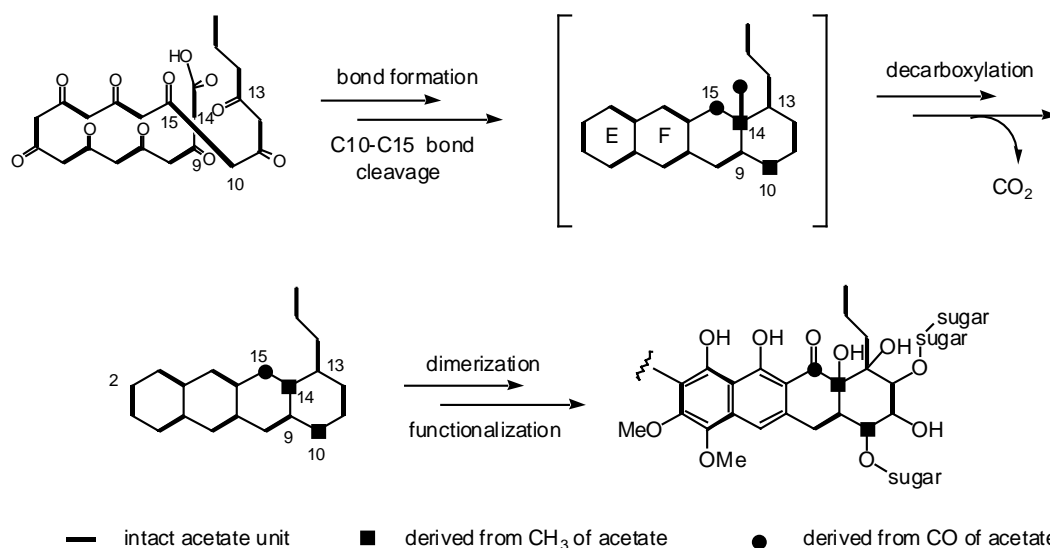


Figure 1.4. Generalized biosynthetic pathway of hibarimicins.

biosynthetically formed through the polyketide pathway, utilizing a dimerization of the two half units formed from the decarboxylation and skeletal rearrangement of the starting undecaketide. Their proposed biosynthetic pathway is shown in Figure 1.4.⁵

Kajiura did not propose a mechanism for the skeletal rearrangement leading to cleavage of the C10-C14 bond to provide the carbon skeleton of the hibarimicins. One possible mechanism for this rearrangement is proposed in Figure 1.5. The first steps of this rearrangement are aldol condensation reactions in order to construct the EF ring system, followed by a deprotonation at C10 and attack of the resulting enolate on the C9

carbonyl. Next, fragmentation results in cleavage of the C9-C14 bond, with 1,3 migration of an acetate unit to C15 (formation of the C14-C15 bond). Another fragmentation then occurs breaking the C15-C10 bond. The next step in the mechanism is a deprotonation at C14 and the resulting enolate attacks the carbonyl at C9, thereby constructing the G ring. A second deprotonation at C14 then occurs, and the resulting enolate adds to the carbonyl at C13 to form the H ring, and decarboxylation completes the carbon skeleton of the EFGH ring system.

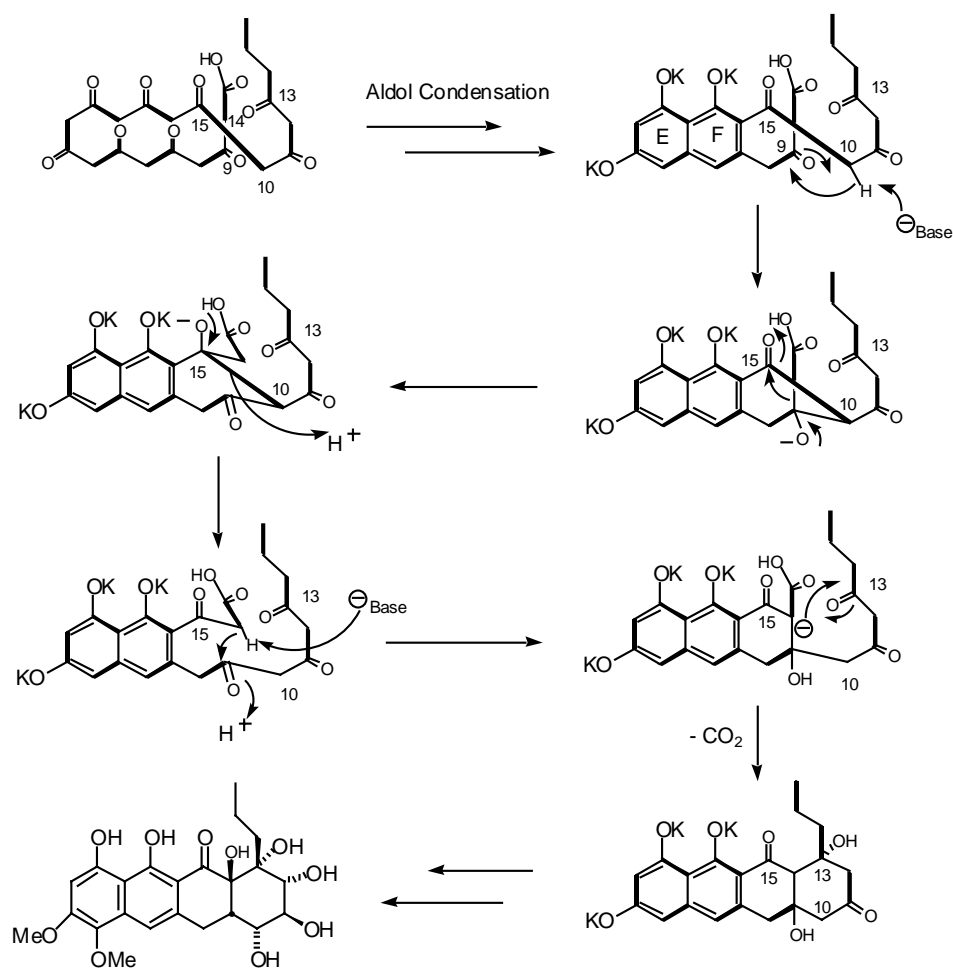


Figure 1.5. Proposed mechanism for the skeletal rearrangement.

Kajiura further investigated the biosynthetic pathway leading to the hibarimicins by the isolation and structure elucidation of shunt metabolites.⁶ The blocked mutants from this experiment were obtained by exposure of *M. rosea* subsp. *hibaria* TP-A012 to the mutagenic agent, N-methyl-N'-nitro-N-nitrosoguanidine (NTG). Initially nine hundred sixty colonies were gathered after mutagenesis, none of which produced

hibarimicins. Five of these colonies possessed the characteristic red color of the hibarimicins and were selected for further analysis.⁶

After further investigation of these mutants by fermentation in various media they isolated key intermediates on the biosynthetic pathway leading to the hibarimicins, summarized in Figure 1.6.⁶ Polyketide (**1.8**) undergoes a cyclization and skeletal rearrangement affording tetracycle (**1.9**), the presumed precursor to the key dimerization. Tetracycle (**1.9**) then undergoes an oxidative coupling to afford the symmetrical metabolite HMP-Y1 (**1.10**). The symmetrical compound then undergoes an oxidation of the E and F rings and formation of the furan linkage bridging the GH ring system to furnish hibarimicinone (**1.6**). Hibarimicinone (**1.6**) then undergoes a series of glycosylations to furnish the hibarimicins, including hibarimicin B (**1.2**).⁶ Isolation of HMP-Y1 (**1.10**) demonstrates that the dimerization of the two half units occurs first on the biosynthetic pathway, followed by oxidation of the E and F rings and furan formation, and then finally the glycosylation reactions that account for the difference in the hibarimicins. From this information we identified HMP-Y1 (**1.10**) and hibarimicinone (**1.6**) to be valuable intermediates in the synthesis of hibarimicin B (**1.2**), and chose these as our synthetic targets in order to correlate our synthetic products with known natural products.

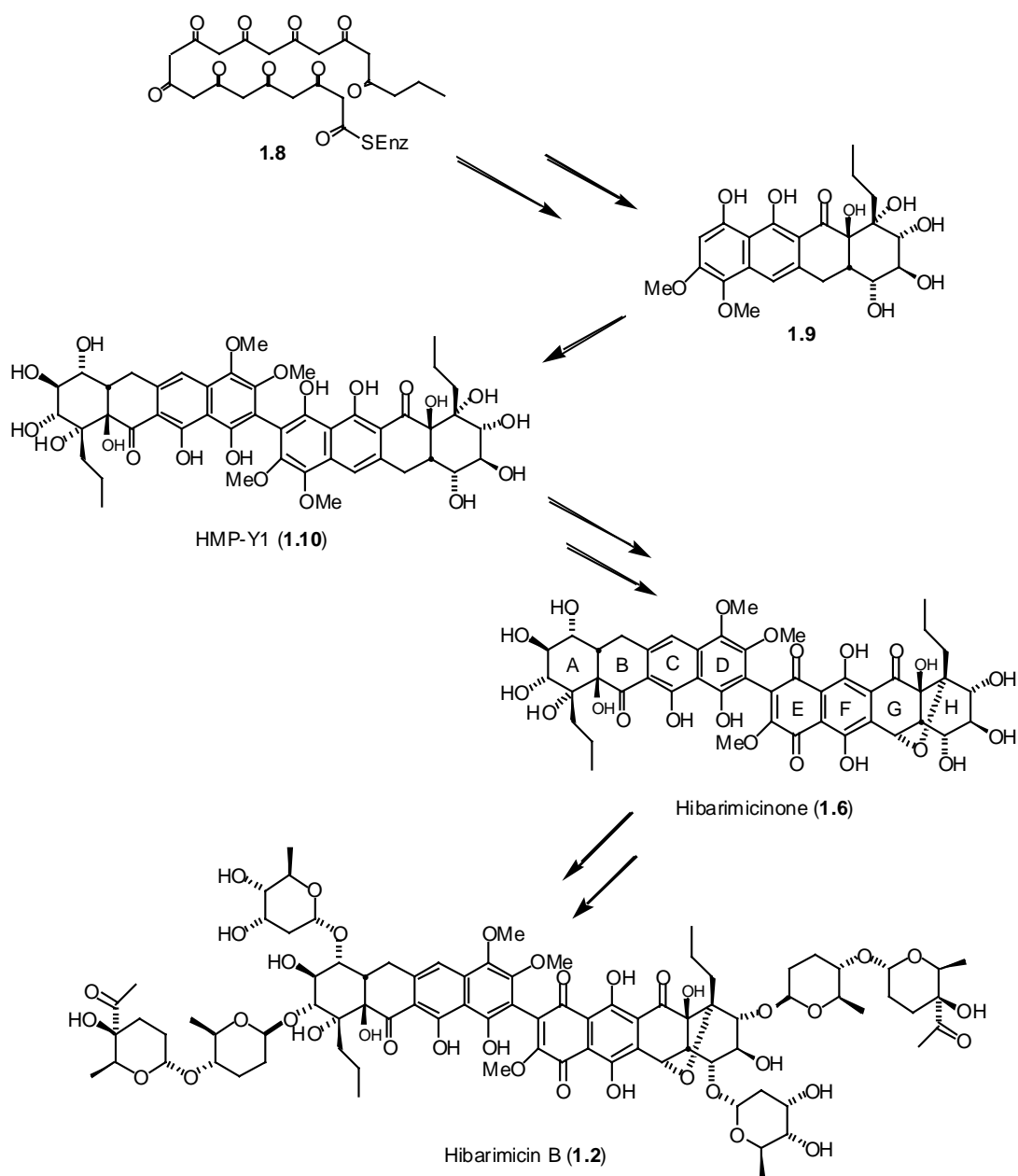
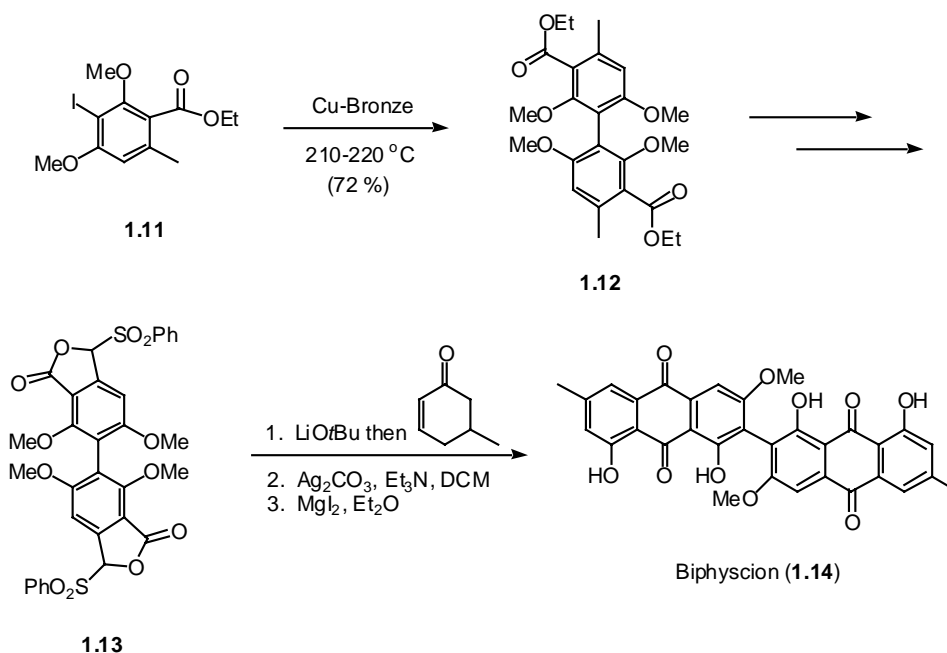


Figure 1.6. Proposed biosynthetic pathway to hibarimicin B (1.2).

1.3 Synthetic Analysis of Hibarimicinone (1.6) and HMP-Y1 (1.10)

From the work done by Kajiura and co-workers, we identified hibarimicinone (**1.6**) and HMP-Y1 (**1.10**) as synthetic targets in our labs. We have contemplated multiple strategies for our synthetic approach to hibarimicinone (**1.6**) and HMP-Y1 (**1.10**). For hibarimicinone (**1.6**) we envision using a palladium mediated Suzuki or Stille cross coupling in the late stages of the synthesis to couple the ABCD and EFGH ring systems. For HMP-Y1 (**1.10**) we have more options for our synthetic strategy, due to the symmetrical nature of the target metabolite. One of our options is the application of a palladium mediated coupling reaction to dimerize the tetracycle in the late stages of our synthesis, similar to our synthetic strategy for hibarimicinone (**1.6**). A second approach is to form the aryl-aryl bond early in the synthesis and utilize a bi-directional approach for the synthesis of HMP-Y1 (**1.10**). This strategy was used by Hauser and co-workers in their synthesis of Biphyscion (**1.13**) (Scheme 1.1).⁷ We are currently investigating all three of these strategies for the total synthesis of hibarimicinone (**1.6**) and HMP-Y1 (**1.10**).

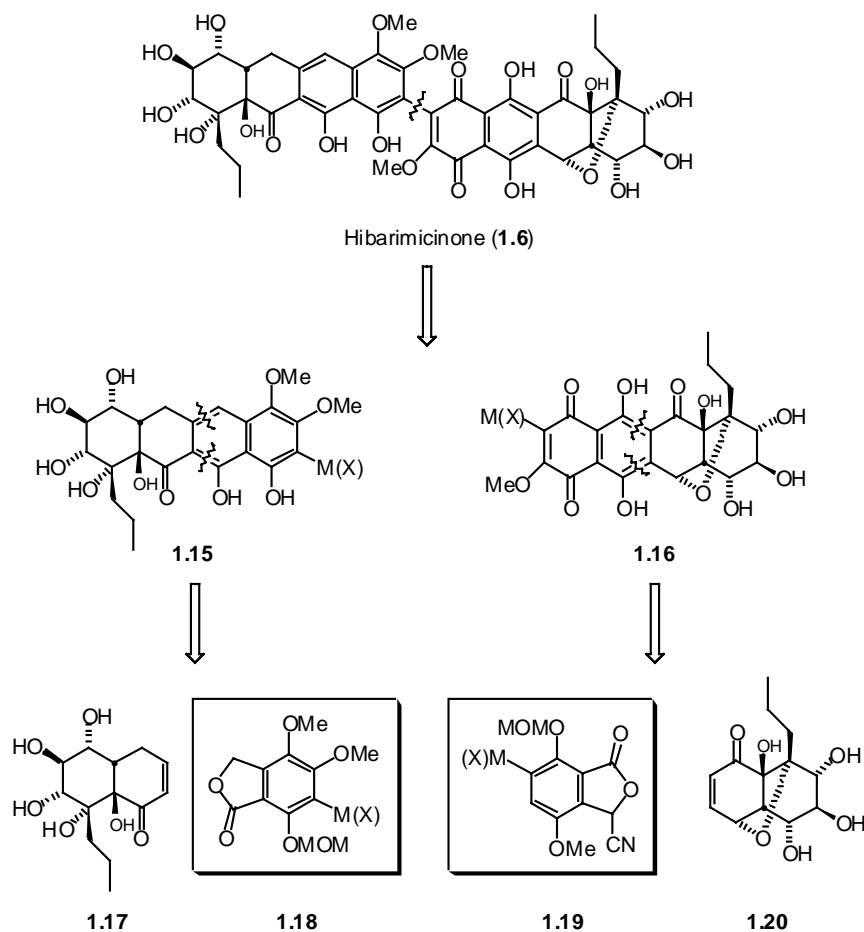
Scheme 1.1. Hauser's Synthesis of Biphyscion (**1.13**).



1.3a Synthetic Analysis of Hibarimicinone (1.6)

Our major disconnections for the total synthesis of hibarimicinone (**1.6**) are shown in Scheme 1.2. We envision that hibarimicinone (**1.6**) can be assembled by a palladium mediated cross coupling between tetracycles, **1.15** and **1.16**. This transformation may be accomplished in one of several ways, including a Suzuki or Stille cross-coupling reaction. The Suzuki coupling reaction would involve the coupling of the aryl-boronic acid **1.15** ($M = B(OR)_2$) with the bromo-quinone **1.16** ($X = Br$). The Stille

Scheme 1.2. Retrosynthetic Analysis of Hibarimicinone (**1.6**).



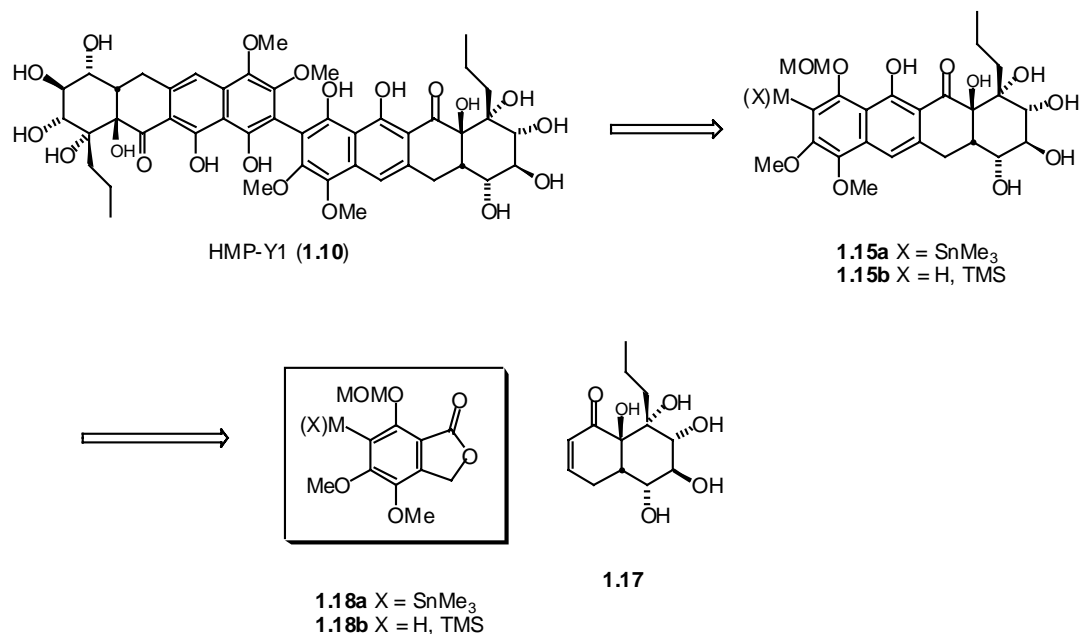
coupling reaction would consist of the coupling of the aryl-stannane **1.15** ($M = \text{SnR}_3$) with the bromo-quinone **1.16** ($X = \text{Br}$). These two tetracycles may be synthesized from a Hauser annulation between enone **1.17** and the lactone **1.18**, and a Hauser annulation with cyanophthalide **1.19** and the furan bridged enone **1.20**. Lactone **1.18** and cyanophthalide **1.19** are therefore points of departure for our synthetic studies. Lactone

1.18 was anticipated to be synthesized from a series of directed ortho-metallations (DoM) starting from MOM protected 3,4 dimethoxyphenol. Similarly, the cyanophthalide **1.19** could be synthesized from a series of DoM reactions starting from MOM protected p-methoxyphenol.

1.3b Synthetic Analysis of HMP-Y1 (1.10): Cross-Coupling Approach

One retrosynthetic analysis for HMP-Y1 (**1.10**), similar to that of hibarimicinone (**1.6**) (Scheme 1.2), is outlined in Scheme 1.3. The metabolite HMP-Y1 (**1.10**) may be constructed using either a palladium mediated dimerization of the aryl-stannane **1.15a** or a oxidative aryl coupling of tetracycle **1.15b**. The tetracycle **1.15** is proposed to be formed from the Hauser annulation of the lactone **1.18** and the enone **1.17**. The lactone **1.18**, which is our synthetic target, may be constructed using a series of DoM reactions. Tetracycle **1.15** for construction of HMP-Y1 (**1.10**) is potentially one of the coupling partners required for construction of hibarimicinone (**1.6**).

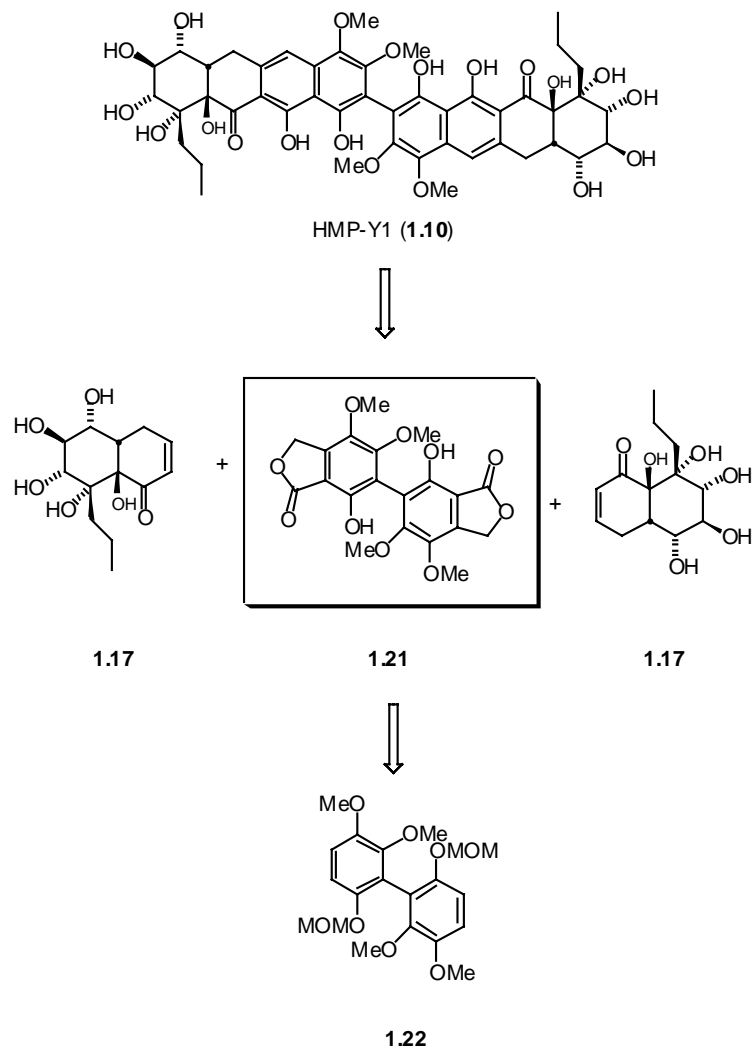
Scheme 1.3. Retrosynthetic Analysis of HMP-Y1 (**1.10**): Cross-Coupling Approach.



1.3c Synthetic Analysis of HMP-Y1 (1.10): Bi-directional Approach

Our second synthetic strategy for the synthesis of HMP-Y1 (**1.10**) involves constructing the central aryl-aryl bond and assembling the target structure in bi-directional fashion, as illustrated in Scheme 1.4. From this retrosynthetic approach we envision that HMP-Y1 (**1.10**) may be synthesized from a bis-Hauser annulation of the bislactone **1.21** and the enone **1.17**. The bislactone **1.21** is our synthetic target and may be synthesized from a series of directed ortho metalation reactions starting from the biaryl compound **1.22**. The biaryl compound **1.22** may be constructed using a palladium mediated dimerization reaction to construct the central aryl-aryl bond.

Scheme 1.4. Retrosynthetic Analysis of HMP-Y1 (**1.10**): Bi-Directional Approach.

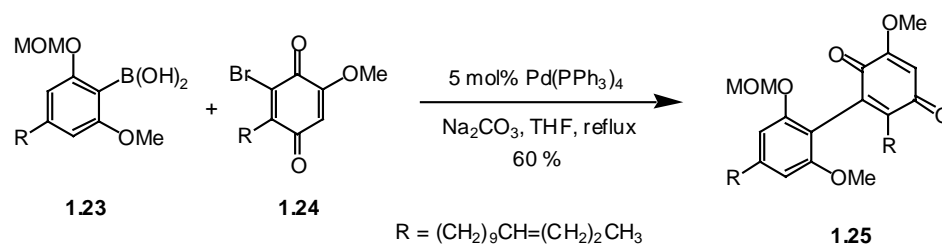


1.4 Literature Precedent for Aryl-Quinone and Aryl-Aryl Bond Formation

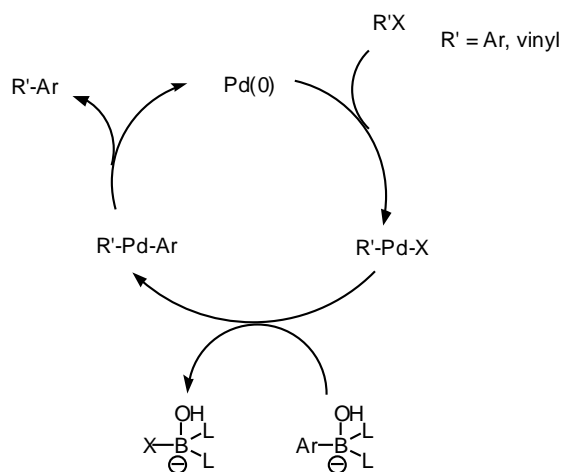
As discussed earlier, there are several methods available for the construction of the aryl-quinone bond required to complete the core carbon structure of hibarimicinone (**1.6**). The most viable of these options would consist of the Suzuki cross coupling

between the aryl-boronic acid and the aryl halide. Fukuyama and co-workers have shown in their synthesis of mastigophorenes A and B, the ability to couple the highly substituted aryl-boronic acid **1.23** with bromo-quinone **1.24** in good yield,⁸ as shown in Scheme 1.5. The most widely accepted mechanism for the Suzuki coupling consists of an oxidative addition-transmetalation-reductive elimination sequence,⁹ as shown in Scheme 1.6. In this reaction, the rate limiting step is the oxidative addition of the palladium catalyst into the R-X bond.⁹

Scheme 1.5. Fukuyama's Aryl-Quinone Suzuki Coupling.

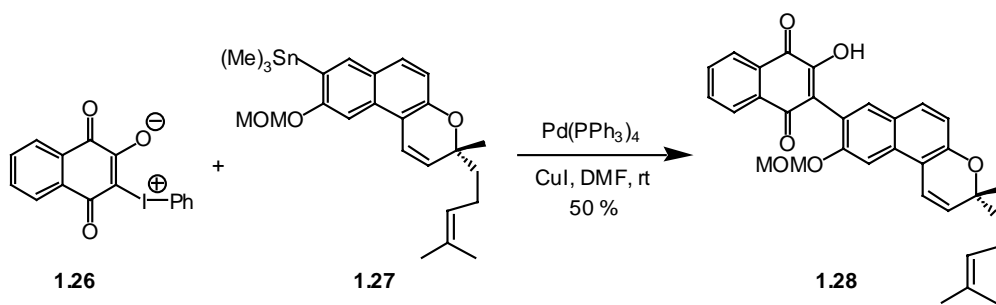


Scheme 1.6. Mechanism of Suzuki Coupling.



Another commonly used method for aryl-quinone bond formation is the Stille coupling which entails the palladium mediated coupling of aryl stannanes with halo-quinones. This has been recently demonstrated by Stagliano and Malinakova, where they coupled the hypervalent iodo-quinone **1.26** with the aryl-stannane **1.27**, (Scheme 1.7).¹⁰ The mechanism of the Stille coupling closely resembles the Suzuki coupling. The initial step is an oxidative addition of the palladium catalyst into the R-X bond, followed by a transmetalation of the aryl group with loss of trialkyltin halide. Reductive elimination of R-R' then occurs to give the desired product and recycle the Pd(II) to Pd(0), which may then repeat the cycle.⁹

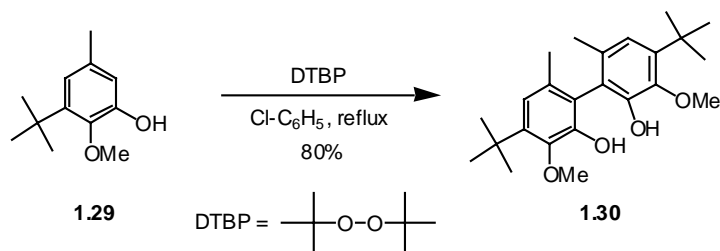
Scheme 1.7. Stagliano's Aryl-Quinone Coupling.



Aryl-aryl bond formation has also been used widely in synthetic chemistry, and is a valuable tool for the formation of a variety of biaryl compounds. A wide variety of methods are available for such transformations, including Suzuki coupling, Stille coupling, and oxidative coupling.⁹ Suzuki and Stille aryl-aryl couplings are closely

related to the aryl-quinone couplings previously discussed. These conditions may be used for the coupling of aryl-halides with aryl-boronic acids and aryl-stannanes, respectively. Another viable route to the formation of biaryl bonds is oxidative coupling. Bringmann and Tasler have shown that dimerization of phenols may occur under oxidative conditions, despite bis-ortho substitution at the coupling site.¹¹ Bringmann used di-*tert*-butyl peroxide (DTBP) as an oxidizing agent for the dimerization of the phenol **1.29** to provide the biaryl complex **1.30** in 80% yield, as shown in Scheme 1.8.¹¹ There is a variety of alternative oxidants available for oxidative coupling such as Cu(II)¹² salts, Pb(OAc)₄, Ag₂O, FeCl₃, a variety of hyper-valent iodine reagents, O₂ and others.¹¹ There is also a variety of possible mechanisms for this type of reaction, and they are widely based on the nature of the substrate. In general two electrons and two protons are removed from the substrates during the oxidation, the location of which is based on the functionality found on the aromatic ring.¹³

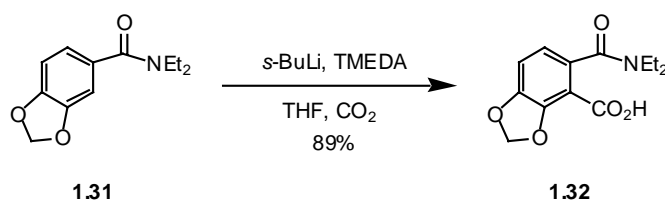
Scheme 1.8. Bringmann's Oxidative Coupling of Phenols.



1.5 Literature Precedent for Directed ortho Metalations

Directed ortho metalation (DoM) reactions have been widely used in the synthesis of highly substituted aromatic rings. The directing metalation group (DMG), a Lewis base, coordinates to an alkyl lithium and directs the deprotonation of the aromatic ring to the ortho position of the DMG.¹⁴ Once deprotonation occurs, the reaction may be quenched with a variety of electrophiles, such as CO₂, TMS-Cl, acid chlorides, DMF, and alkyl halides.¹⁵ Strong alkyl lithium bases are the preferred bases for DoM reactions, and are usually used in combination with a bidentate ligand such as TMEDA. TMEDA helps break the aggregates of alkyl lithiums into monomers and dimers, thereby making them stronger and more reactive bases.¹⁴ One example of DoM reactions reported by Snieckus is shown in Scheme 1.9.¹⁵ In this reaction, *s*-BuLi is added to the benzamide **1.31** at -78°C and quenched with CO₂ to give the benzoic acid **1.32** in 89% yield.

Scheme 1.9. Example of Directed ortho Metallation Reaction.



In summary, we propose a synthesis of hibarimicinone (**1.6**) and HMP-Y1 (**1.10**). We have chosen to use aryl-quinone, aryl-aryl bond formation, and directed ortho metallations in order to synthesize the target compounds. These types of reactions are

well preceded in the literature and provide ample methods for the eventual synthesis of hibarimicinone (**1.6**) and HMP-Y1 (**1.10**).

CHAPTER II

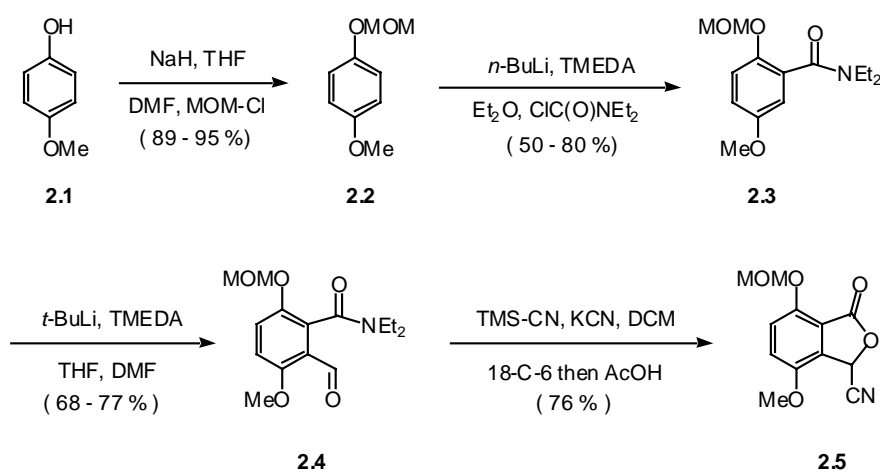
SYNTHETIC PROGRESS TOWARD THE AB AND GH RING

SYSTEM OF HIBARIMICINONE AND HMP-Y1

2.1 Synthetic Progress Toward Hibarimicinone (1.6): Model Study

As illustrated in the retrosynthetic analysis of hibarimicinone (**1.6**), Scheme 1.2, a Hauser annulation between the cyanophthalide **1.19** and the enone **1.20** will be used to construct the EFGH ring system. A model study was performed in order to test the viability of the Hauser annulation and the subsequent reactions necessary to complete the EFGH fragment of hibarimicinone (**1.6**). The model study initially consisted of the synthesis of the known cyanophthalide **2.5** from commercially available *p*-methoxy phenol **2.1** as outlined in Scheme 2.1.

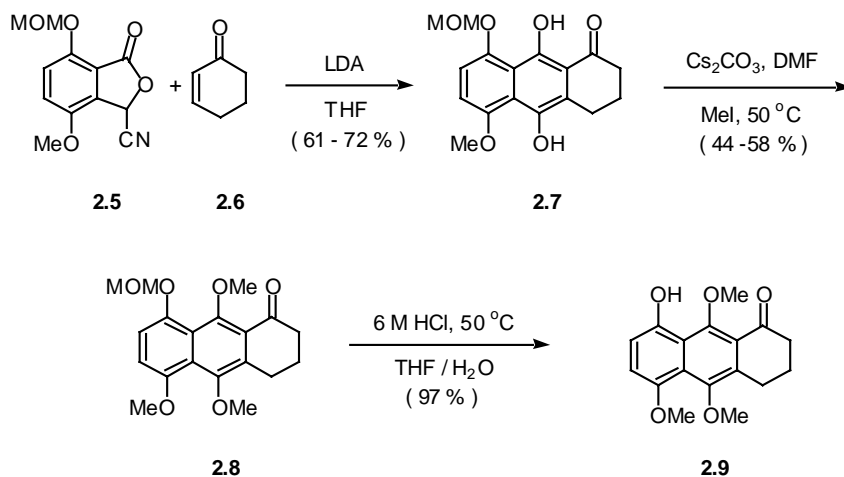
Scheme 2.1. Synthesis of the known cyanophthalide **2.5**.



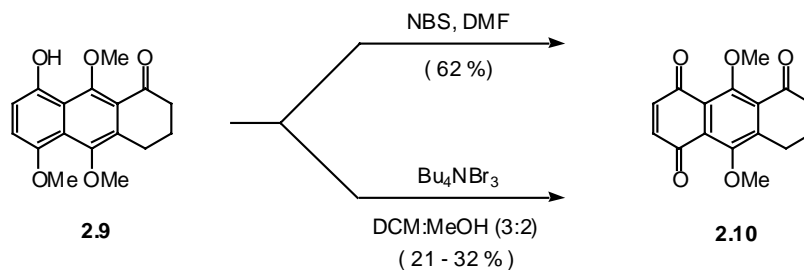
Commercially available *p*-methoxyphenol **2.1** was protected using NaH and MOM-Cl in 89 - 95% yield.¹⁶ The resulting MOM protected phenol **2.2** underwent a DoM reaction using *n*-BuLi and TMEDA followed by quenching with diethylcarbonyl chloride to afford the aryl amide **2.3** in 50 - 80% yield.¹⁵ This compound was then subjected to a second DoM reaction using *t*-BuLi, TMEDA, and quenching with DMF to afford the formylated compound **2.4** in yields ranging from 68 to 77%.¹⁵ The formylated product **2.4** underwent a lactonization using a combination of TMS-CN, KCN, and 18-crown-6 followed by stirring in AcOH to afford the cyanophthalide **2.5** in 76% yield.¹⁷

With the cyanophthalide **2.5** in hand, we investigated the Hauser annulation with commercially available 2-cyclohexen-1-one **2.6** using LDA as the base which provided the dihydroquinone (**2.7**) in 61 - 72% yield,¹⁸ (Scheme 2.2). The dihydroquinone **2.7** was then methylated using Cs₂CO₃ and MeI to provide the tricycle **2.8** in 44 - 58% yield.¹⁹ Upon treatment of **2.8** with 6 M HCl the free phenol **2.9** was obtained in 97% yield.²⁰ Surprisingly, in our attempt to perform an ortho-bromination reaction on phenol **2.9** using either NBS²¹ or Bu₄NBr₃²² we observed no halogen incorporation. The only observed product was the quinone **2.10**, as determined by NMR analysis, resulting from oxidation of the free phenol, Scheme 2.3.

Scheme 2.2. Synthesis of phenol **2.9**.



Scheme 2.3. Synthesis of quinone **30**.



This model study provided valuable information for the synthesis of the EFGH ring system of hibarimicinone (**1.6**). Specifically, we developed reaction conditions for the key Hauser annulation for our synthesis. We also determined that a second route must be developed in order to incorporate the halide/metal functional group, necessary for the coupling of the tetracycles **1.14** and **1.15**, prior to deprotection of the phenol.

Finally, the model study showed us that oxidation of the terminal aromatic ring should be the preferred ring for oxidation over the internal aromatic ring.

2.2 Synthetic Progress Toward HMP-Y1 (1.10): Cross-Coupling Approach

Examination of the retrosynthetic analysis for hibarimicinone (**1.6**) and HMP-Y1 (**1.10**), shown in Schemes 1.2 and 1.3, reveals that the ABCD tetracycle is a common intermediate that may be used in the synthesis of both of these target structures. This intermediate will be derived from lactone **2.11** (Figure 2.1).

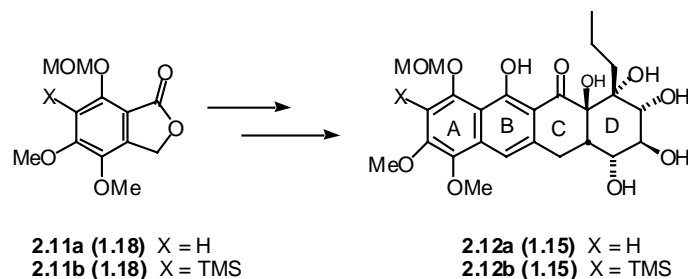


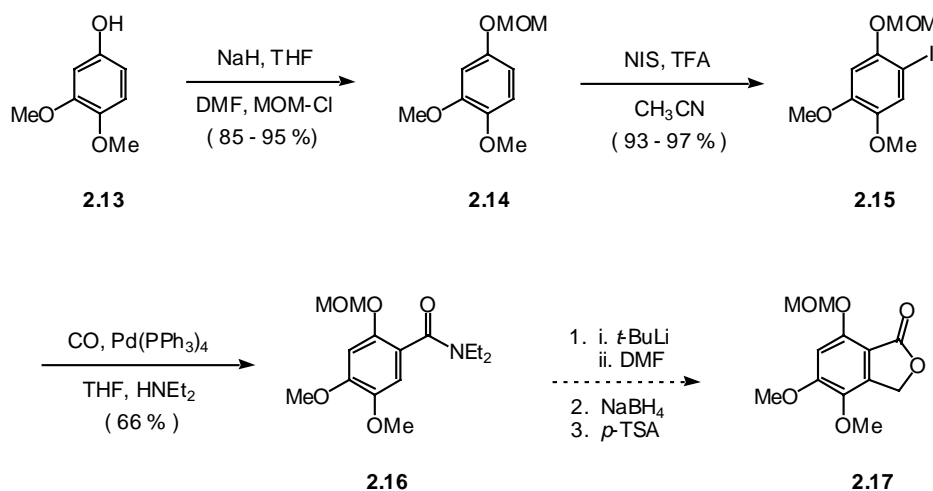
Figure 2.1. Common intermediate in the synthesis of hibarimicinone (**1.6**) and HMP-Y1 (**1.10**).

We have examined the synthesis of intermediates **2.11a** and **2.11b**. For **2.11a** the synthesis starts from 3,4 dimethoxy phenol **2.13** which was alkylated to yield MOM ether **2.14** in 85 -95% yield, (Scheme 2.4).¹⁶ The MOM ether **2.14** was treated with NIS and a catalytic amount of TFA in CH₃CN to afford the aryl iodide **2.15** in 93 - 97% yield.²³ The aryl iodide was then subjected to a carbonylation reaction using Pd(PPh₃)₄

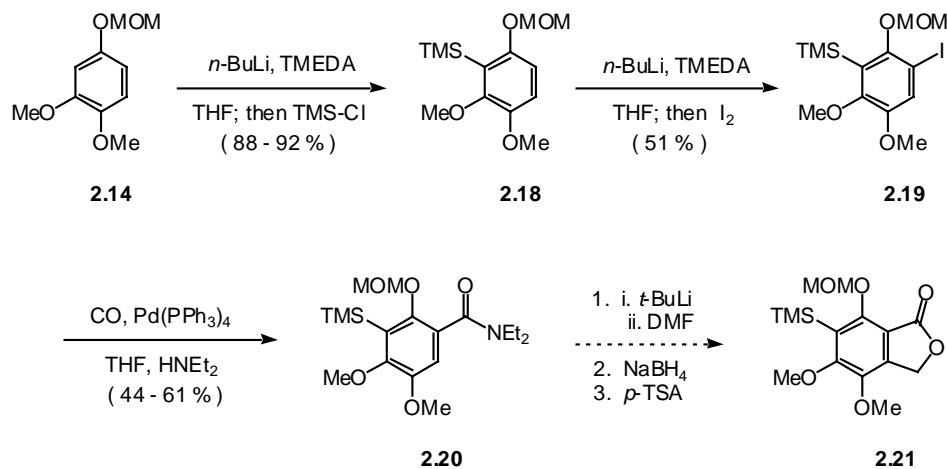
as a catalyst in THF containing fifteen equivalents of diethylamine under 1 atm of CO to afford the aryl amide **2.16** in 66% yield.²⁴ We anticipate formylation using DoM methodology followed by reduction of the formyl group and cyclization are necessary to synthesize lactone **2.11a**. This work is currently under investigation in our laboratory.

In addition to the synthetic work developed in connection with lactone **2.11a** we have also worked toward intermediate **2.11b**, (Scheme 2.5). The MOM ether **2.14** was treated with *n*-BuLi and TMEDA followed by a TMS-Cl quench to furnish the aryl silane **2.18** in 88 - 92% yield.¹⁵ The aryl silane **2.18** underwent another DoM reaction using *n*-BuLi and TMEDA, and quenching with iodine to furnish the aryl iodide **2.19** in 51% yield.¹⁵ The aryl iodide **2.19** underwent a carbonylation reaction using the previously described carbonylation conditions to afford the aryl amide **2.20** in 44 - 61% yield.²⁴ The formylation, reduction of the resulting aldehyde, and cyclization are currently under investigation in our laboratory.

Scheme 2.4. Synthetic Work Toward lactone **2.11a**.



Scheme 2.5. Synthetic Work Toward lactone **2.11b**.

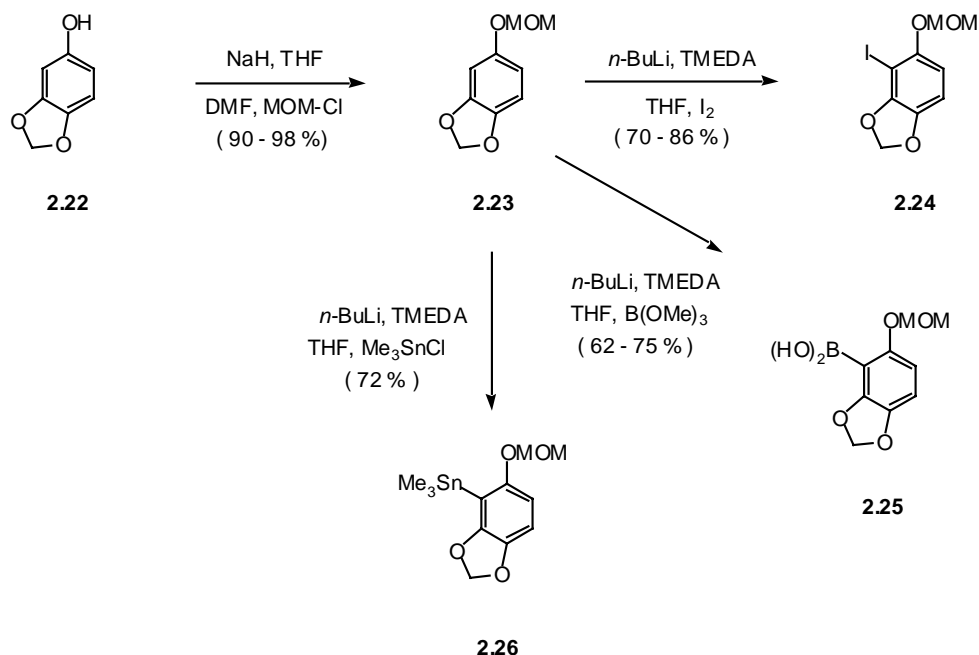


2.3 Synthetic Work Toward HMP-Y1 (1.10): Bi-Directional Approach

In addition to the work previously discussed, we have investigated an alternate strategy for the synthesis of HMP-Y1 (**1.10**). This strategy involves the formation of the central aryl-aryl bond then utilizing a bi-directional approach to the synthesis of HMP-Y1 (**1.10**), as shown in Scheme 1.4. Sesamol derivatives were used for a model study to investigate the coupling chemistry needed to construct the central aryl-aryl bond. The synthesis of these sesamol derivatives are summarized in Scheme 2.6. Sesamol **2.22** was MOM protected using NaH and MOM-Cl to afford the protected phenol **2.23** in 90 - 98% yield.¹⁶ The MOM protected phenol **2.23** was treated with *n*-BuLi and TMEDA followed by quenching with I₂ to afford the aryl iodide **2.24** in 70 - 86% yield.¹⁵ Similarly, when the MOM ether **2.23** was subjected to *n*-BuLi and TMEDA, quenching with B(OMe)₃ the boronic acid **2.25** was achieved in 62 - 75% yield.¹⁵ Utilizing the

same deprotonation conditions and quenching with Me_3SnCl , the aryl stannane **2.26** was achieved in 72% yield.¹⁵

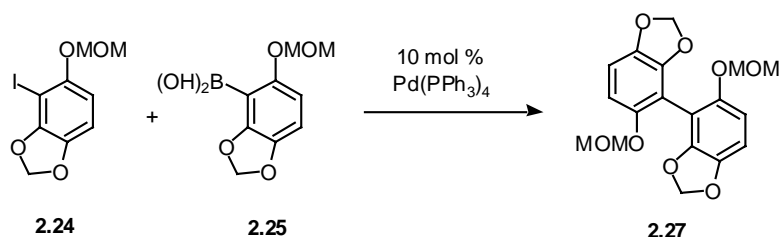
Scheme 2.6. Synthesis of Sesamol Derivatives.



With the aryl iodide **2.24** and the boronic acid **2.25** in hand, we investigated the Suzuki coupling reaction of these two substrates to afford the coupled biaryl complex **2.27**. A variety of conditions were investigated and summarized in Table 2.1.^{25,26} The best yield for the Suzuki coupling reaction of the aryl iodide **2.24** with the boronic acid **2.25** was achieved when Na_2CO_3 was used as the base at room temperature in a solution of DMF : H_2O (9:1).²⁵ However, optimal conditions required 5.0 equivalents of the boronic acid **2.25** and afforded the coupled product **2.27** in only 30% yield. In addition,

Suzuki coupling reaction also requires the synthesis of two structurally distinct substrates. Collectively, this information persuaded us to investigate another synthetic route to biaryl **2.27**.

Table 2.1. Conditions for Suzuki Coupling Reaction.

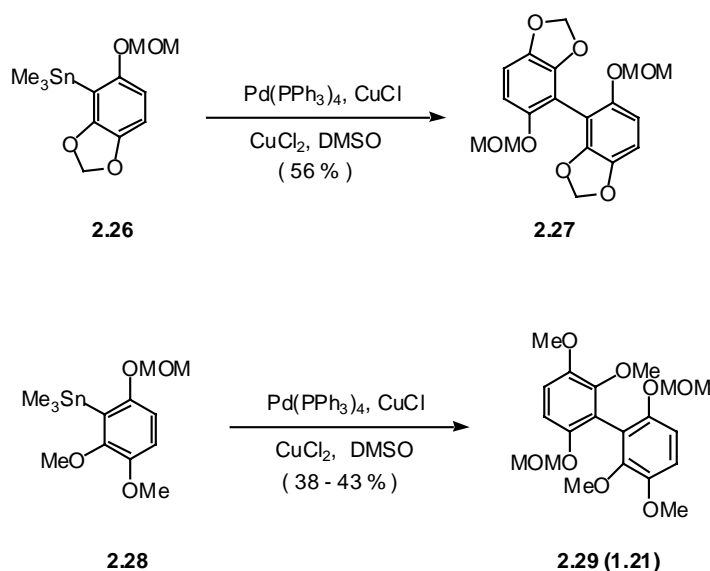


Base	Temp	Solvent	Eq. Boronic Acid	Yield
NaOH (4 eq.)	rt	DMF:H ₂ O (9 : 1)	2	4 %
TIOEt (1.8 eq.)	rt	THF:H ₂ O (3 : 1)	2	No Rxn
NaOH (5 eq.)	rt	DMF:H ₂ O (9 : 1)	5	28 %
NaOH (5 eq.)	50 °C	DMF:H ₂ O (9 : 1)	5	8 %
TIOEt (5 eq.)	rt	DMF:H ₂ O (9 : 1)	5	Trace
Na ₂ CO ₃ (5 eq.)	rt	DMF:H ₂ O (9 : 1)	5	30 %

In 1999, Corey and co-workers developed a new dimerization method using $\text{Pd}(\text{PPh}_3)_4$ as a catalyst, CuCl , and CuCl_2 , in a solution of DMSO.²⁷ When the aryl stannane **2.26** was subjected to these conditions, the dimerized product **2.27** was

obtained in 56% yield, (Scheme 2.7).²⁷ However, when the aryl stannane **2.28** was subjected to these conditions a diminished yield of 38 - 43% of the dimerized product **2.29** was achieved. One possible explanation for this occurrence is that the free methoxy groups add more steric hinderance at the coupling site, compared to the less sterically hindered sesamol derivative.

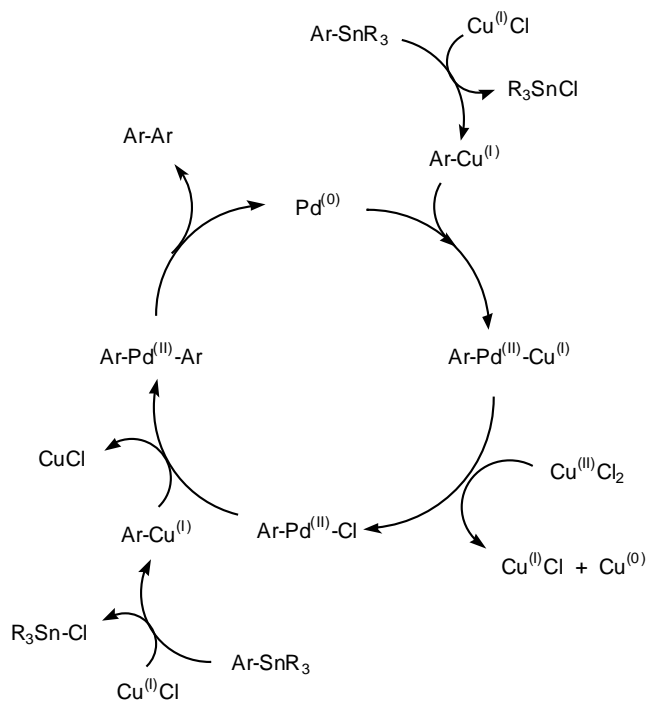
Scheme 2.7. Corey Conditions for Dimerization Reaction.



Corey did not propose a mechanism for the dimerization of the aryl-stannane. A possible mechanism is shown in Scheme 2.8. The first step in the proposed mechanism is a transmetalation of the aryl group, with loss of R_3SnCl , followed by an oxidative addition of the $\text{Pd}(0)$ into the resulting aryl-Cu bond. A ligand exchange then occurs replacing the Cu ligand with a chloride, with the reduction of CuCl_2 to CuCl . The

palladium inserts into a second Ar-Cu bond with loss of CuCl to afford the Ar-Pd-Ar complex, which then undergoes a reductive elimination to afford the biaryl product and recycle the Pd(II) to Pd(0), which may then repeat the cycle.

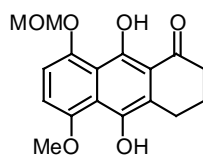
Scheme 2.8. Proposed Mechanism for the Corey Dimerization.



This comprises the work done to date on the previously mentioned target structures in our synthesis of hibarimicinone (**1.6**) and HMP-Y1 (**1.10**). Further research toward the completion of these target compounds is currently under investigation in our laboratories.

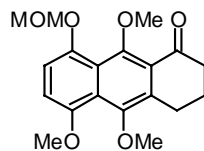
2.4 Experimental Section

Materials and Methods. All reactions were carried out under an argon atmosphere using dry glassware which had been flame-dried *in vacuo* unless otherwise noted. Diethyl amine, TMEDA, and diisopropyl amine were all distilled from CaH₂ and stored over KOH prior to use. Reactions were monitored by thin-layer chromatography using 0.25-mm E. Merck precoated silica gel plates. Visualization was accomplished with UV light and aqueous potassium permanganate solution or aqueous phosphomolybdic acid solution as a stain followed by charring on a hot plate. Purification was accomplished using flash liquid chromatography with the stated solvents using silica gel 60 (particle size 0.040-0.063 mm). All yields correspond to chromatographically and spectroscopically pure compounds unless otherwise noted. Unless otherwise stated, melting points are uncorrected values. ¹H and ¹³C NMR spectra were obtained from a Varian-300 or 500 spectrometers at ambient temperature. ¹H and ¹³C NMR are reported using δ values relative to CDCl₃ unless otherwise noted. Infrared spectra were recorded using a Nicolet Impact 410 spectrometer. Low and High-resolution mass spectra were obtained from the Texas A&M University Mass Spectrometry Service Center on a PE Sciex Qstar Electrospray Ionization (ESI) mass spectrometer.

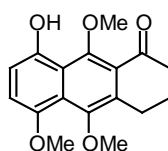


2.7

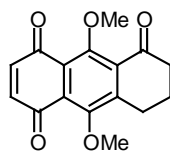
Dihydroquinone 2.7. To a solution of diisopropyl amine (0.13 mL, 0.93 mmol) in THF (3 mL) was added *n*-BuLi (0.58 mL of a 1.6 M solution in hexanes, 0.93 mmol) dropwise at $-78\text{ }^{\circ}\text{C}$. The resulting solution was stirred at $-78\text{ }^{\circ}\text{C}$ for 0.5 h and **2.5** (116 mg, 0.467 mmol) in THF (4 mL) was added dropwise. The reaction mixture was stirred at $-78\text{ }^{\circ}\text{C}$ for 1 h. 2-cyclohexen-1-one **2.6** (45 μL , 0.47 mmol) was added dropwise to the reaction at $-78\text{ }^{\circ}\text{C}$ and the mixture was stirred at $21\text{ }^{\circ}\text{C}$ for 25 min. Water (5 mL) was added and the aqueous layer extracted with EtOAc (3 x 5 mL), dried (MgSO_4), concentrated *in vacuo* and the residue was purified by flash liquid chromatography (2:1 hexane : EtOAc) to afford 88 mg of **2.7** (61 %) as an orange solid: mp $126\text{-}130\text{ }^{\circ}\text{C}$ (DCM); IR (CH_2Cl_2) $3452, 1660, 1527\text{ cm}^{-1}$; ^1H NMR (500 MHz, CDCl_3) δ 9.45 (s, 1H), 6.98 (d, $J = 8.5\text{ Hz}$, 1H), 6.90 (d, $J = 9\text{ Hz}$, 1H), 5.24 (s, 2H), 4.02 (s, 3H), 3.60 (s, 3H), 2.98 (t, $J = 6.5\text{ Hz}$, 2H), 2.73 (t, $J = 6.5\text{ Hz}$, 2H), 2.09 (m, 2H), -1.71 (s, 1H); ^{13}C NMR (126 MHz, CDCl_3) δ 205.8, 157.2, 151.6, 150.9, 141.6, 121.3, 121.0, 118.1, 113.8, 112.7, 109.9, 97.6, 57.2, 56.7, 39.4, 23.1, 22.2; HRMS (ESI) m/z 325.1222 $[(\text{M} + \text{Li})^+]$, calcd for $\text{C}_{17}\text{H}_{18}\text{O}_6$ 325.1263].

**2.8**

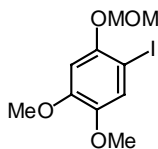
Tricycle 2.8. To a solution of **2.7** (212 mg, 0.688 mmol) in DMF (24 mL) was added Cs₂CO₃ (1.2 g, 3.4 mmol) followed by iodomethane (0.86 mL, 14 mmol). The resulting mixture was heated at 50 °C for 22 h. Water (30 mL) was added and the aqueous layer extracted with EtOAc (3 x 50 mL), washed with water (2 x 30 mL) and brine (30 mL), dried (MgSO₄), concentrated *in vacuo* and the residue was purified by flash liquid chromatography (2 :1 hexane : EtOAc) to afford 100 mg of **2.8** (44 %) as an orange solid: mp 77-82 °C (DCM); IR (CH₂Cl₂) 2926, 1652 cm⁻¹; ¹H NMR (500 MHz, CDCl₃) δ 7.06 (d, *J* = 8.5 Hz, 1H), 6.88 (d, *J* = 8.5 Hz, 2H), 5.15 (s, 2H), 3.95 (s, 3H), 3.89 (s, 3H), 3.75 (s, 3H), 3.58 (s, 3H), 3.09 (t, *J* = 10 Hz, 2H), 2.68 (t, *J* = 10 Hz, 2H), 2.07 (m, 2H); ¹³C NMR (126 MHz, CDCl₃) δ 198.3, 154.8, 151.6, 149.1, 149.1, 133.1, 125.4, 124.8, 123.4, 115.7, 109.6, 98.2, 63.5, 61.8, 57.1, 56.7, 41.3, 23.9, 22.5; HRMS (ESI) *m/z* 347.1387 [(M + H)⁺, calcd for C₁₉H₂₂O₆ 347.1495].

**2.9**

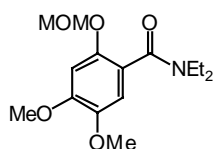
Phenol 2.9. To a solution of **2.8** (8.8 mg, 0.026 mmol) in THF (0.9 mL) was added water (0.36 mL) and 6M HCl (0.92 mL). The resulting solution was heated at 50 °C for 4.5 h. The reaction was then poured into brine (3 mL), extracted with EtOAc (3 x 3 mL), dried (MgSO₄), concentrated *in vacuo*, and the residue was purified by flash liquid chromatography (2 :1 hexane : EtOAc) to afford 7.5 mg of **2.9**, (97 %) as an orange solid: mp 114-117 °C (DCM); IR (CH₂Cl₂) 3432, 1650, 1521 cm⁻¹; ¹H NMR (500 MHz, CDCl₃) δ 9.88 (s, 1H), 6.98 (d, *J* = 8.5 Hz, 1H), 6.83 (d, *J* = 9 Hz, 1H), 4.00 (s, 3H), 3.94 (s, 3H), 3.78 (s, 3H), 3.13 (t, *J* = 6 Hz, 2H), 2.71 (t, *J* = 6.5 Hz, 2H), 2.11 (m, 2H); ¹³C NMR (126 MHz, CDCl₃) δ 197.7, 155.2, 150.6, 149.7, 148.4, 132.6, 124.6, 121.4, 118.7, 113.0, 110.8, 64.6, 61.8, 57.8, 41.3, 24.0, 22.4; HRMS (ESI) *m/z* 303.1246 [(M + H)⁺, calcd for C₁₇H₁₈O₅ 303.1232].

**2.10**

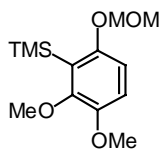
Quinone 2.10. To a solution of **2.9** (22.3 mg, 0.075 mmol) in DMF (1.5 mL), was added NBS (14.6 mg, 0.082 mmol) at 0 °C and the reaction was allowed to warm to 21 °C over 7 h. Water (3 mL) was added and aqueous layer was extracted with EtOAc (3 x 3 mL), washed with water (2 x 3 mL) and brine (3 mL), dried (MgSO₄), concentrated *in vacuo*, and the residue was purified by flash liquid chromatography (4 :1 hexane : EtOAc) to afford 13 mg of **2.10** (62 %) as an orange solid: mp 163-167 °C (DCM); IR (CH₂Cl₂) 2969, 1644, 1604 cm⁻¹; ¹H NMR (500 MHz, CDCl₃) δ 6.87 (d, *J* = 10Hz, 1H), 6.85 (d, *J* = 10.5 Hz, 1H), 3.95 (s, 3H), 3.87 (s, 3H), 3.05 (t, *J* = 6 Hz, 2H), 2.70 (t, *J* = 6 Hz, 2H), 2.13 (m, 2H); ¹³C NMR (126 MHz, CDCl₃) δ 196.2, 184.5, 183.6, 157.1, 153.7, 148.8, 139.6, 138.2, 134.1, 128.0, 125.2, 63.7, 62.0, 40.4, 24.3, 22.0; HRMS (ESI) *m/z* 287.0923 [(M + H)⁺, calcd for C₁₆H₁₄O₅ 287.0919].

**2.15**

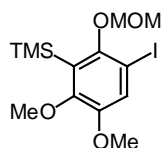
Aryl-Iodide 2.15. To a solution of NIS (101 mg, 0.451 mmol) and TFA (0.010 mL, 12 mmol) in CH₃CN (0.64 mL) was added **2.14** (81.2 mg, 0.410 mmol) in CH₃CN (1 mL) at 21 °C. The reaction stirred at 21 °C for 2 h and was poured into saturated NaHCO₃ (2mL), the aqueous layer was extracted with EtOAc (3 x 5 mL), washed with saturated Na₂S₂O₃ (3 mL) and brine (3 mL), dried (MgSO₄), concentrated *in vacuo* and the residue was purified by flash chromatography (4:1 hexane : EtOAc) to afford 0.12 g of **2.15** (93 %) as a dark pink solid: mp 67-70 °C (DCM); IR (CH₂Cl₂) 2949, 1577, 1498 cm⁻¹; ¹H NMR (500 MHz, CDCl₃) δ 7.19 (s, 1H), 6.76 (s, 1H), 5.17 (s, 2H), 3.87 (s, 3H), 3.84 (s, 3H), 3.55 (s, 3H); ¹³C NMR (126 MHz, CDCl₃) δ 151.1, 150.3, 145.5, 121.5, 101.6, 96.4, 74.8, 56.8, 56.7, 56.3; HRMS (ESI) *m/z* 331.0020 [(M + Li)⁺ calcd for C₁₀H₁₃O₄I 331.0019].

**2.16**

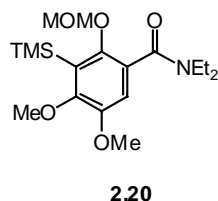
Aryl-Amide 2.16. A flask containing Pd(PPh₃)₄ (769 mg, 0.666 mmol) was purged with CO, and **2.15** (360 mg, 1.11 mmol) in THF (11 mL) and then HNEt₂ (1.7 mL, 17 mmol) were then added at 21 °C. Carbon monoxide was bubbled into the reaction mixture for 20 min and the reaction was stirred at 21 °C for 22 h under 1 atm of CO. The reaction was diluted with Et₂O (30 mL), filtered through a plug of silica gel, concentrated *in vacuo* and the residue was purified by flash chromatography (1:2 hexane : EtOAc) to afford 0.22 g of **2.16** (66 %) as a light orange solid: mp 81-81 °C (CH₂Cl₂); IR (CH₂Cl₂) 2941, 1664, 1551 cm⁻¹; ¹H NMR (500 MHz, CDCl₃) δ 7.47 (s, 1H), 6.77 (s, 1H), 5.13 (s, 2H), 3.95 (s, 3H), 3.91 (s, 3H), 3.51 (q, *J* = 7.0 Hz, 2H), 3.51 (s, 3H), 3.26 (q, *J* = 7.0 Hz, 2H), 1.27 (t, *J* = 7.9 Hz, 3H), 1.20 (t, *J* = 7.0 Hz, 3H); ¹³C NMR (126 MHz, CDCl₃) δ 189.3, 168.7, 156.0, 155.0, 144.9, 111.2, 99.6, 95.7, 56.6, 56.5, 56.4, 41.9, 38.5, 13.7, 13.0; LRMS (ESI) *m/z* 298 [(M + H)⁺, calcd for C₁₅H₂₃NO₅ 298].

**2.18**

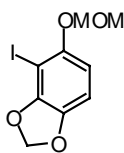
Aryl-Silane 2.18. To a solution of **2.14** (434 mg, 2.19 mmol) and TMEDA (0.36 mL, 2.4 mmol) in THF (5.5 mL) at 0 °C was added *n*-BuLi (0.91 mL of a 2.6 M solution of hexanes, 2.4 mmol) dropwise. The ice bath was removed and the reaction mixture stirred at 21 °C for 1 h. The mixture was then cooled to 0 °C and trimethylsilyl chloride (0.84 mL, 6.6 mmol) was added and the mixture was allowed to warm to 21 °C over 3.5 h. The reaction was then diluted with water (10 mL) and the aqueous layer extracted with EtOAc (3 x 10 mL), dried (MgSO₄), concentrated *in vacuo* and the residue was purified by flash chromatography (20:1 hexane : EtOAc) to afford 0.52 g **2.18** (88 %) as light yellow oil: IR (CH₂Cl₂) 2950, 1583, 1465 cm⁻¹; ¹H NMR (500 MHz, CDCl₃) δ 6.85 (d, *J* = 8.5 Hz, 1H), 6.79 (d, *J* = 8.5 Hz, 1H), 5.10 (s, 2H), 3.82 (s, 3H), 3.80 (s, 3H), 3.47 (s, 3H), 0.34 (s, 9H); ¹³C NMR (126 MHz, CDCl₃) δ 156.3, 154.6, 147.8, 122.1, 114.7, 108.9, 94.8, 61.1, 56.4, 56.1, 1.6; HRMS (ESI) *m/z* 277.1442 [(M + Li)⁺. Calcd for C₁₃H₂₂O₄Si 277.1447].

**2.19**

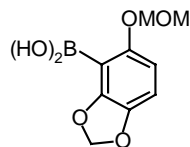
Aryl-Iodide 2.19. To a solution of **2.18** (488 mg, 1.80 mmol) and TMEDA (0.30 mL, 2.0 mmol) in THF (9 mL) at 0 °C was added *n*-BuLi (0.84 mL of a 2.36 M solution in hexanes, 2.0 mmol) dropwise. The ice bath was removed and the mixture stirred at room temperature for 2 h. Iodine (503 mg, 1.98 mmol) in THF (5.8 mL) was added at 0 °C and the reaction mixture was allowed to warm to 21 °C over 2.5 h. The reaction was then poured into saturated Na₂S₂O₃ (10 mL), extracted with EtOAc (3 x 10 mL), washed with brine (10 mL), dried (MgSO₄), concentrated *in vacuo* and the residue was purified by flash chromatography (20:1 hexane : EtOAc) to afford 0.36 g **2.19** (50 %) as an orange oil: IR (CH₂Cl₂) 2940, 1646 cm⁻¹; ¹H NMR (300 MHz, CDCl₃) δ 7.30 (s, 1H), 4.93 (s, 2H), 3.84 (s, 3H), 3.83 (s, 3H), 3.62 (s, 3H), 0.35 (s, 9H); ¹³C NMR (126 MHz CDCl₃) δ 155.1, 153.8, 149.9, 128.2, 124.4, 100.7, 84.8, 61.0, 58.9, 56.3, 1.7; HRMS (ESI) *m/z* 403.0423 [(M + Li)⁺, calcd for C₁₃H₂₁IO₄Si 403.0414].



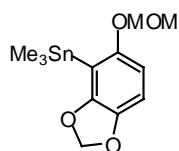
Aryl-Amide 2.20. A flask containing Pd(PPh₃)₄ (61 mg, 0.052 mmol) was purged with CO, and **2.19** (35 mg, 0.087 mmol) in THF (0.87 mL) and HNEt₂ (0.14 mL, 1.3 mmol) were then added at 21 °C. Carbon monoxide was bubbled into the reaction for 20 min and the reaction stirred at 21 °C overnight under 1 atm CO. The solution was diluted with Et₂O (3 mL), filtered through a silica plug, concentrated *in vacuo* and the residue was purified by flash chromatography (3 :1 hexane : EtOAc) to afford 20 mg of **2.20** (60 %) as a thick orange oil: IR (CH₂Cl₂) 2940, 1646 cm⁻¹; ¹H NMR (500 MHz, CDCl₃) δ 7.34 (s, 1H), 4.94 (s, 2H), 3.94 (s, 3H), 3.86 (s, 3H), 3.51 (q, *J* = 7.0 Hz, 2H), 3.34 (s, 3H), 3.25 (q, *J* = 7.0 Hz, 2H), 1.25 (t, *J* = 7.0 Hz, 3H), 1.16 (t, *J* = 7.0 Hz, 3H), 0.35 (s, 9H); ¹³C NMR (126 MHz, CDCl₃) δ 190.3, 167.4, 160.2, 157.7, 148.8, 123.3, 116.0, 102.3, 61.1, 58.6, 56.1, 42.3, 38.8, 14.0, 12.7, 1.6; HRMS (ESI) *m/z* 370.2081 [(M + H)⁺, calcd for C₁₈H₃₁NO₅Si 370.2050].

**2.24**

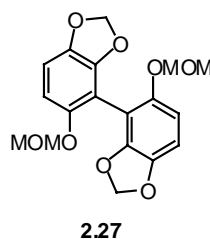
Aryl-iodide 2.24. To a solution of **2.23** (507 mg, 2.79 mmol) and TMEDA (0.46 mL, 3.1 mmol) in THF (7 mL) at 0 °C was added *n*-BuLi (1.3 mL in a 2.4 M solution of hexanes, 3.1 mmol) dropwise. The ice bath was removed and the reaction mixture stirred at 21 °C for 13 min and then cooled to 0 °C. Iodine (1.42 g, 5.58 mmol) in THF (7 mL) was added dropwise. The mixture was allowed to warm to 21 °C over 4.5 h. The reaction mixture was poured into saturated Na₂S₂O₃ (10 mL) and the aqueous layer extracted with EtOAc (3 x 10 mL) dried (MgSO₄), concentrated *in vacuo* and the residue was purified by flash chromatography (10:1 hexane : EtOAc) to afford 0.74 g **2.24** (86 %) as a pink solid: mp 56-58 °C (CH₂Cl₂); IR (CH₂Cl₂) 2900, 1613, 1454 cm⁻¹; ¹H NMR (500 MHz, CDCl₃) δ 6.69 (d, *J* = 8.5 Hz, 1H), 6.56 (d, *J* = 8.5 Hz, 1H), 6.02 (s, 2H), 5.16 (s, 2H), 3.53 (s, 3H); ¹³C NMR (126 MHz, CDCl₃) δ 151.6, 150.5, 141.8, 108.3, 107.9, 107.7, 101.2, 96.3, 56.7; HRMS (ESI) *m/z* 314.9714 [(M + Li)⁺, calcd for C₉H₉IO₄ 314.9706].

**2.25**

Boronic Acid 2.25. To a solution of **2.23** (1.10 g, 6.05 mmol) and TMEDA (1.0 mL, 6.7 mmol) in THF (15 mL) at 0 °C was added *n*-BuLi (2.8 mL in a 2.4 M solution of hexanes, 6.7 mmol) dropwise. The ice bath was removed and the reaction mixture stirred at 21 °C for 13 min and then cooled to 0 °C. Trimethyl borate (3.4 mL, 30 mmol) was added and the reaction mixture was allowed to warm to 21 °C over 3 h. Water (15 mL) was added and the aqueous layer was extracted with EtOAc (3 x 15 mL), dried (MgSO₄), concentrated *in vacuo* and the residue was purified by flash chromatography (4:1 to 2:1 hexane : EtOAc) to afford 0.95 g **2.25** (70 %) as a gray solid: mp 71-74 °C (CH₂Cl₂); IR (CH₂Cl₂) 3432, 1634, 1460 cm⁻¹; ¹H NMR (500 MHz, CDCl₃) δ 6.84 (d, *J* = 14 Hz, 1H), 6.63 (d, *J* = 14 Hz, 1H), 6.31 (s, 2H), 6.03 (s, 2H), 5.23 (s, 2H), 3.51 (s, 3H); ¹³C NMR (126 MHz, CDCl₃) δ 156.6, 153.3, 142.1, 111.1, 106.5, 101.7, 96.7, 95.0, 56.7; HRMS (ESI) *m/z* 249.0563 [(M + Na)⁺, calcd for C₉H₁₁BO₆ 249.0546].

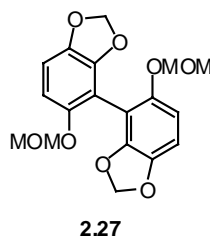
**2.26**

Aryl-Stannane 2.26. To a solution of **2.23** (1.02 g, 5.61 mmol) and TMEDA (0.93 mL, 6.2 mmol) in THF (14 mL) at 0 °C was added *n*-BuLi (2.8 mL of a 2.2 M solution in hexanes, 6.2 mmol) dropwise. The ice bath was removed and the reaction mixture was stirred at 21 °C for 13 min and then cooled to 0 °C. Trimethyltin chloride (11 mL, of a 1 M solution in THF, 11 mmol) was added and the reaction was allowed to warm to room temperature over 4 h. Water (15 mL) was added and the aqueous layer was extracted with EtOAc (3 x 15 mL), dried (MgSO₄), concentrated *in vacuo* and the residue was purified by flash chromatography (10:1 hexane : EtOAc) to afford 1.4 g **2.26** (72 %) as yellow oil: IR (CH₂Cl₂) 2904, 1624, 1434 cm⁻¹; ¹H NMR (500 MHz, CDCl₃) δ 6.68 (d, *J* = 8 Hz, 1H), 6.50 (d, *J* = 8 Hz, 1H), 5.87 (s, 2H), 5.08 (s, 2H), 3.46 (s, 3H), 0.35 (s, 9H); ¹³C NMR (126 MHz, CDCl₃) δ 157.2, 154.0, 141.4, 110.5, 108.5, 104.8, 100.4, 95.1, 56.1, -7.7; HRMS (ESI) *m/z* 353.0403 [(M + Li)⁺, calcd for C₁₂H₁₈O₄Sn 353.0387].

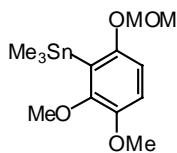


Example Procedure for Synthesis of Biaryl 2.27 Using Suzuki Conditions.

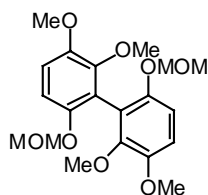
To a solution of **2.24** (36 mg, 0.12 mmol), **2.25** (132 mg, 0.586 mmol), and Pd(PPh₃)₄ (14 mg, 0.012 mmol) in DMF:H₂O (9:1) (0.5 mL) was added Na₂CO₃ (62 mg, 0.59 mmol) at 21 °C. The reaction mixture was stirred at room temperature for 2 d. The solution was diluted with Et₂O (3 mL) and the resulting mixture was filtered through a plug of silica gel, washed with water (3 x 3 mL) and then brine (3 mL), dried (MgSO₄), concentrated *in vacuo* and the residue was purified by flash chromatography (4:1 hexane : EtOAc) to afford 14 mg **2.27** (33 %) of an orange oil: IR (CH₂Cl₂) 2922, 1639, 1445 cm⁻¹; ¹H NMR (500 MHz, CDCl₃) δ 6.77 (d, *J* = 8.5 Hz, 1H), 6.70 (d, *J* = 8.5 Hz, 1H), 5.95 (d, *I* = 1.5 Hz, 1H), 5.93 (d, *J* = 1.5 Hz, 1H), 5.01 (d, *J* = 1.5 Hz, 2H), 3.36 (s, 3H); ¹³C NMR (126 MHz, CDCl₃) δ 150.8, 146.8, 142.8, 108.6, 107.9, 107.0, 101.6, 96.6, 56.1; HRMS (ESI) 369.1161 [(M + Li)⁺, calcd for C₁₈H₁₈O₈ 369.1162].



Biaryl 2.27. A flask containing Pd(PPh₃)₄ (36 mg, 0.031 mmol), CuCl (156 mg, 1.58 mmol), and CuCl₂ (85 mg, 0.63 mmol) was purged with argon (3x) and **2.26** (109 mg, 0.315 mmol) in DMSO (3.2 mL) was added dropwise at 21 °C. The reaction mixture was stirred at 21 °C for 10 min and then heated at 60 °C for 1.5 h. The reaction mixture was diluted with EtOAc (6 mL) and the resulting solution was washed with brine (6 mL) and then NH₄OH (6 mL). The combined aqueous layers were extracted with EtOAc (2 x 6 mL). The combined organic layers were washed with water (2 x 6 mL) and then washed with brine (2 x 6 mL), dried (Na₂SO₄), concentrated *in vacuo* and purified by flash chromatography (6:1 to 4:1 hexane : EtOAc) to afford 32 mg of **2.27** (56 %) of an orange oil: IR (CH₂Cl₂) 2922, 1639, 1445 cm⁻¹; ¹H NMR (500 MHz, CDCl₃) δ 6.77 (d, *J* = 8.5 Hz, 1H), 6.70 (d, *J* = 8.5 Hz, 1H), 5.95 (d, *I* = 1.5 Hz, 1H), 5.93 (d, *J* = 1.5 Hz, 1H), 5.01 (d, *J* = 1.5 Hz, 2H), 3.36 (s, 3H); ¹³C NMR (126 MHz, CDCl₃) δ 150.8, 146.8, 142.8, 108.6, 107.9, 107.0, 101.6, 96.6, 56.1; HRMS (ESI) 369.1161 [(M + Li)⁺, calcd for C₁₈H₁₈O₈ 369.1162].

**2.28**

Aryl-stannane 2.28. To a solution of **2.14** (1.03 g, 5.21 mmol) and TMEDA (0.87 mL, 5.7 mmol) in THF (13 mL) at 0 °C was added *n*-BuLi (3.7 mL of a 1.6 M solution in hexanes, 5.7 mmol) dropwise. The ice bath was removed and the reaction mixture was stirred at 21 °C for 1 h and then cooled to 0 °C. Trimethyltin chloride (5.7 mL of a 1 M solution in THF, 5.7 mmol) was added and the reaction mixture was allowed to warm to 21 °C over 1.5 h. The resulting solution was poured into saturated NaHCO₃ (15 mL) and the product was extracted with EtOAc (3 x 15 mL), dried (MgSO₄), concentrated *in vacuo* and the resulting residue was purified by flash chromatography (10:1 hexane : EtOAc) to afford 1.3 g **2.28** (68 %) as a yellow oil: IR (CH₂Cl₂) 2918, 1577, 1467 cm⁻¹; ¹H NMR (500 MHz, CDCl₃) δ 6.84 (d, *J* = 9 Hz, 1H), 6.80 (d, *J* = 8.5 Hz, 1H), 5.10 (s, 2H), 3.83 (s, 3H), 3.82 (s, 3H), 3.47 (s, 3H), 0.35 (s, 9H); ¹³C NMR (126 MHz, CDCl₃) δ 156.1, 154.3, 147.7, 124.7, 114.4, 108.6, 94.8, 61.1, 56.4, 56.1, -6.8; HRMS (ESI) *m/z* 385.0415 [(M + Na)⁺, calcd for C₁₃H₂₂O₄Sn 385.0438].

**2.29**

Biaryl 2.29. A flask containing Pd(PPh₃)₄ (2.09 g, 1.82 mmol), CuCl (9.00 g, 90.9 mmol), and CuCl₂ (4.88 g, 36.3 mmol) was purged with argon (3x) and **2.28** (6.58 g, 18.2 mmol) in DMSO (182 mL) was added dropwise at 21 °C and the reaction mixture stirred at 21 °C for 3 d. The mixture was diluted with EtOAc (200 mL) and resulting solution was washed with brine (2 x 180 mL) and then washed with NH₄OH (180 mL). The combined aqueous layers were extracted with EtOAc (2 x 180 mL). The combined organic layers were washed with water (2 x 180 mL) and then washed with brine (2 x 180 mL), dried (MgSO₄), concentrated *in vacuo* and the resulting residue was purified by flash chromatography (6:1 hexane : EtOAc) to afford 1.3 g **2.29** (38 %) as a light yellow solid: mp 27-29 °C (CH₂Cl₂); IR (CH₂Cl₂) 2944, 1595, 1480 cm⁻¹; ¹H NMR (500 MHz, CDCl₃) δ 6.91 (d, *J* = 9 Hz, 1H), 6.77 (d, *J* = 9.5 Hz, 1H), 5.19 (s, 2H), 3.89 (s, 3H), 3.85 (s, 3H), 3.54 (s, 3H); ¹³C NMR (126 MHz, CDCl₃) δ 149.2, 147.9, 146.8, 119.7, 111.9, 110.8, 96.2, 60.9, 56.7, 56.6; LRMS (ESI) *m/z* 395 [(M + H)⁺, calcd for C₂₀H₂₆O₈ 395].

CHAPTER III

CONCLUSION

3.1 Summary

Our recent synthetic efforts have focused on the synthesis of hibarimicinone (**1.6**) and HMP-Y1 (**1.10**), which are key intermediates on the biosynthetic pathway leading to the more complex hibarimicin B (**1.2**). Completion of these synthetic targets will enable us to correlate our synthetic products with the natural products, thereby confirming structural assignment. Our retrosynthetic analysis of hibarimicinone (**1.6**) and HMP-Y1 (**1.10**) are illustrated in Schemes 1.2, 1.3, and 1.4. The synthetic work accomplished toward these target intermediates was discussed in Chapter Two.

3.2 Future Work Toward the Synthesis of Hibarimicinone (**1.6**)

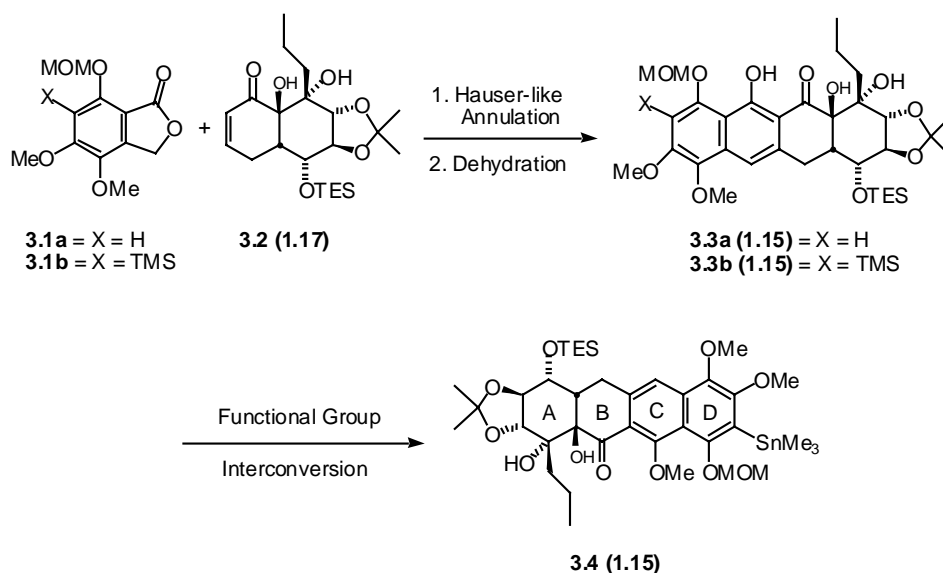
Our synthesis of hibarimicinone (**1.6**) requires the completion of the Hauser annulation precursors, followed by a Hauser annulation, and a series of subsequent reactions to afford the ABCD and EFGH ring systems, which then will be coupled to afford hibarimicinone (**1.6**).

3.2a Future Work Toward the ABCD Ring System

The ABCD ring system will be constructed using the chemistry described in Scheme 1.2, and shown in detail in Scheme 3.1. We anticipate utilizing a Hauser annulation between the lactone **3.1** and the enone **3.2** to afford the tetracycle **3.3**. The

tetracycle **3.3** will then undergo a series of functional group interconversions to afford the ABCD ring system, and provide one of the necessary coupling partners for the synthesis of hibarimicinone (**1.6**).

Scheme 3.1. Future Work Toward the Synthesis of ABCD Ring System.

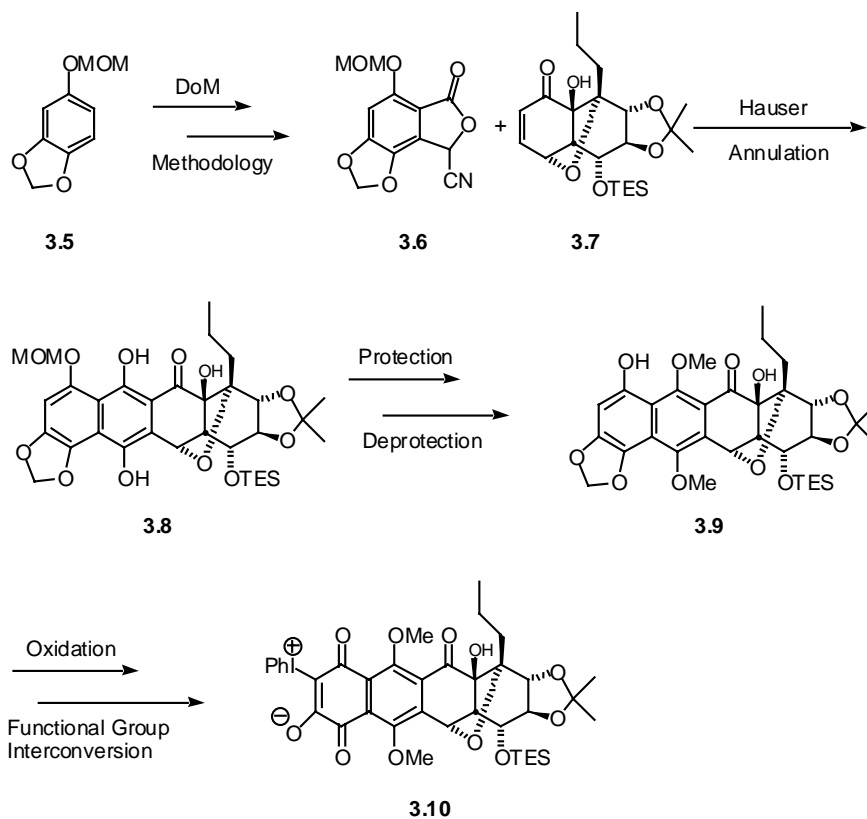


3.2b Future Work Toward the Synthesis of EFGH Ring System

The model study for the EFGH ring system, Section 2.1, provided some valuable information for the synthesis of the EFGH ring system. Using a second generation approach we envision starting from MOM protected sesamol **3.5** and applying DoM methodology to derive cyanophthalide **3.6**, which may then undergo a Hauser annulation with the enone **3.7** to afford the dihydroquinone **3.8** as seen in Scheme 3.2. The dihydroquinone **3.8** will then be methylated and the MOM ether deprotected to afford

the free phenol **3.9**. The free phenol **3.9** may be oxidized followed by functional group interconversion to complete the EFGH ring system **3.10**. The EFGH ring system is the second tetracycle needed for the palladium cross coupling to furnish hibarimicinone (**1.6**).

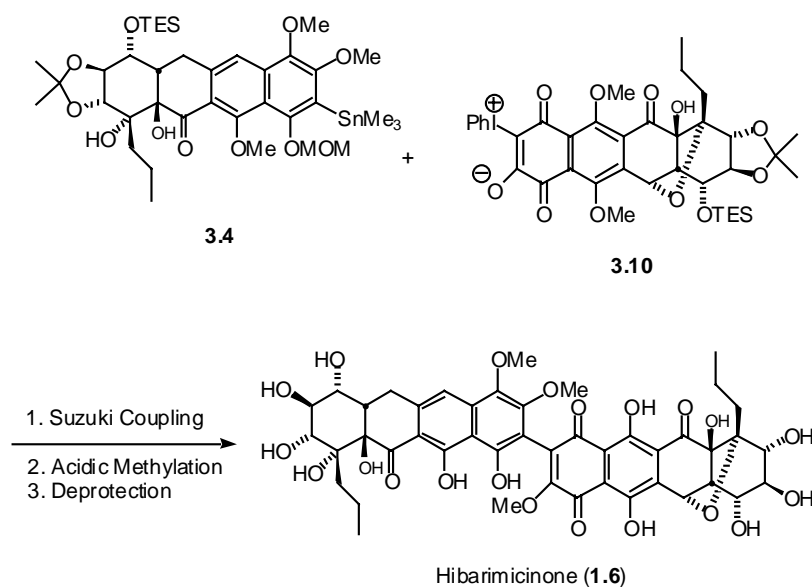
Scheme 3.2. Future Work Toward the Synthesis of EFGH Ring System.



3.2c Palladium Mediated Cross-Coupling

Once the ABCD and EFGH ring systems are in hand, we envision using a palladium mediated cross coupling to couple the tetracycles **3.4** and **3.10**, as illustrated in Scheme 3.3. This transformation may be accomplished in one of several ways, including a Suzuki or Stille cross-coupling reaction, as previously discussed. Upon completion of the cross coupling reaction, the synthesis of hibarimicinone (**1.6**) will be complete.

Scheme 3.3. Future Work Toward the Synthesis of Hibarimicinone (**1.6**).

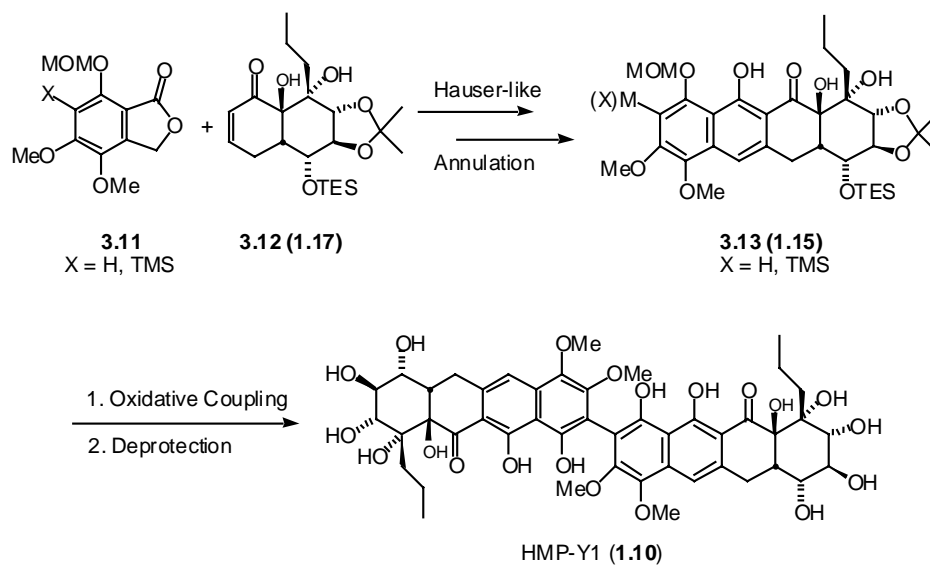


3.3 Future Work Toward the Synthesis of HMP-Y1 (**1.10**)

The most promising approach to the synthesis of HMP-Y1 involves a dimerization of the tetracycle **3.13**, as shown in Scheme 3.4. This may be accomplished by utilizing an

oxidative coupling of tetracycle **3.13**. A Hauser-like annulation between the lactone **3.11** and the enone **3.12** should furnish the tetracycle **3.13**, which may then be oxidatively coupled followed by deprotection to afford HMP-Y1 (**1.10**).

Scheme 3.4. Future Work Toward the Synthesis of HMP-Y1 (**1.10**).



REFERENCES

1. Kajiura, T., Furumai, T., Igarashi, Y., Hori, H., Higashi, K., Ishiyama, T., Uramoto, M., Uehara, Y., Oki, T., *J. Antibiotics*, **1998**, *51*, 394-401.
2. Hori, H., Igarashi, Y., Kajiura, T., Furumai, T., Higashi, K., Ishiyama, T., Uramoto, M., Uehara, Y., Oki, T., *J. Antibiotics*, **1998**, *51*, 402-417.
3. Uehara, Y., Li, P.-M., Fukazawa, H., Mizuno, S., Nihei, Y., Nishio, M., Hanada, M., Yamamoto, C., Furumai, T., Oki, T., *J. Antibiotics*, **1993**, *46*, 1306-1308.
4. Cho, S., I., Fukazawa, H., Honma, Y., Kajiura, T., Hori, H., Igarashi, Y., Furumai, T., Oki, T., Uehara, Y., *J. Antibiotics*, **2002**, *55*, 270-280.
5. Hori, H., Kajiura, T., Igarashi, Y., Furumai, T., Higashi, K., Ishiyama, T., Uramoto, M., Uehara, Y., Oki, T., *J. Antibiotics*, **2002**, *55*, 46-52.
6. Kajiura, T., Furumai, T., Igarashi, Y., Hori, H., Higashi, K., Ishiyama, T., Uramoto, M., Uehara, Y., Oki, T., *J. Antibiotics*, **2002**, *55*, 53-60.
7. Hauser, F., Gauvan, P., J., F., *Org. Lett.*, **1999**, *4*, 671-672.
8. Fukuyama, Y., Kiriyama, Y., Kodama, M., *Tetrahedron Lett.*, **1993**, *34*, 7637-7638.
9. Hassen, J., Sevignon, M., Gozzi, C., Schulz, E., Lemaire, M., *Chem. Rev.*, **2002**, *102*, 1359-1469.
10. Stagliano, K., W., Malinakova, H., C., *J. Org. Chem.*, **1999**, *64*, 8034-8040.
11. Bringmann, G., Tasler, S., *Tetrahedron*, **2001**, *57*, 331-343.
12. Mulrooney, C., A., Li, X., DiVirgilio, E., S., Kozlowski, M., C., *J. Am. Chem. Soc.* **2003**, *125*, 6856-6857.

13. Whiting, D., A., In *Comprehensive Organic Chemistry*, Trost, B., M., Fleming, I., Eds.; Pergamon: New York, 1991; Vol. 3, Chapter 2.9.
14. Snieckus, V., *Chem. Rev.*, **1990**, *90*, 879-933.
15. de Silva, S.,O., Reed, J., N., Billedeau, R.,J., Wang, X., Norris, D.,J., Sniekus, V., *Tetrahedron*, **1992**, *48*, 4863-4878.
16. Simas, A., B., C., Coelho, A., L., Costa, P., R., R., *Synthesis*, **1999**, *6*, 1017-1021.
17. Okazaki, K., Nomura, K., Yoshii, E., *Synth. Commun.*, **1987**, *17*, 1021-1027.
18. Lee, C. S. PhD. Thesis, Texas A&M University, May, 2001.
19. Collini, M., D., Miller, C., P., *Tetrahedron Lett.*, **2001**, *42*, 8429-8431.
20. Meyers, A., I., Durandetta, J., L., Munavu, R., *J. Org. Chem.*, **1975**, *40*, 2025-2029.
21. Uno, H., Sakamoto, K., Honda, E., Fukuhara, K., Ono, N., Tanaka, J., Sakanaka, M., *J., Chem. Soc. Perkin Trans. 1*, **2001**, *3*, 229-238.
22. Kajigaeshi, S., Kakinami, T., *Bull. Chem. Soc. Jpn.*, **1987**, *60*, 4187-4189.
23. Castanet, A., Colobert, F., Broutin, P., *Tetrahedron Lett.*, **2002**, *43*, 5047-5048.
24. Karimi, F., Kihlberg, T., Langstrom, B., *J. Chem. Soc. Perkin Trans. 1*, **2001**, *42*, 1528-1531.
25. Zembower, D., E., Zhang, H., *J. Org. Chem.*, **1998**, *63*, 9300-9305.
26. Frank, S., A., Chen, H., Kunz, R., K., Schnaderbeck, M., J., Roush, W., R., *Org. Lett.*, **2000**, *2*, 2691-2694.
27. Han, X., Stoltz, B., M., Corey, E., J., *J. Am. Chem. Soc.*, **1999**, *121*, 7600-7605.

APPENDIX A
SPECTRA RELEVANT TO CHAPTER II

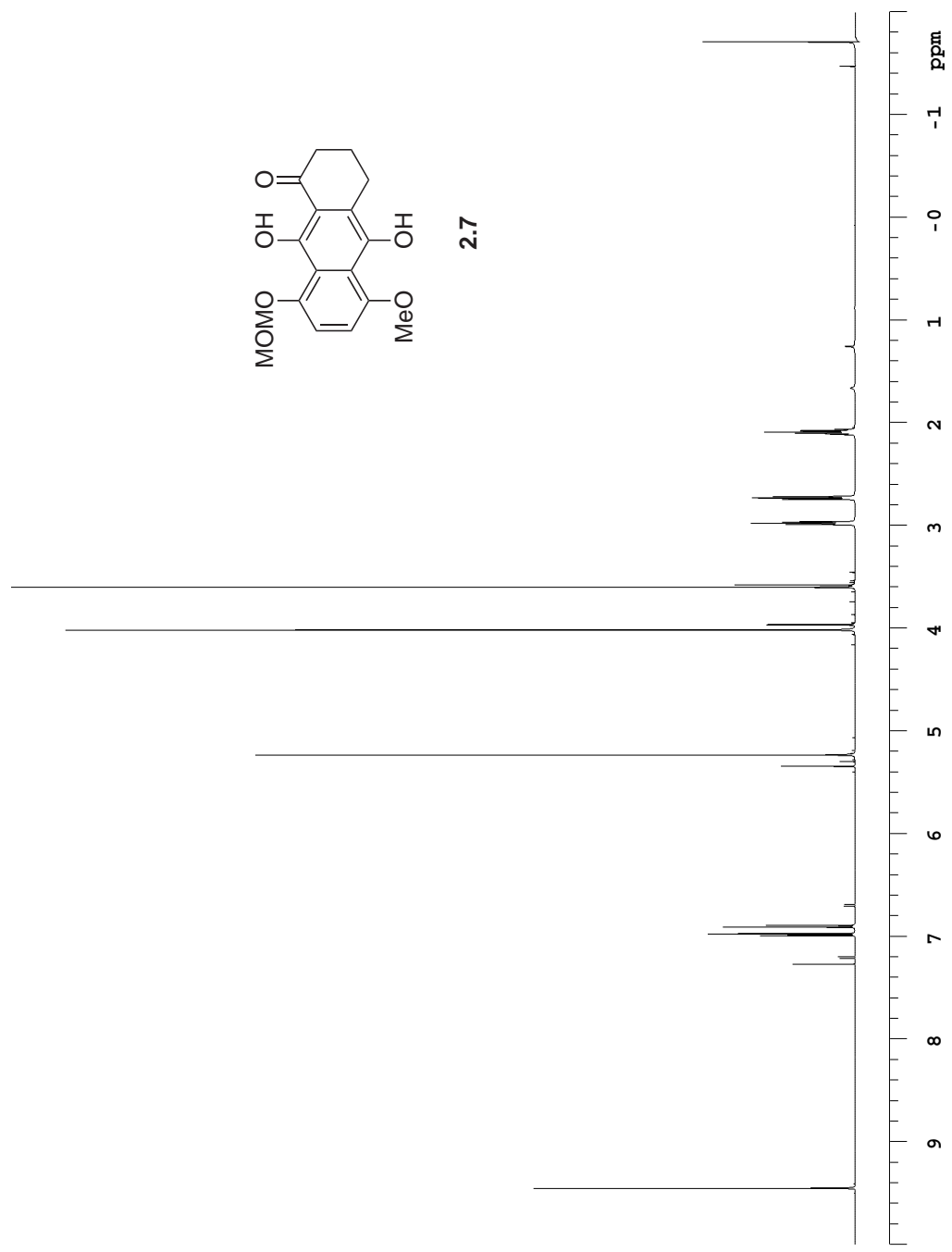
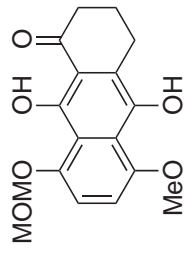


Figure A.1a The 500 MHz ¹H NMR spectrum of dihydroquinone **2.7** in CDCl₃.



2.7

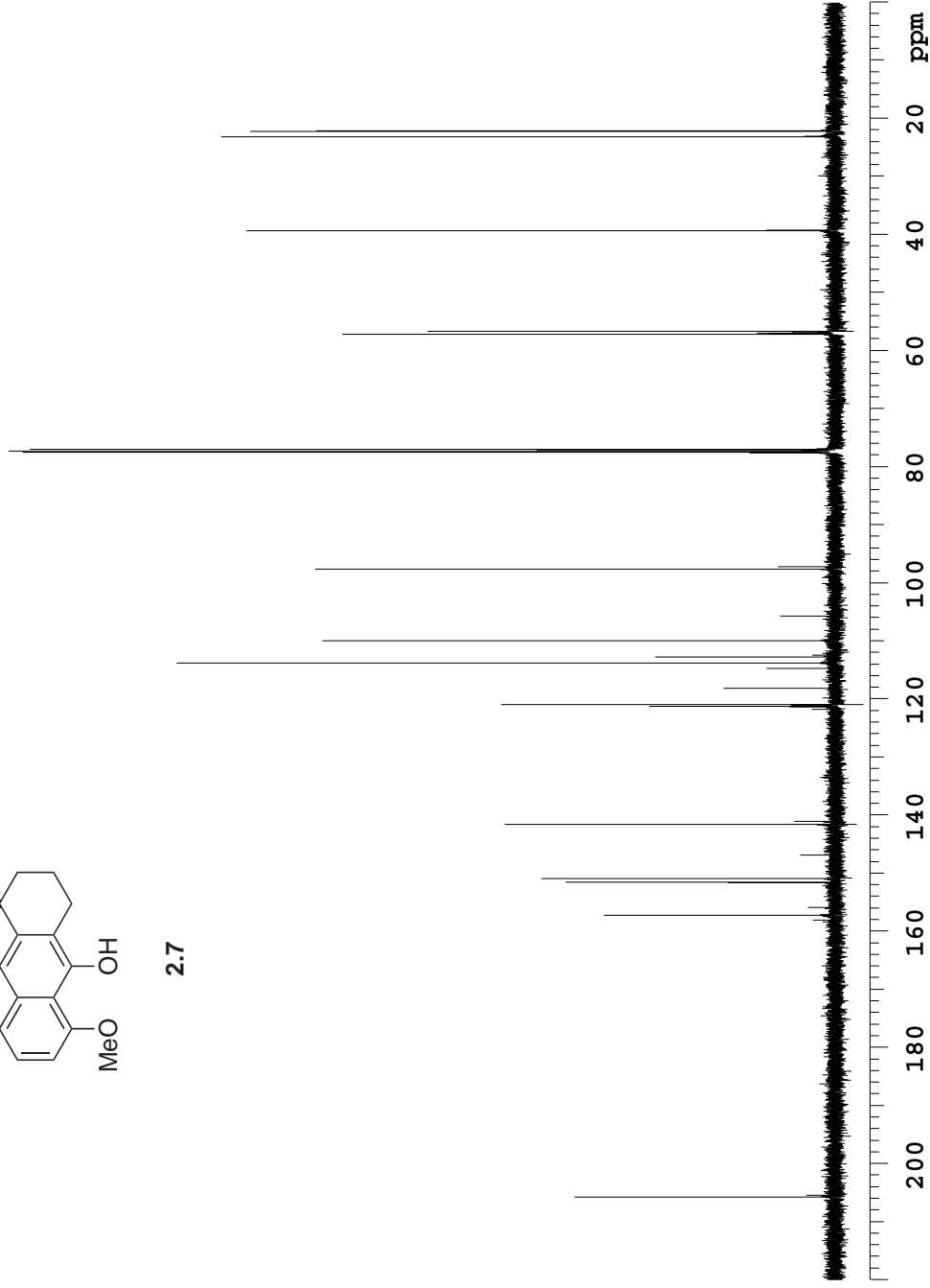


Figure A.1b The 126 MHz ^{13}C NMR spectrum of dihydroquinone **2.7** in CDCl_3 .

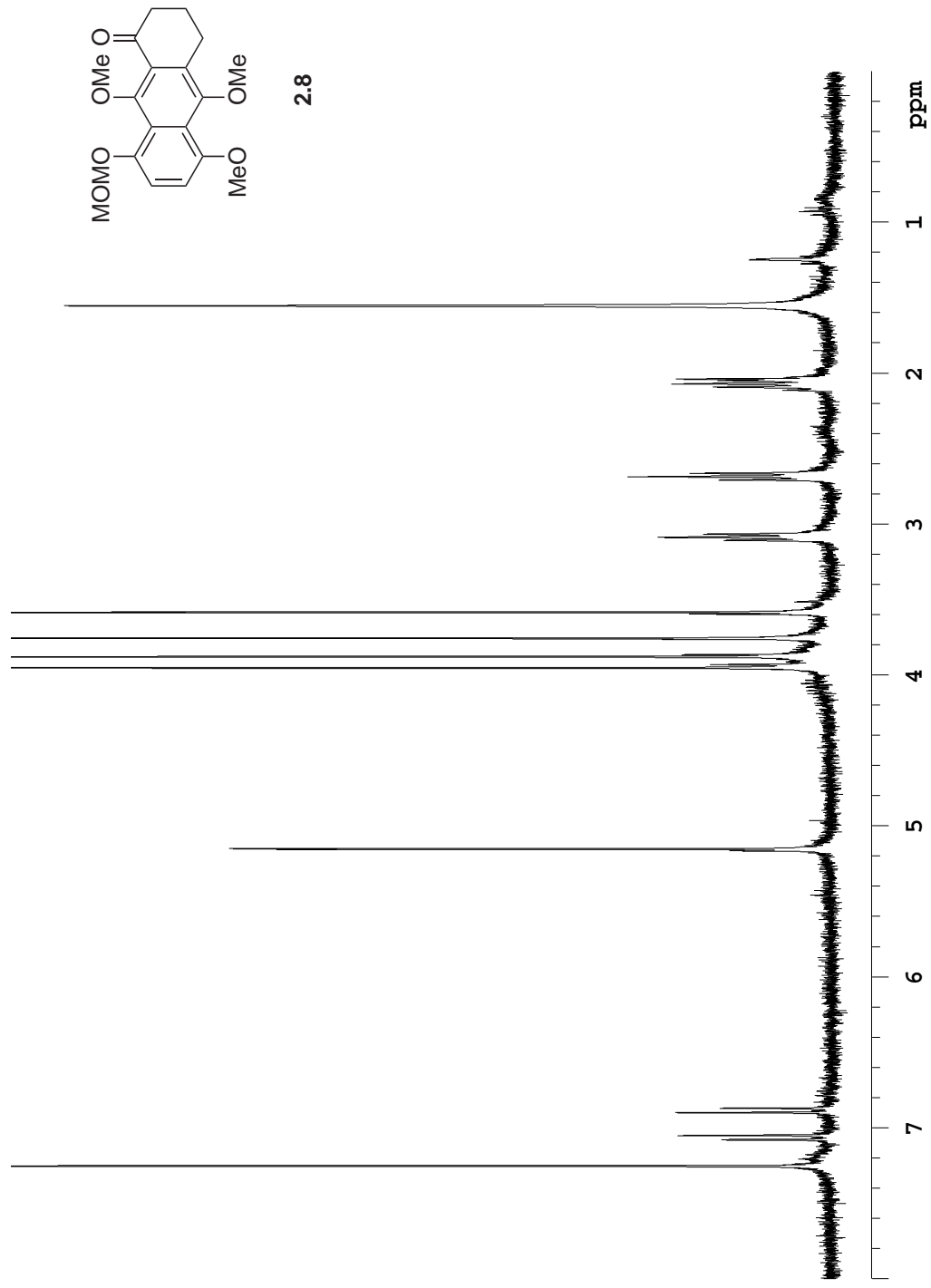


Figure A.2a The 500 MHz ¹H NMR spectrum of tricyclic **2.8** in CDCl₃.

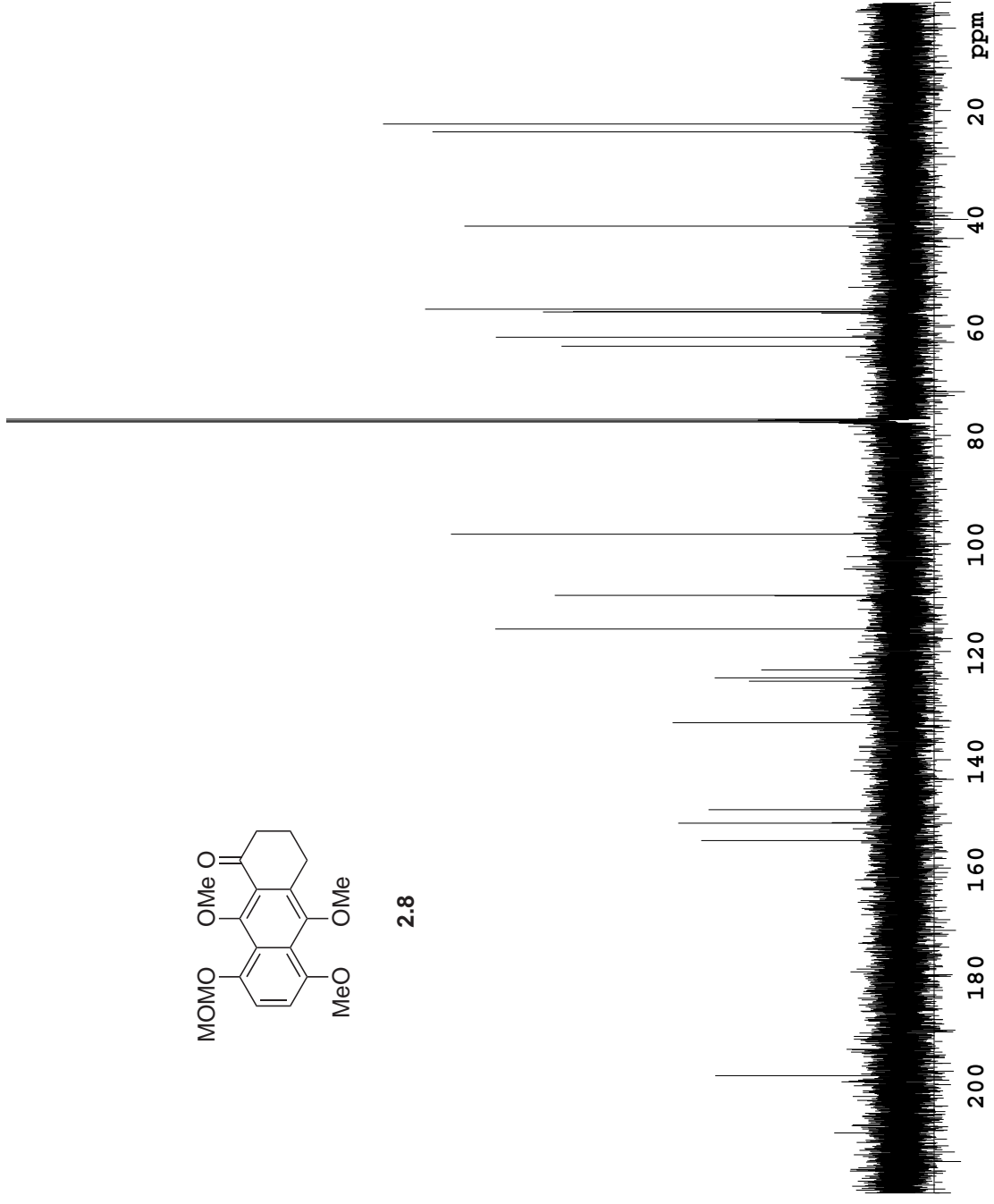
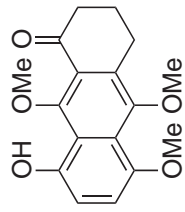


Figure A.2b The 126 MHz ^{13}C NMR spectrum of tricycle 2.8 in CDCl_3 .



2.9

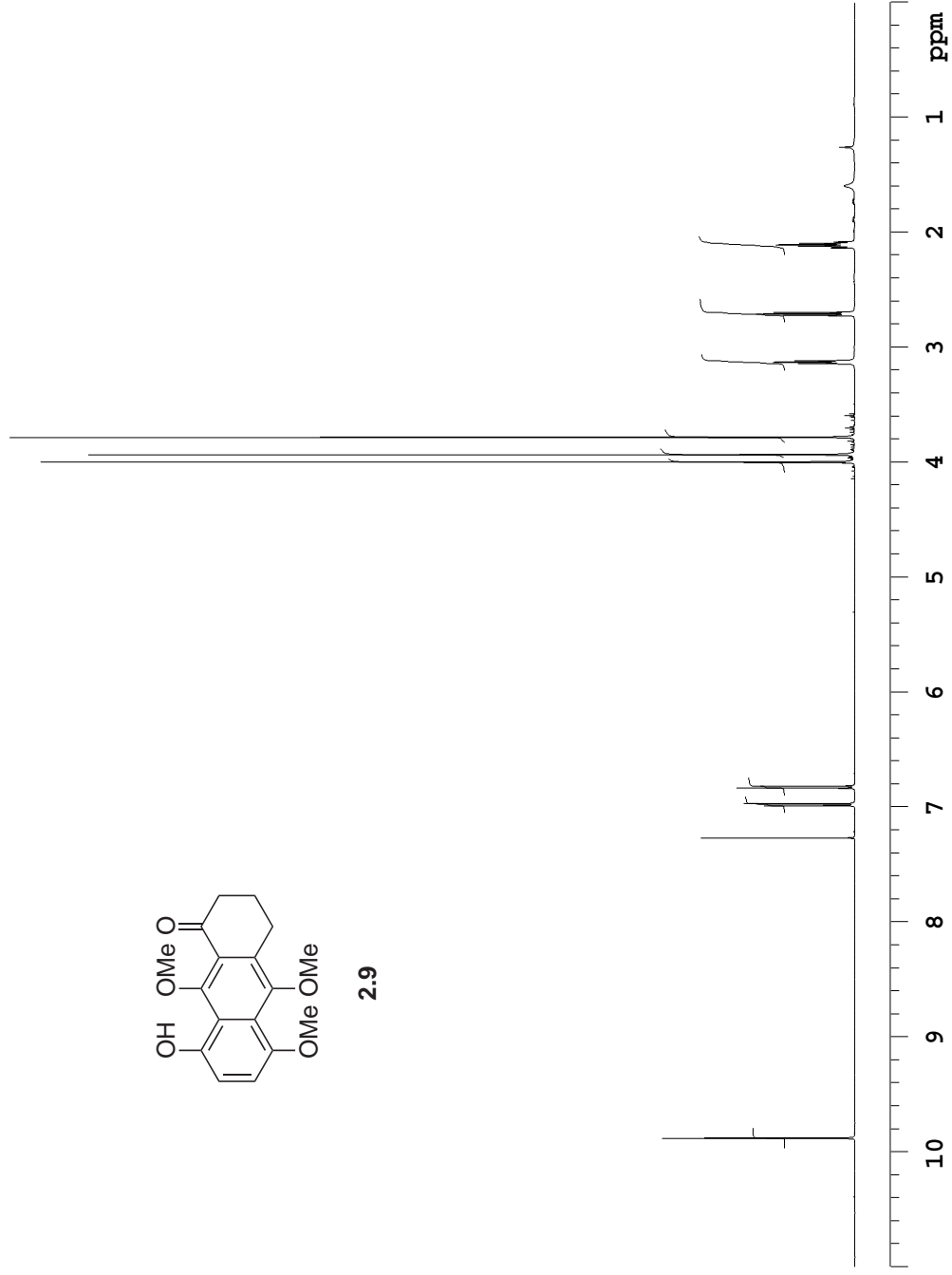
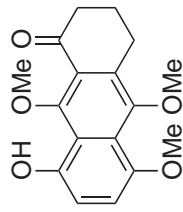


Figure A.3a The 500 MHz ^1H NMR spectrum of phenol 2.9 in CDCl_3 .



2.9

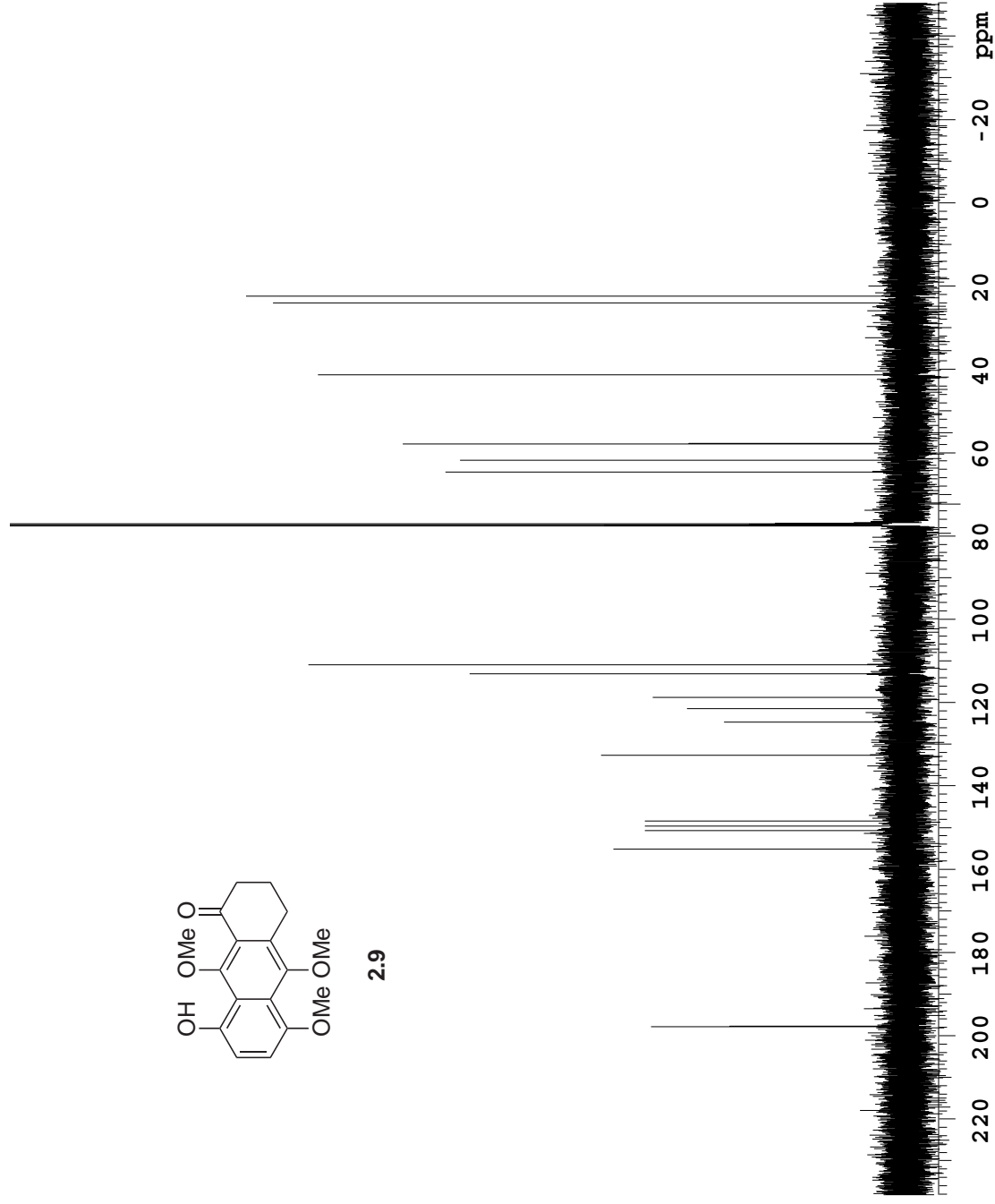


Figure A.3b The 126 MHz ^{13}C NMR spectrum of phenol 2.9 in CDCl_3 .

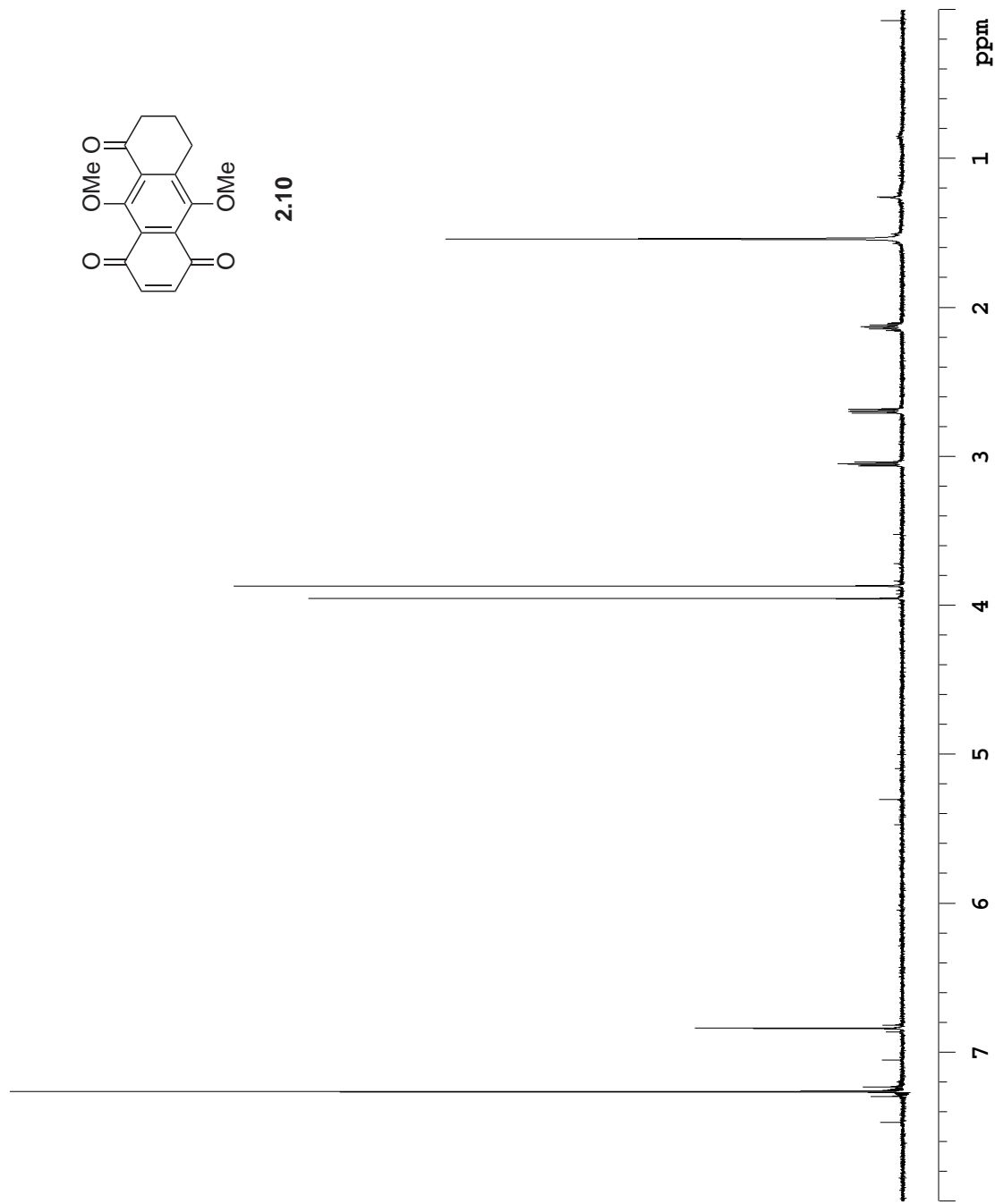


Figure A.4a The 500 MHz ¹H NMR spectrum of quinone **2.10** in CDCl₃.

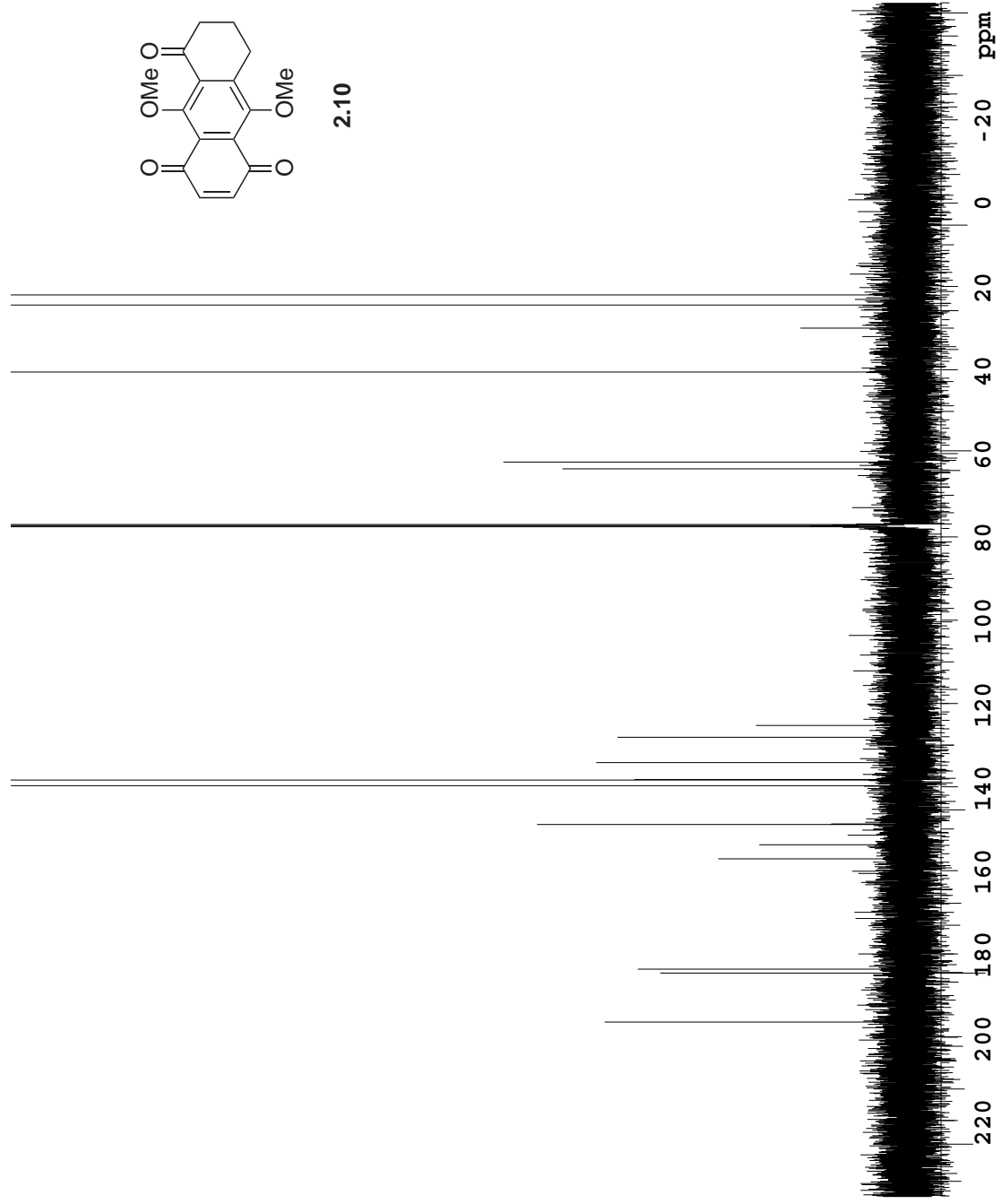


Figure A.4b The 126 MHz ^{13}C NMR spectrum of quinone **2.10** in CDCl_3 .

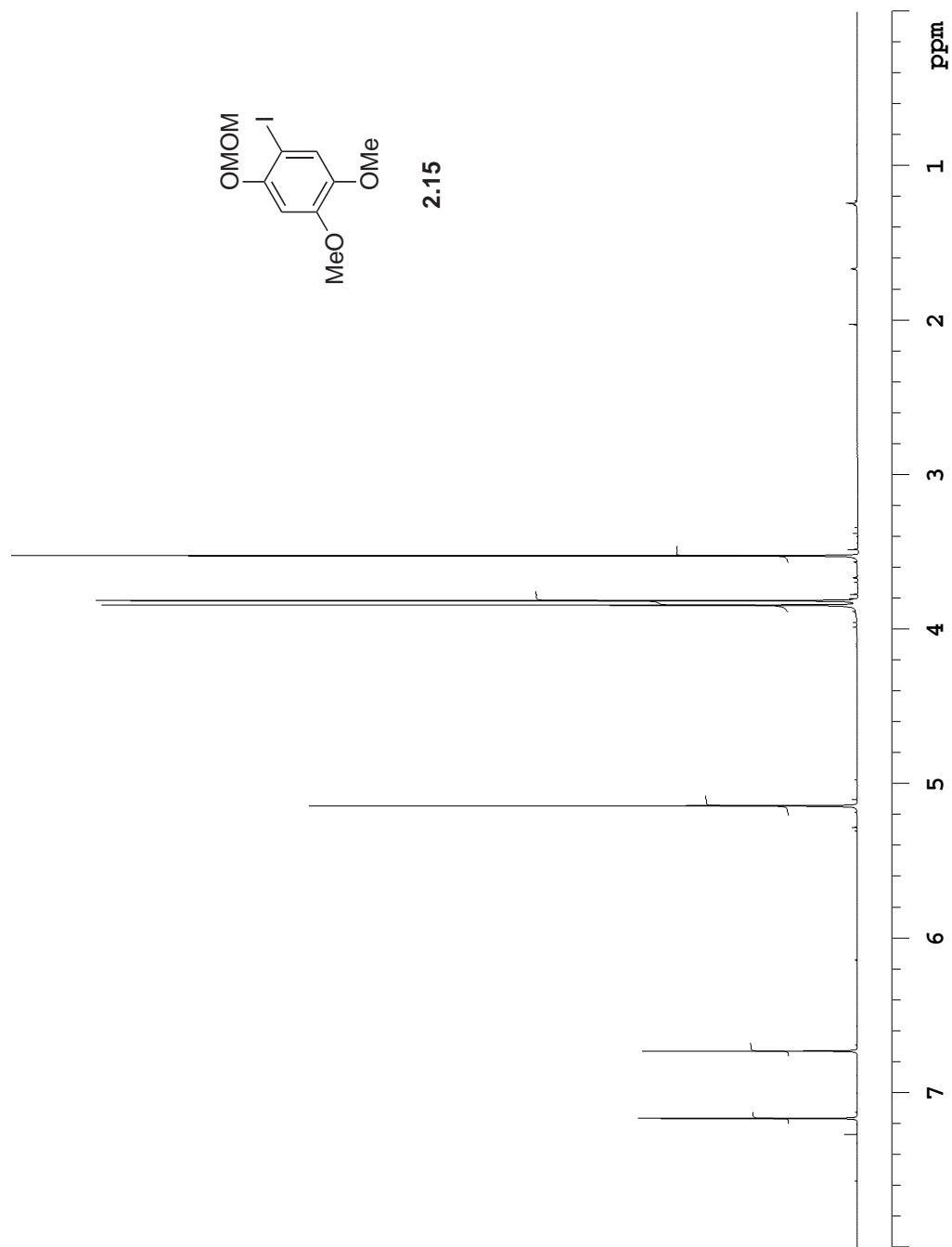


Figure A.5a The 500 MHz ^1H NMR spectrum of aryl-iodide **2.15** in CDCl_3 .

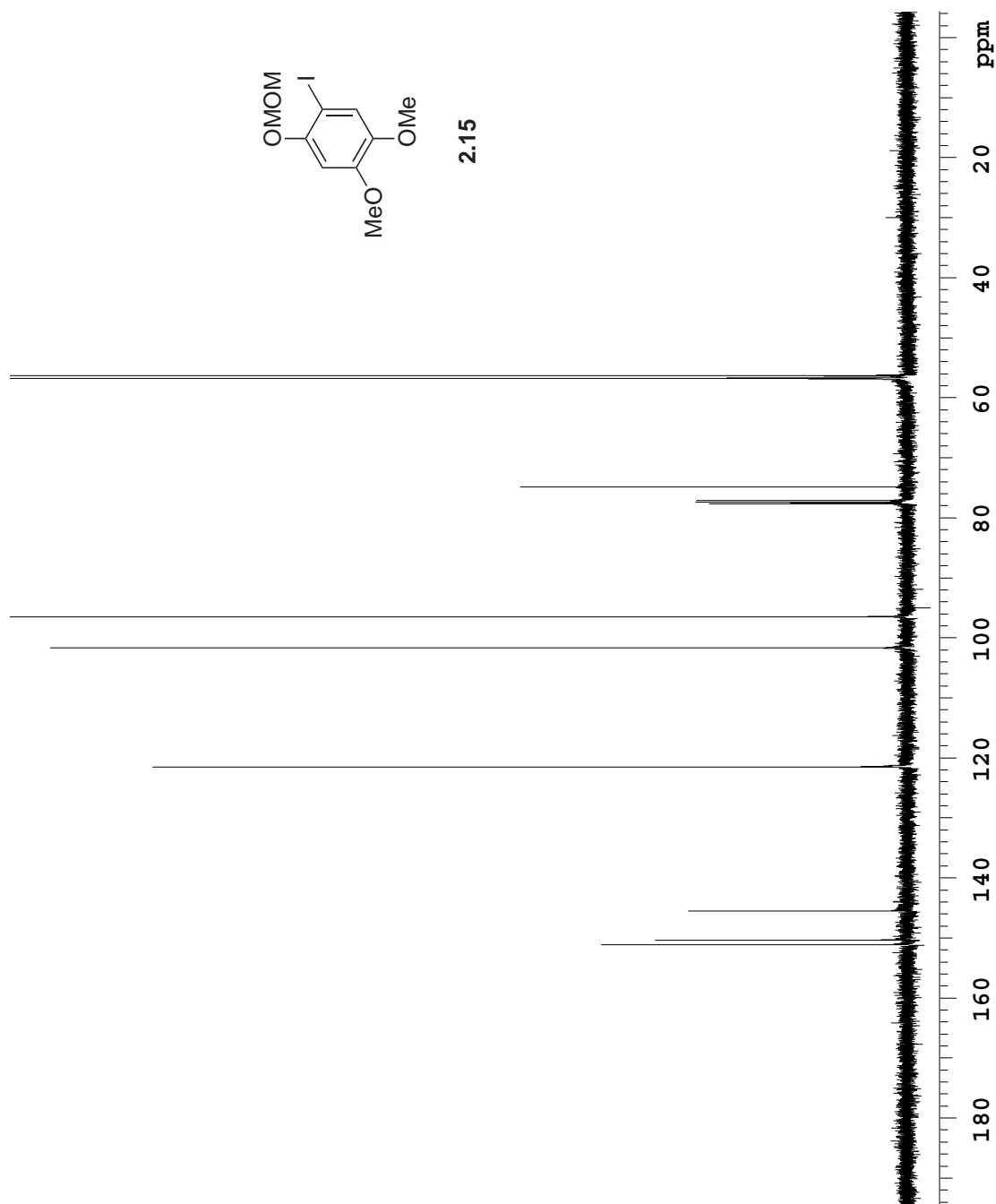


Figure A.5b The 126 MHz ^{13}C NMR spectrum of aryl-iodide **2.15** in CDCl_3 .

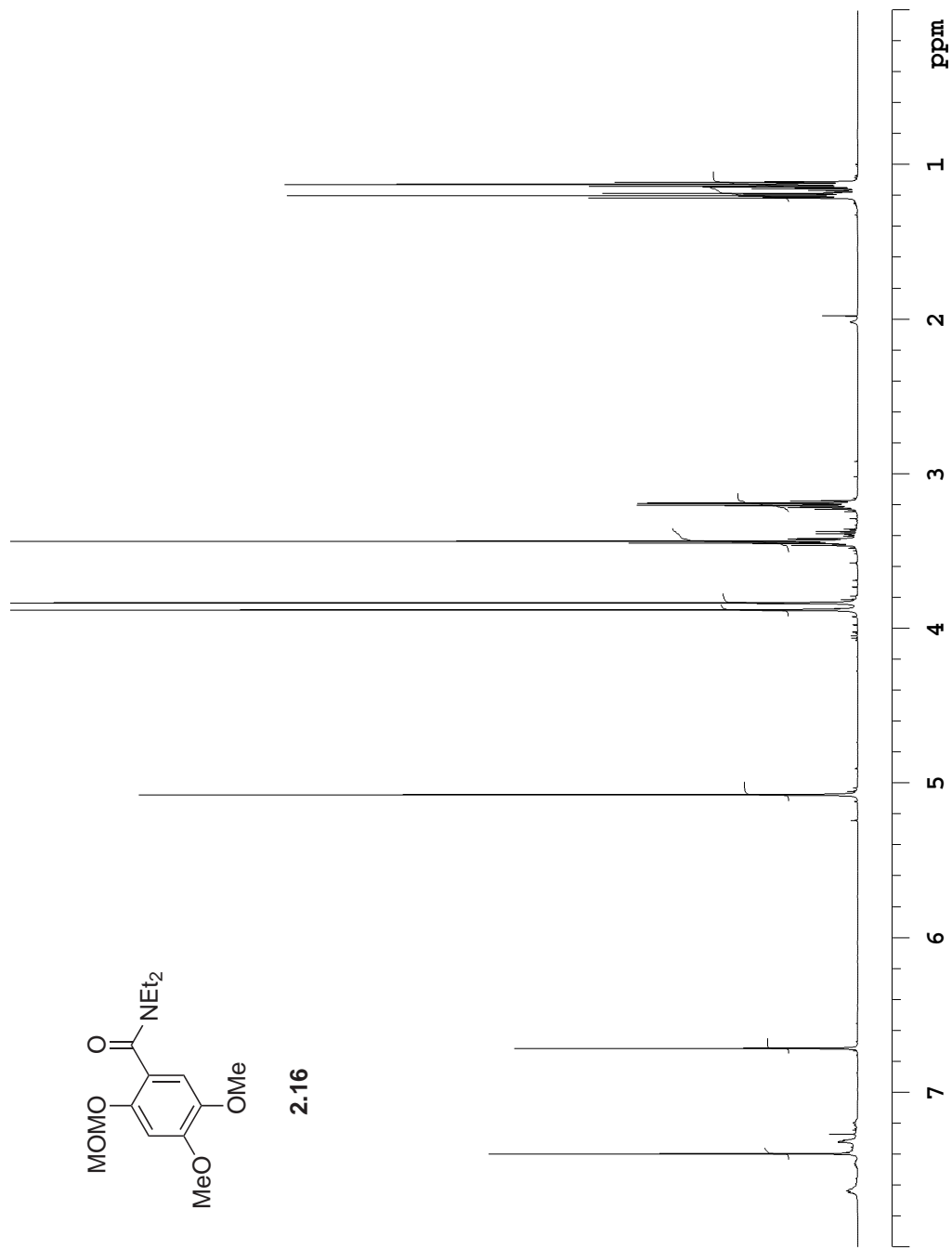


Figure A.6a The 500 MHz ¹H NMR spectrum of aryl-amide **2.16** in CDCl₃.

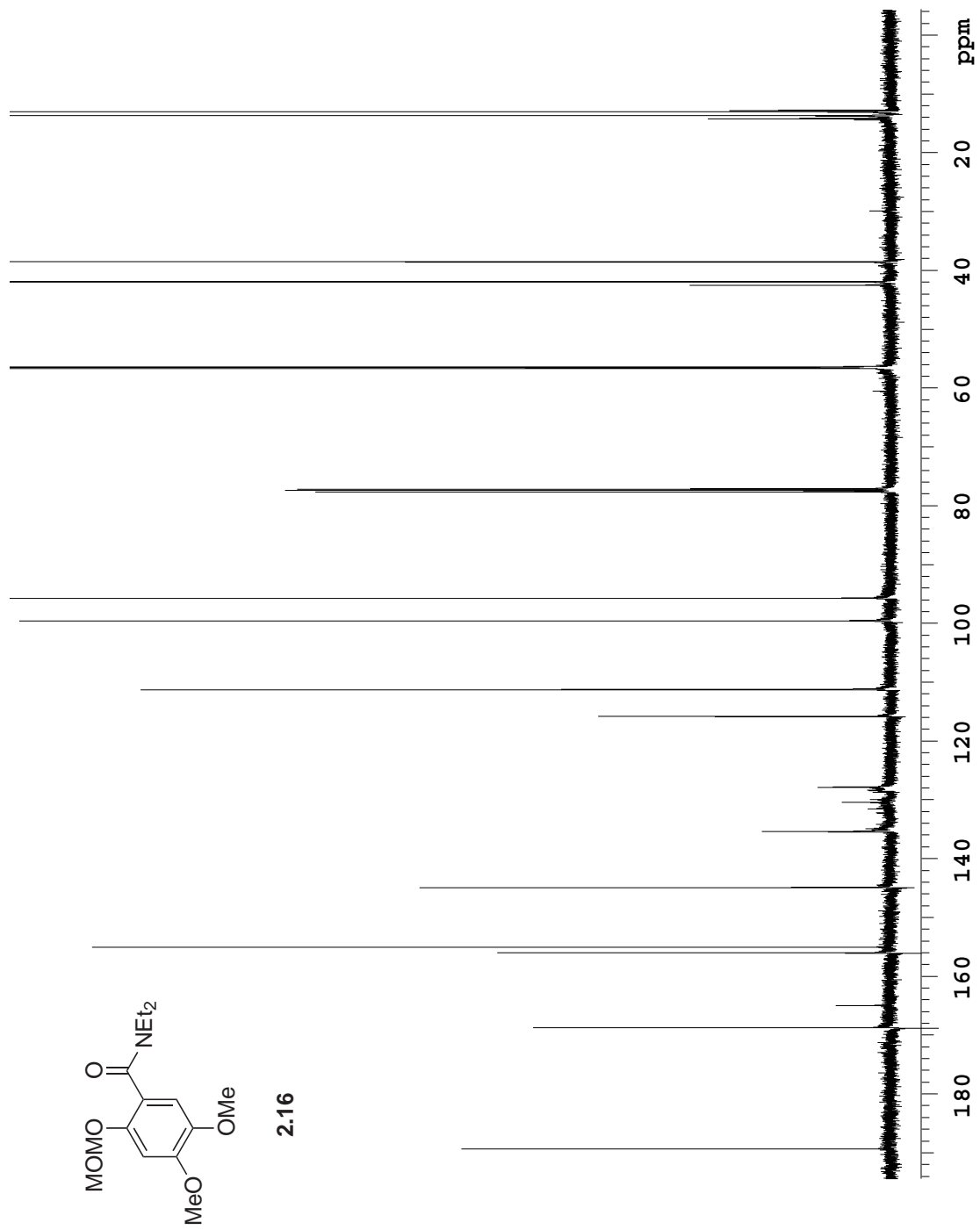


Figure A.6b The 126 MHz ¹³C NMR spectrum of aryl-amide **2.16** in CDCl₃.

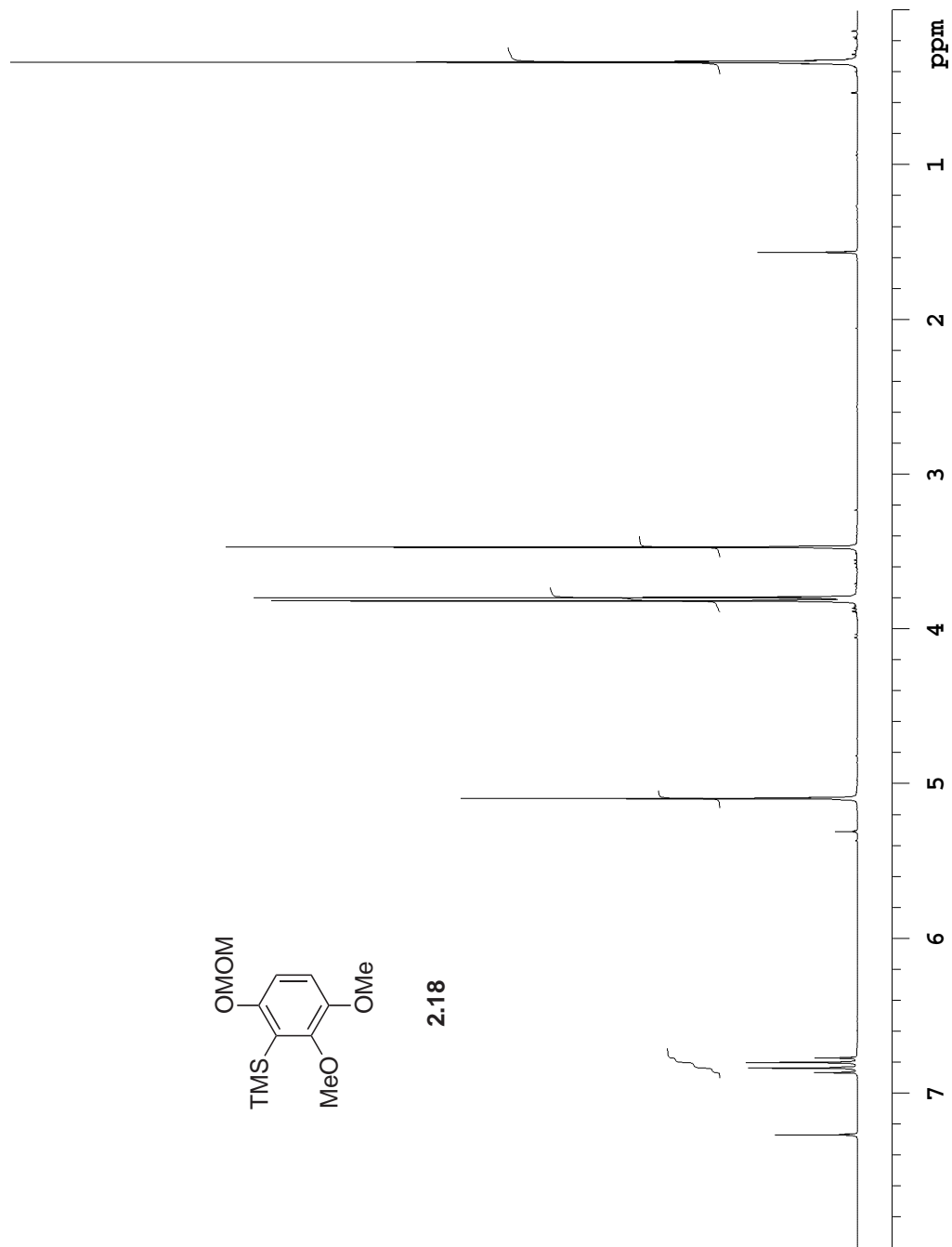


Figure A.7a The 500 MHz ^1H NMR spectrum of aryl-silane **2.18** in CDCl_3 .

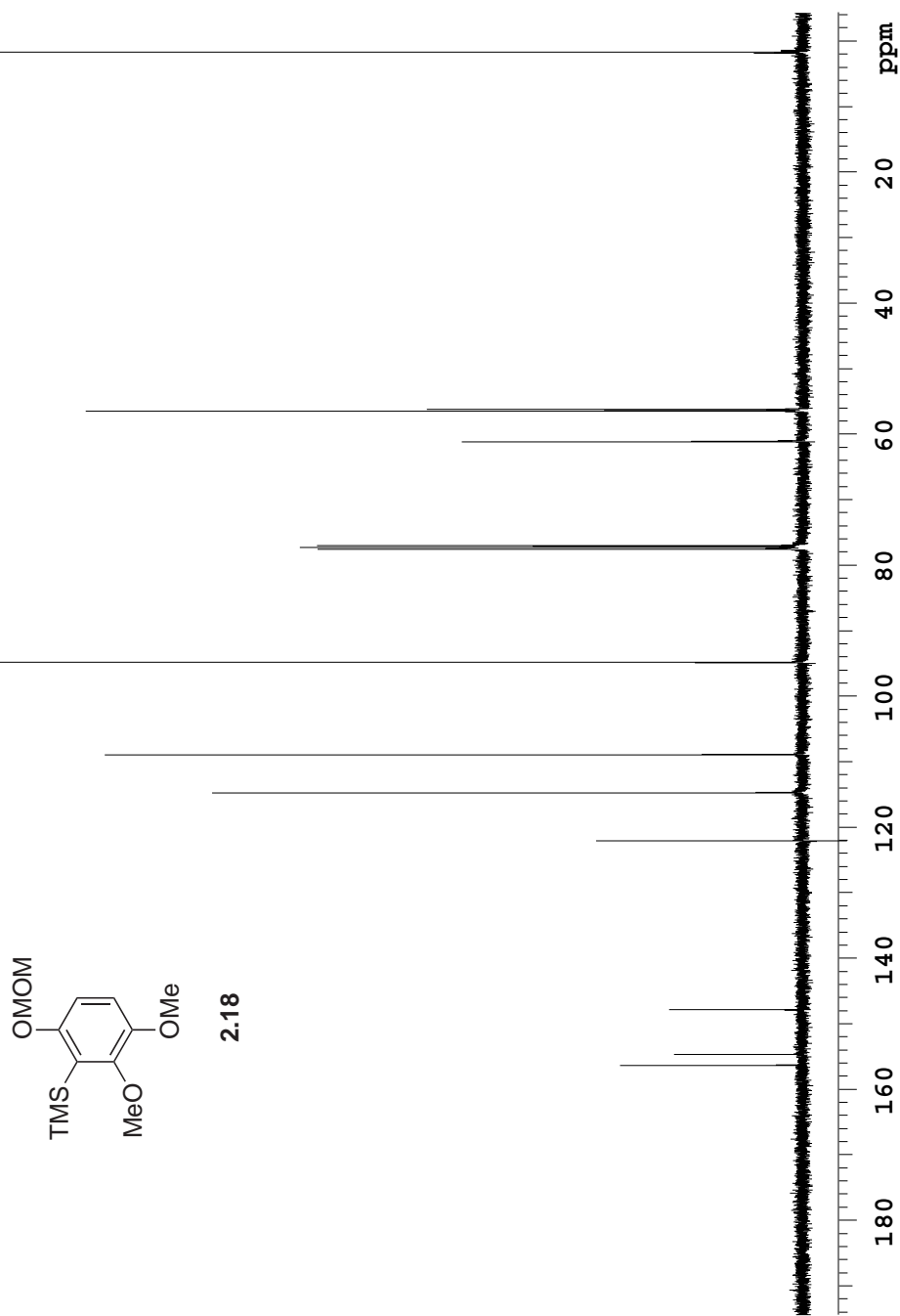


Figure A.7b The 126 MHz ^{13}C NMR spectrum of aryl-silane **2.18** in CDCl_3 .

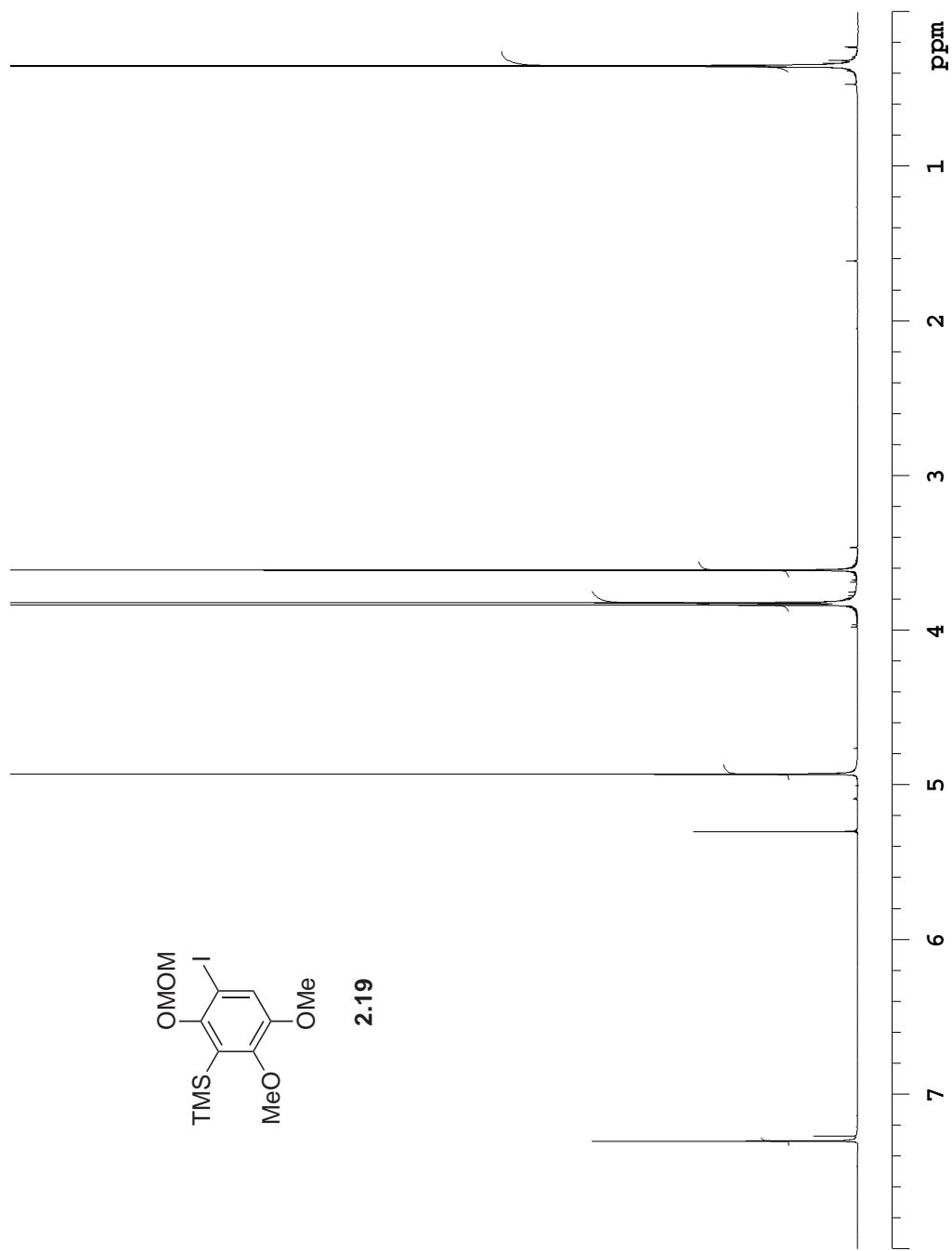
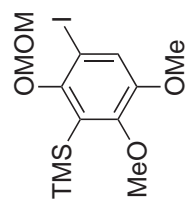


Figure A.8a The 500 MHz ^1H NMR spectrum of aryl-iodide **2.19** in CDCl_3 .



2.19

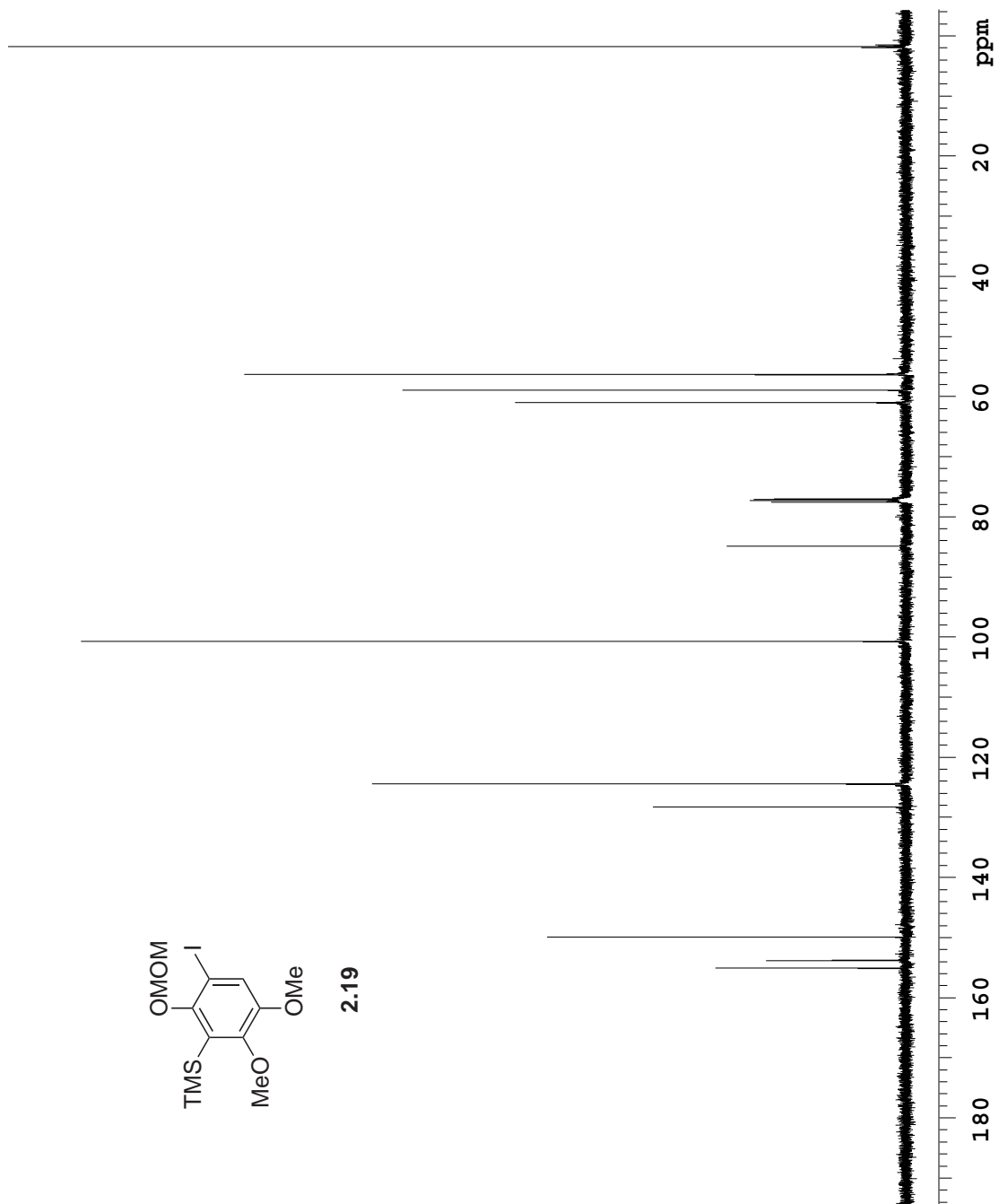


Figure A.8b The 126 MHz ^{13}C NMR spectrum of aryl-iodide 2.19 in CDCl_3 .

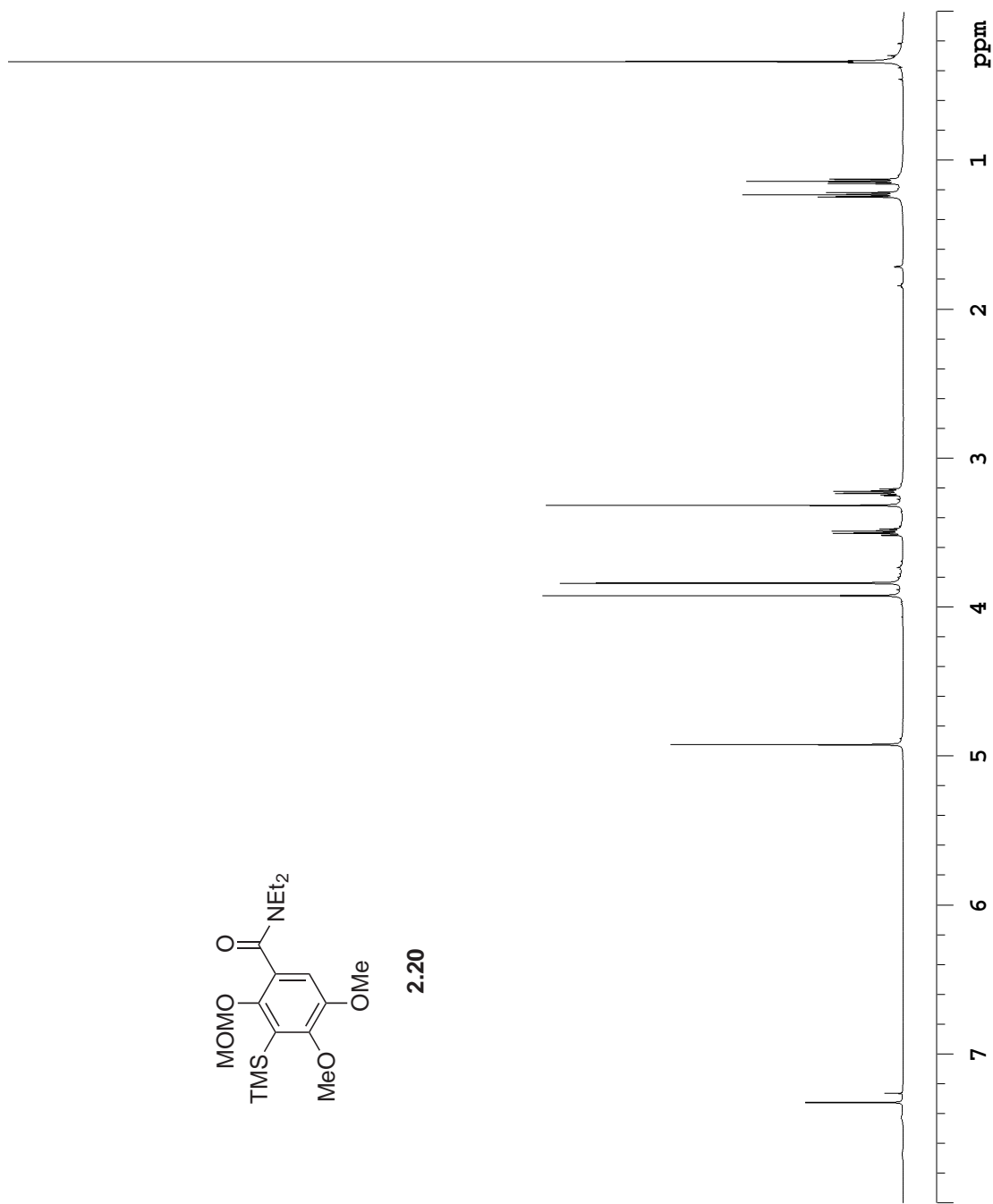
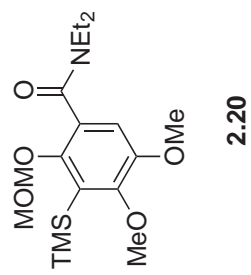


Figure A.9a The 500 MHz ¹H NMR spectrum of aryl-amide **2.20** in CDCl₃.

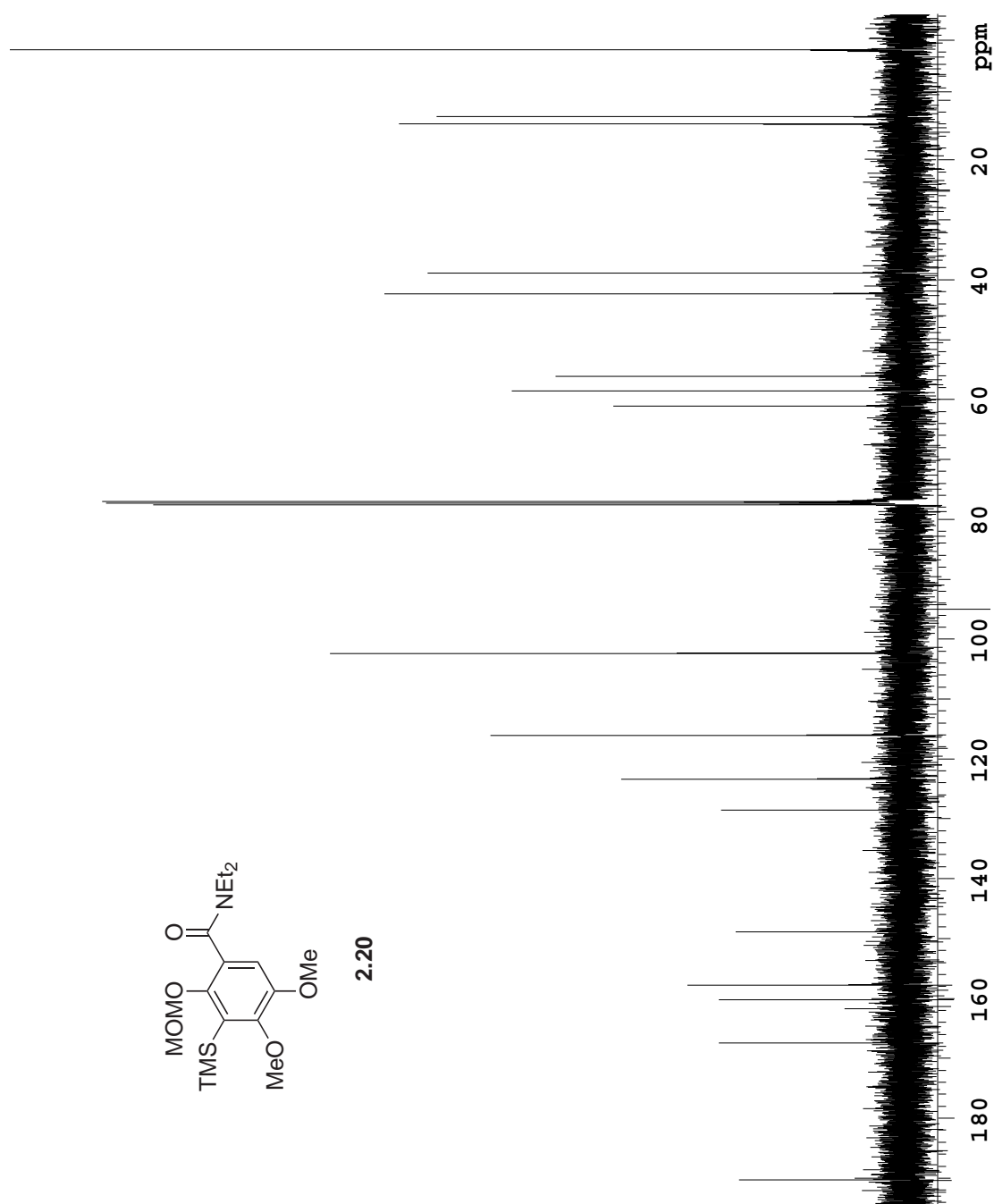


Figure A.9b The 126 MHz ^{13}C NMR spectrum of aryl-amide **2.20** in CDCl_3 .

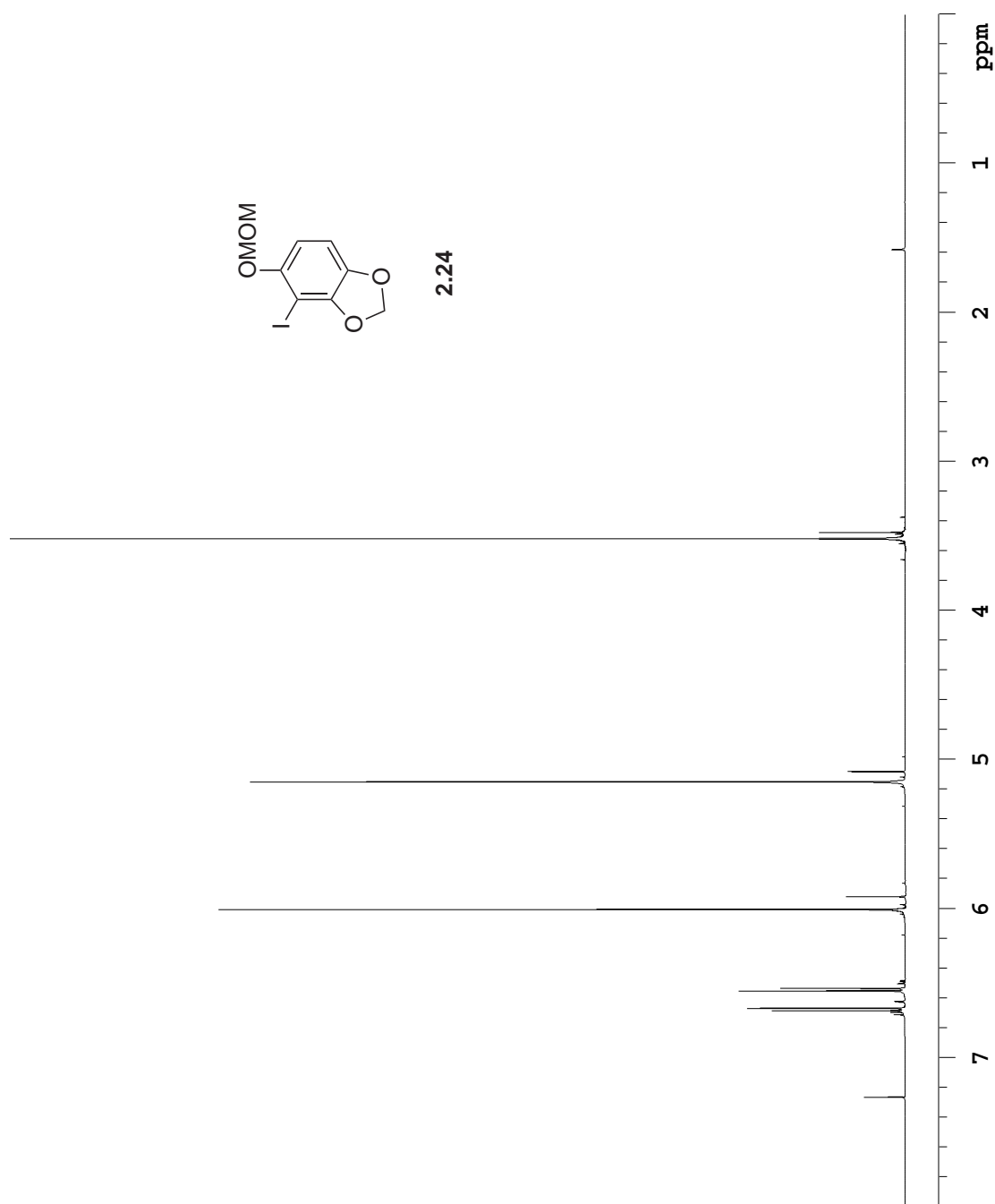


Figure A.10a The 500 MHz ^1H NMR spectrum of aryl-iodide 2.24 in CDCl_3 .

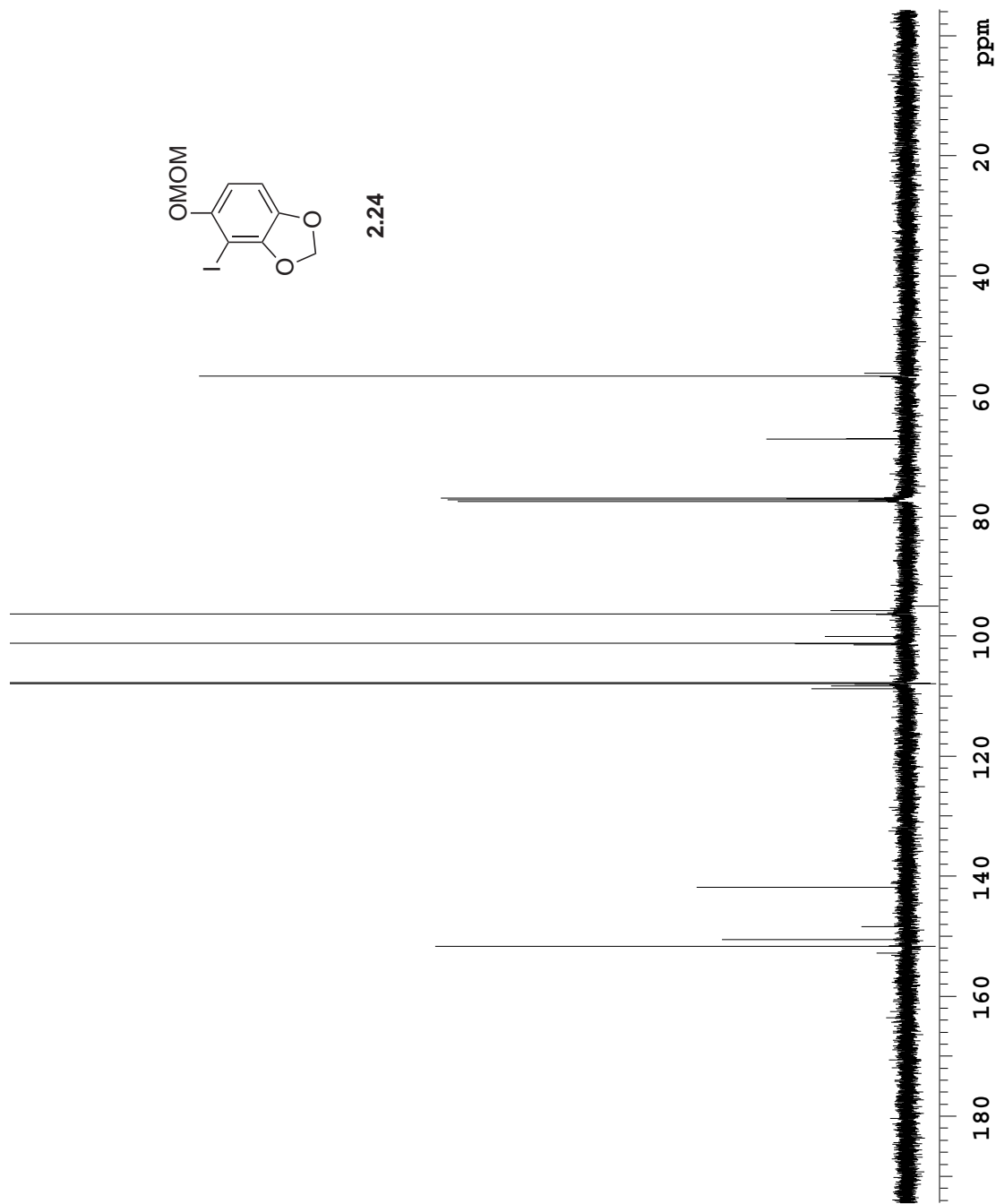


Figure A.10b The 126 MHz ^{13}C NMR spectrum of aryl-iodide 2.24 in CDCl_3 .

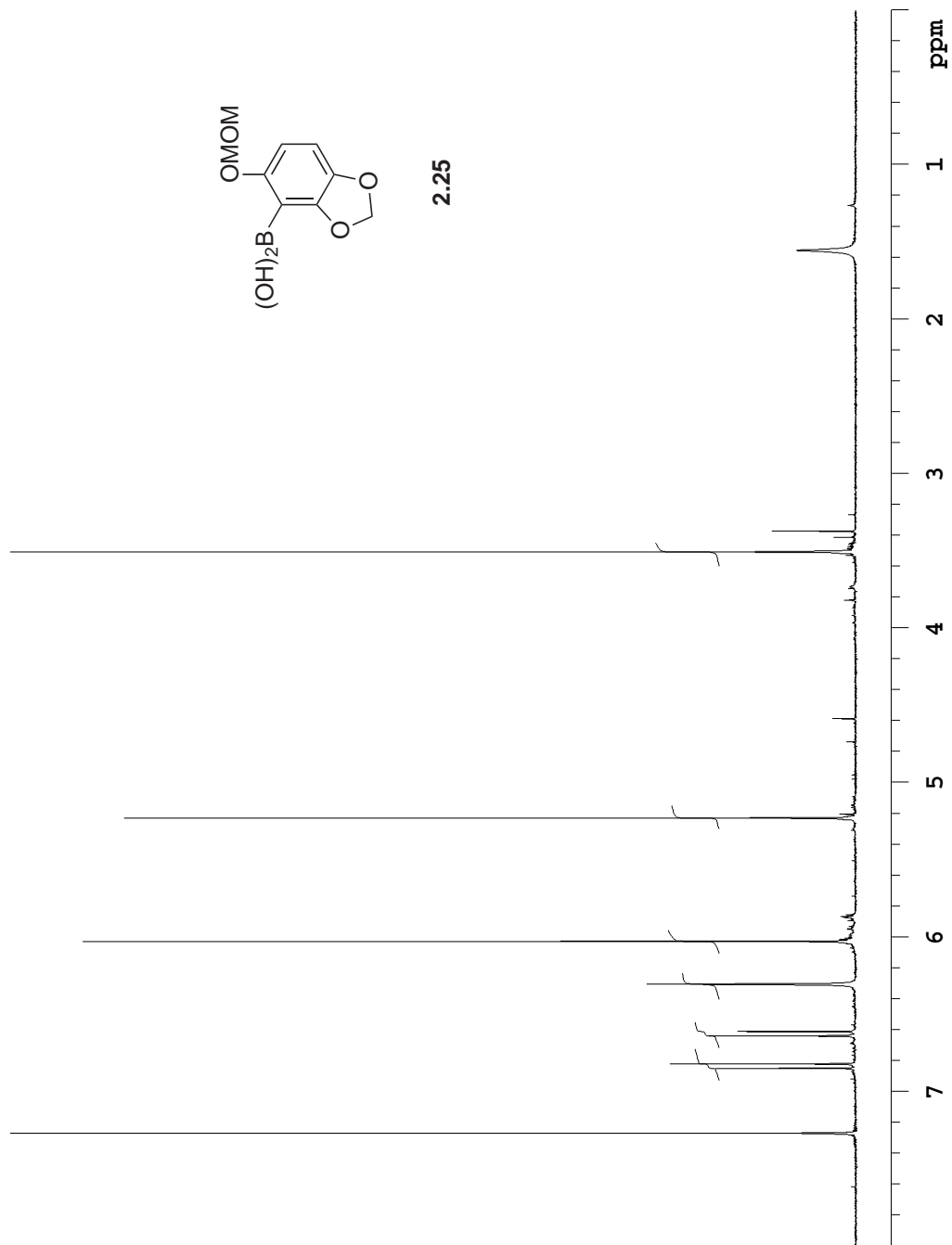
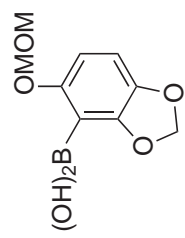


Figure A.11a The 500 MHz ¹H NMR spectrum of boronic acid **2.25** in CDCl₃.



2.25

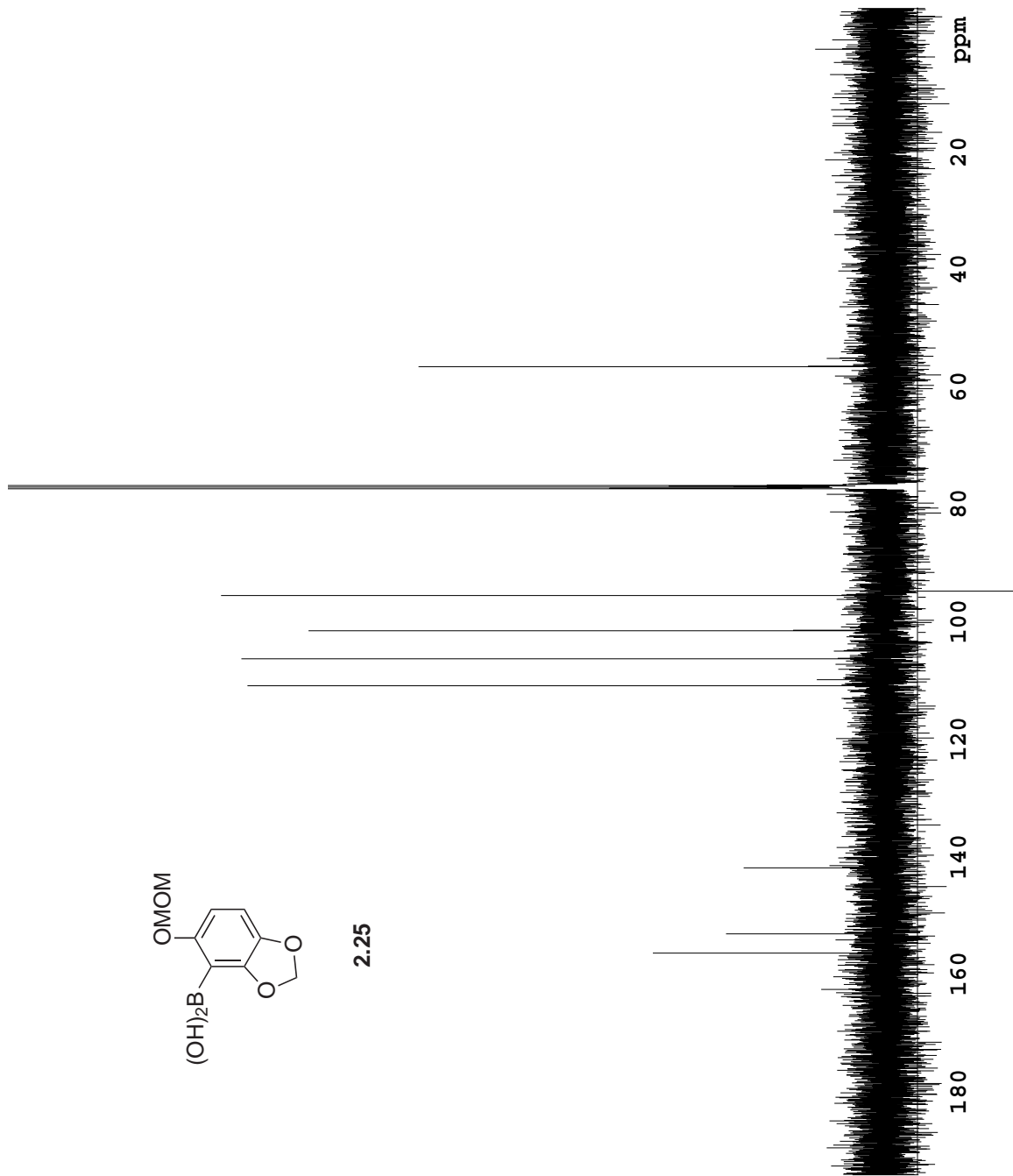
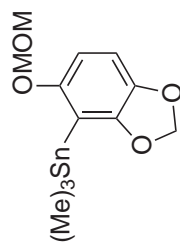


Figure A.11b The 126 MHz ¹³C NMR spectrum of boronic acid 2.25 in CDCl₃.



2.26

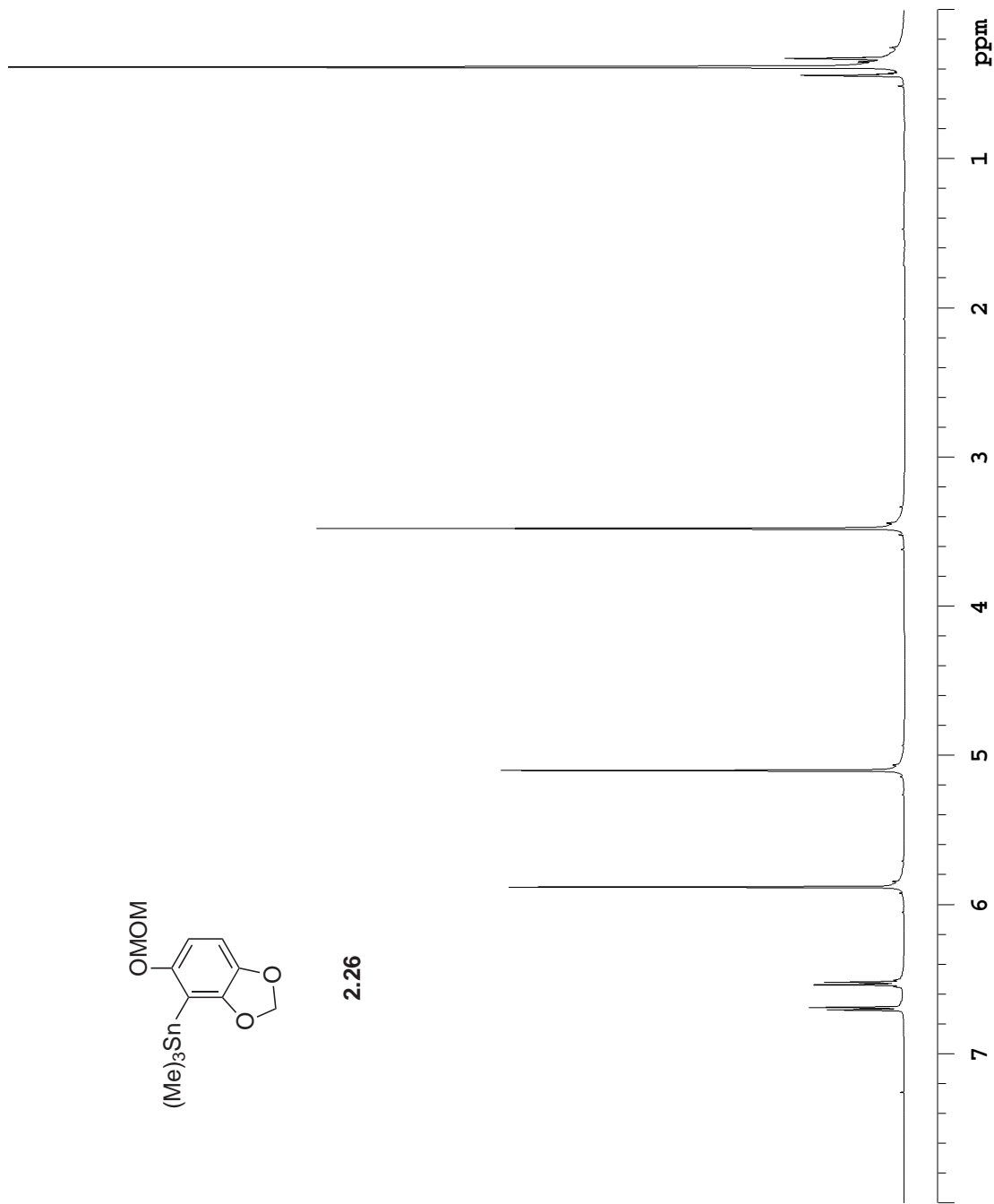


Figure A.12a The 500 MHz ¹H NMR spectrum of aryl-stannane 2.26 in CDCl₃.

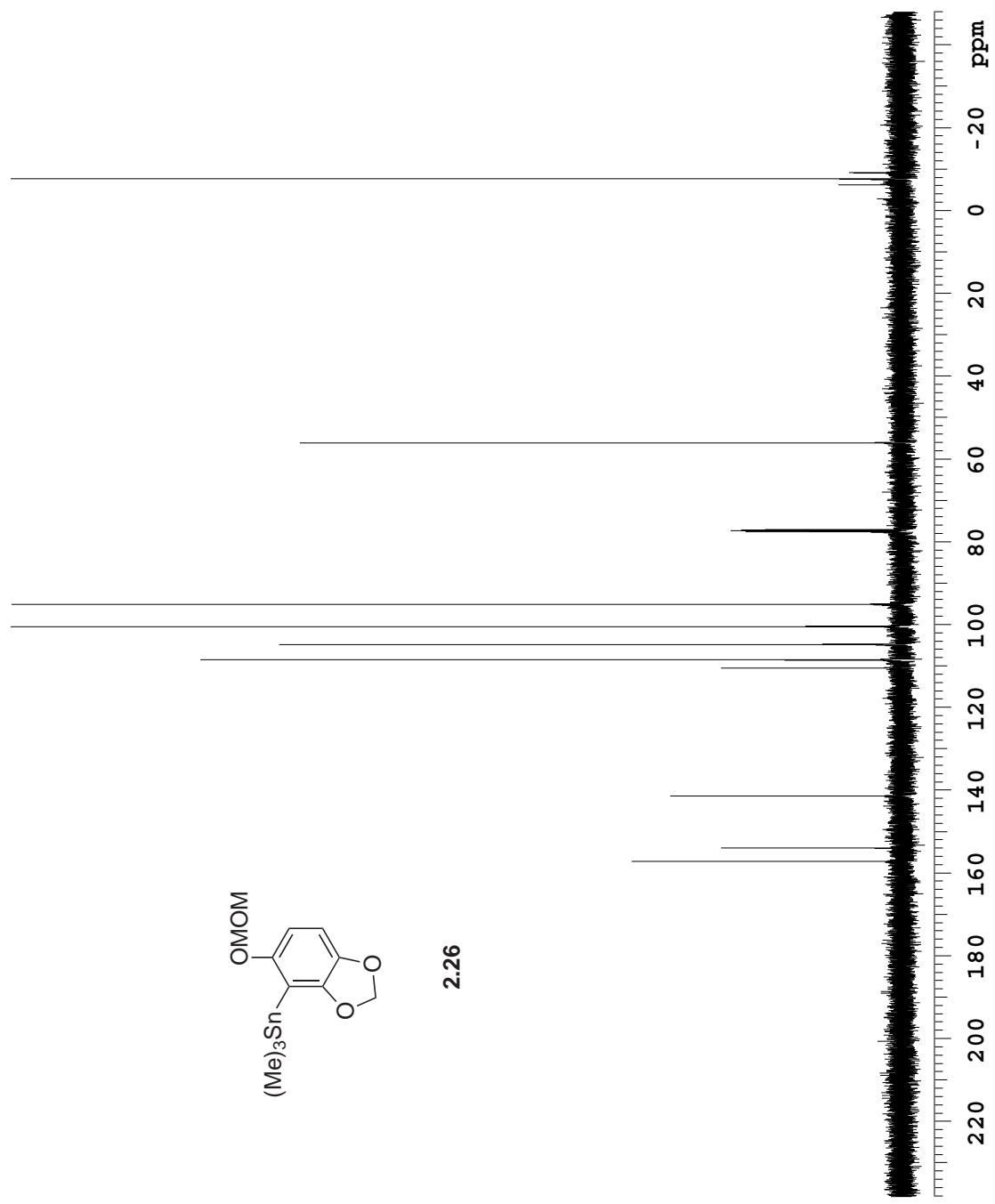


Figure A.12b The 126 MHz ¹³C NMR spectrum of aryl-stannane **2.26** in CDCl₃.

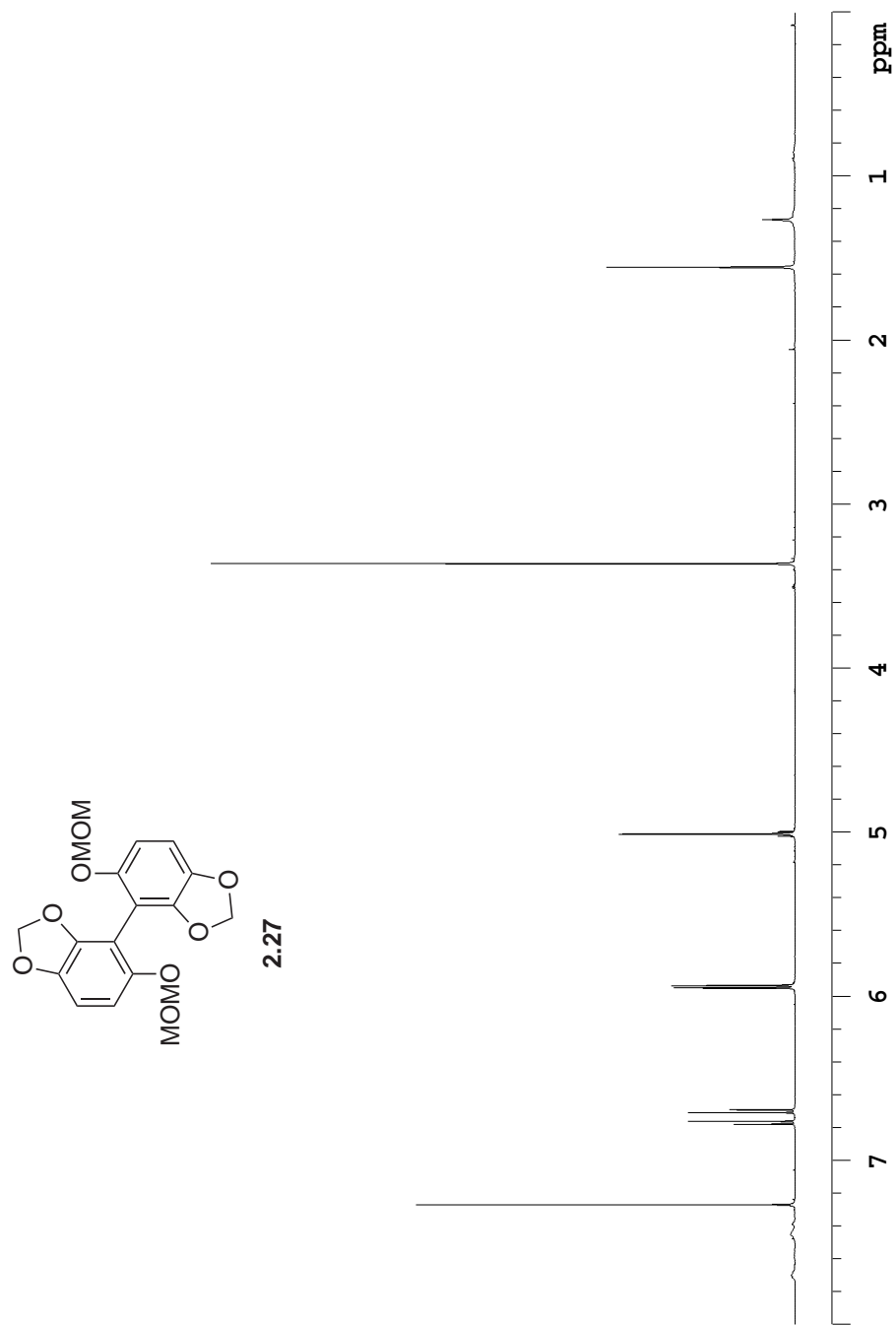


Figure A.13a The 500 MHz ¹H NMR spectrum of biaryl 2.27 in CDCl₃.

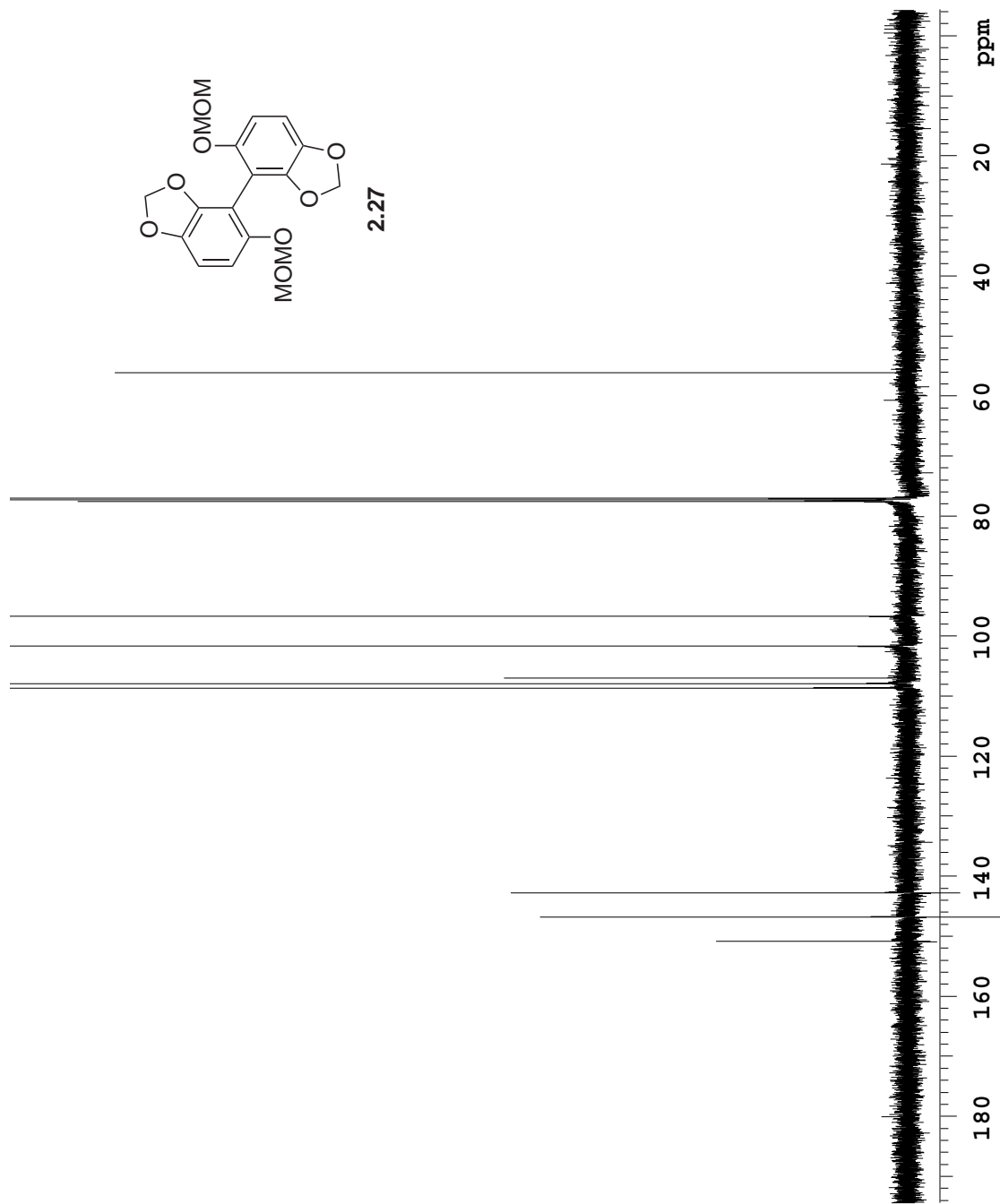
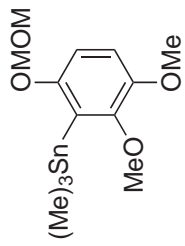


Figure A.13b The 126 MHz ^{13}C NMR spectrum of biaryl 2.27 in CDCl_3 .



2.28

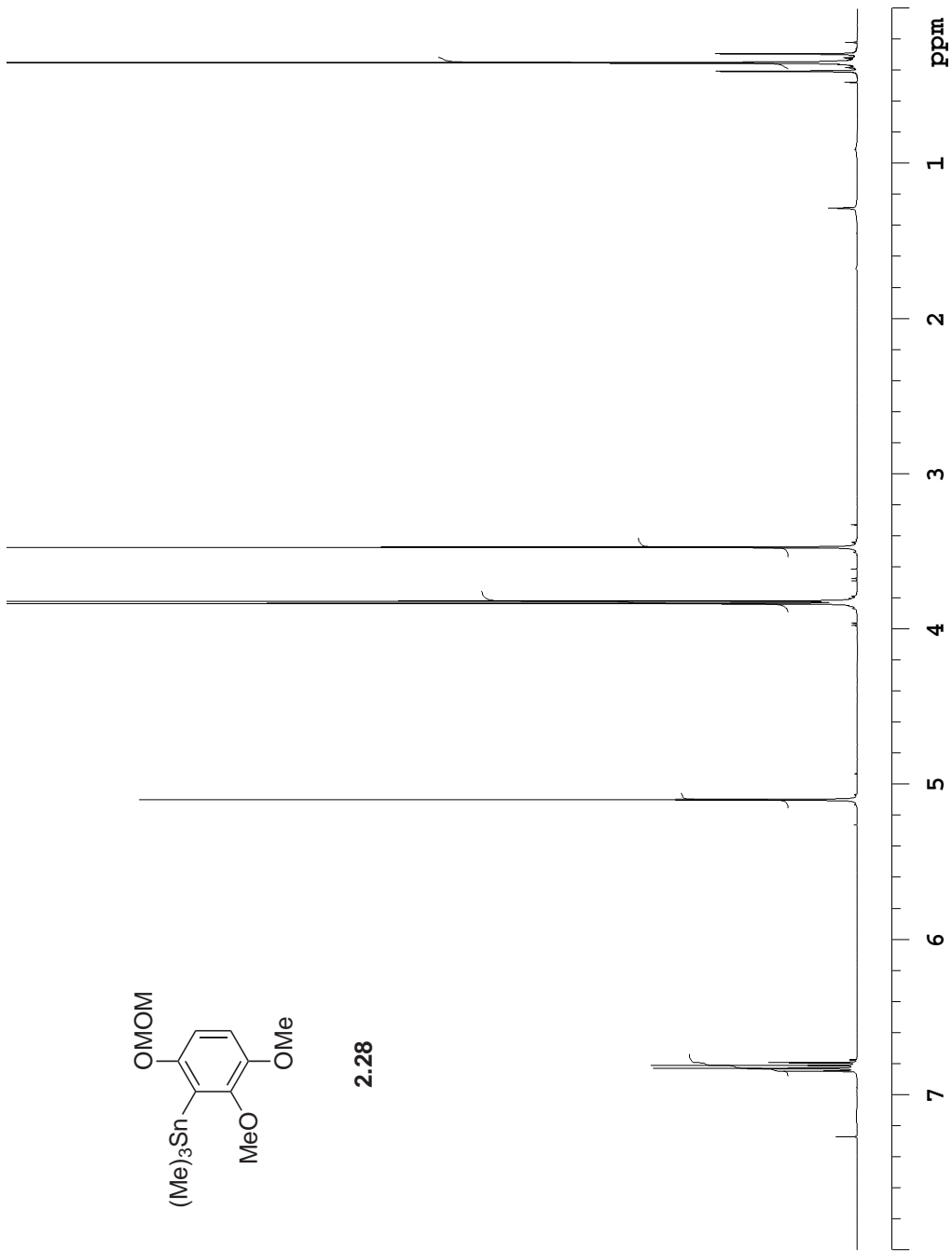
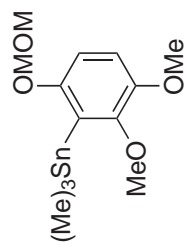


Figure A.14a The 500 MHz ¹H NMR spectrum of aryl-stannane 2.28 in CDCl₃.



2.28

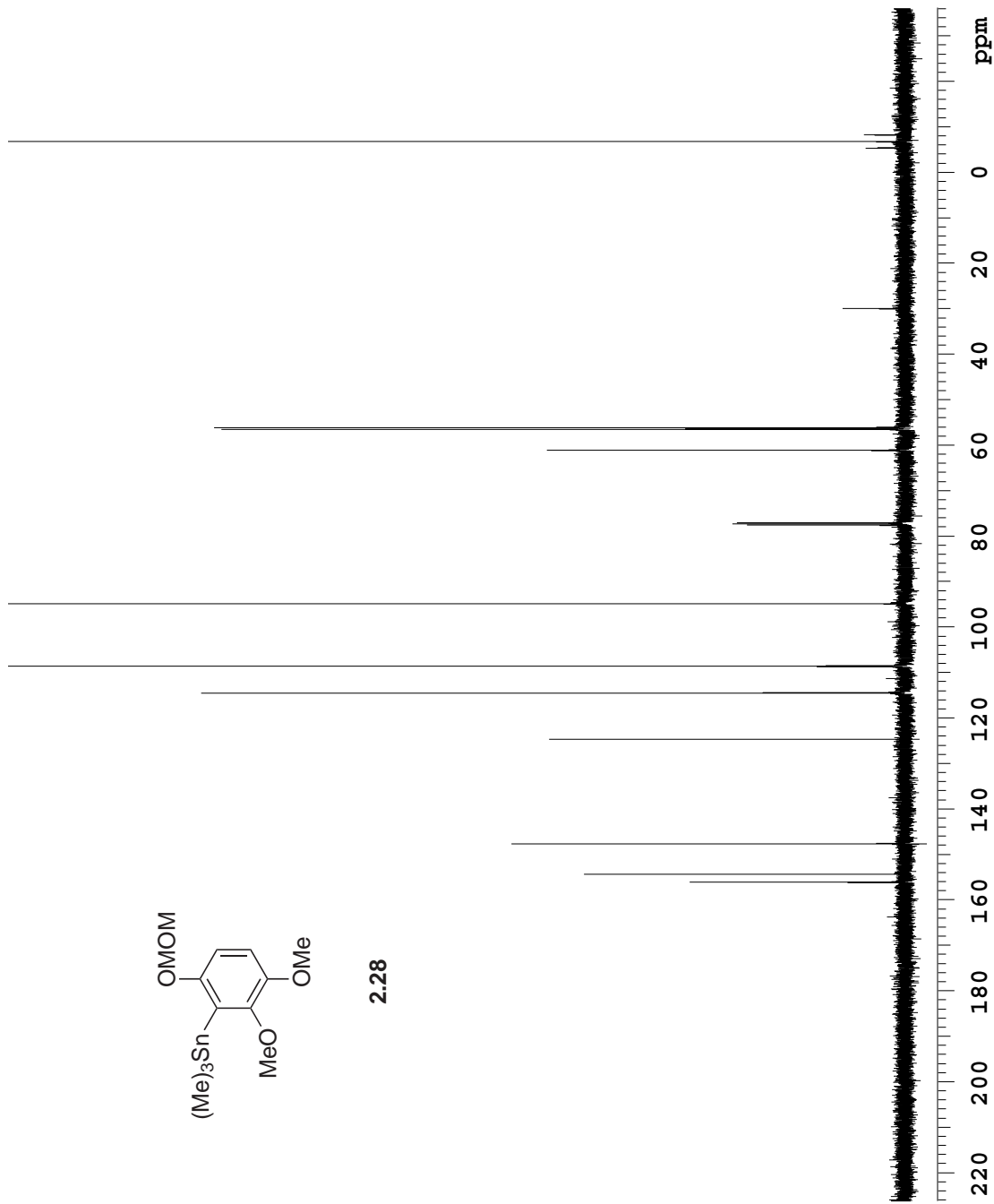


Figure A.14b The 126 MHz ¹³C NMR spectrum of aryl-stannane 2.28 in CDCl₃.

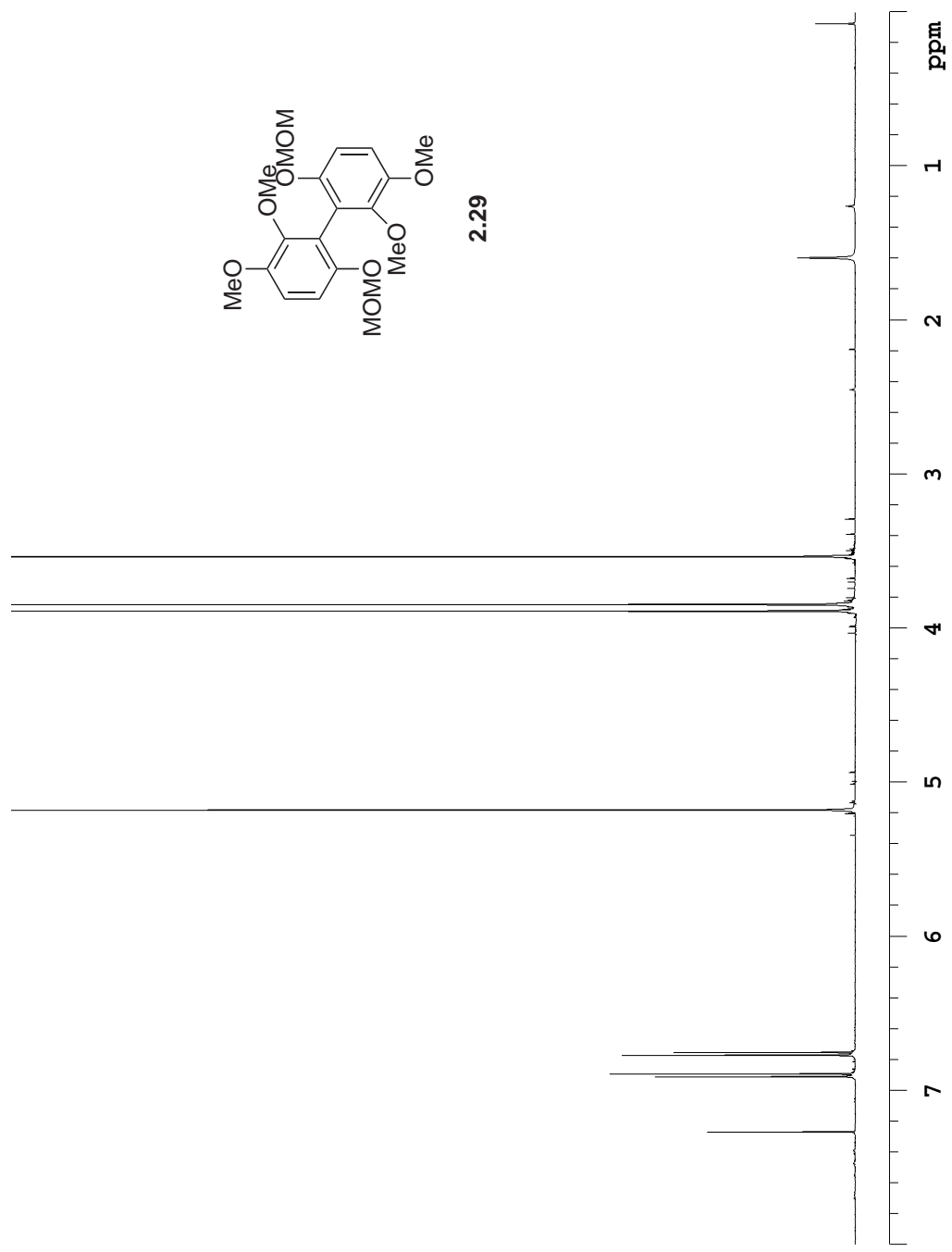


Figure A.15a The 500 MHz ¹H NMR spectrum of biaryl 2.29 in CDCl₃.

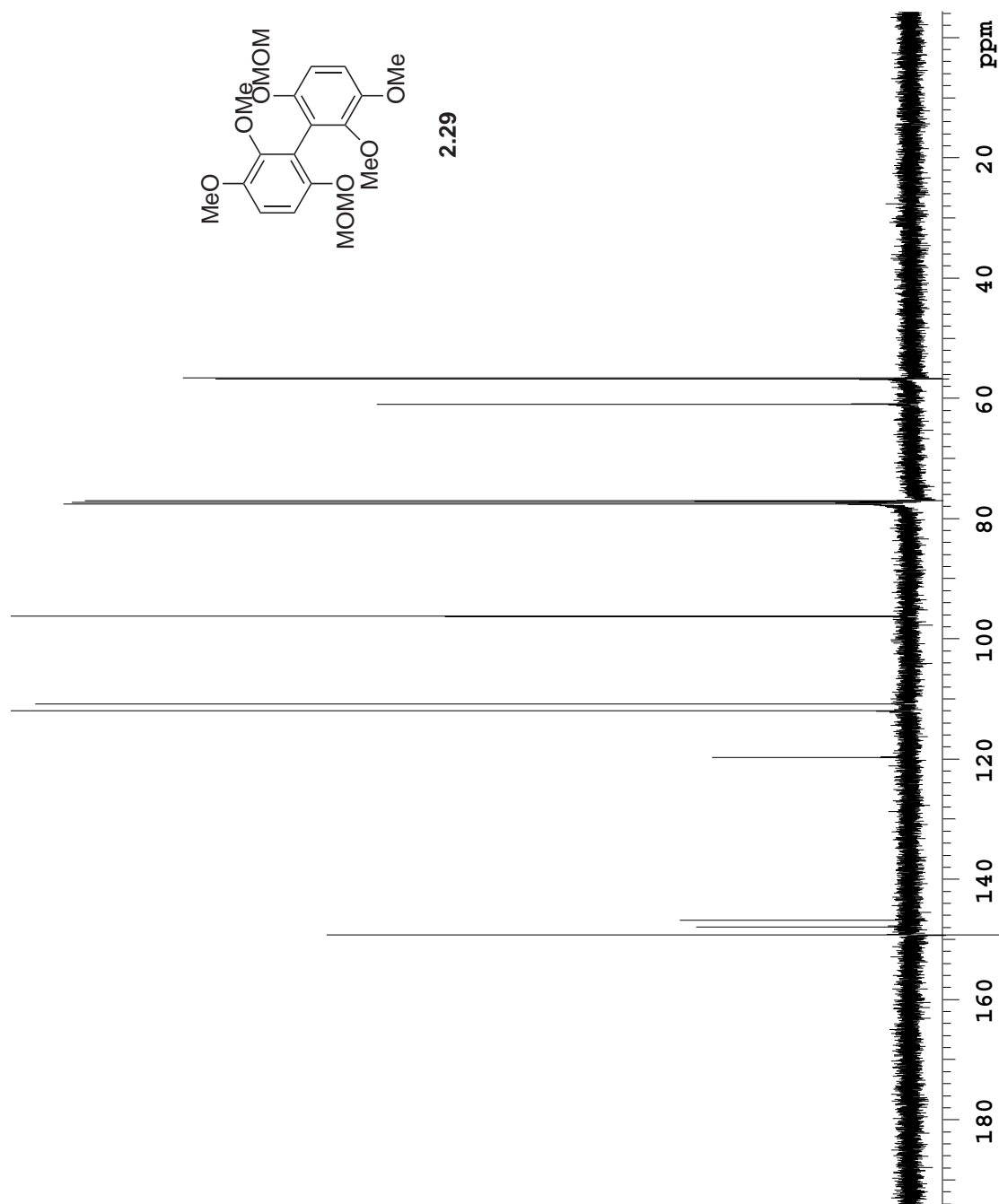


Figure A.15b The 126 MHz ^{13}C NMR spectrum of biaryl **2.29** in CDCl_3 .

VITA

NATHAN PAUL REISING

Permanent Address:

822 W. 5th St.

Marion, IN, 46953

U. S. A.

Educational Background:

B.A. Chemistry, Wabash College, Crawfordsville, IN, 1999.